NASA CR- 132629

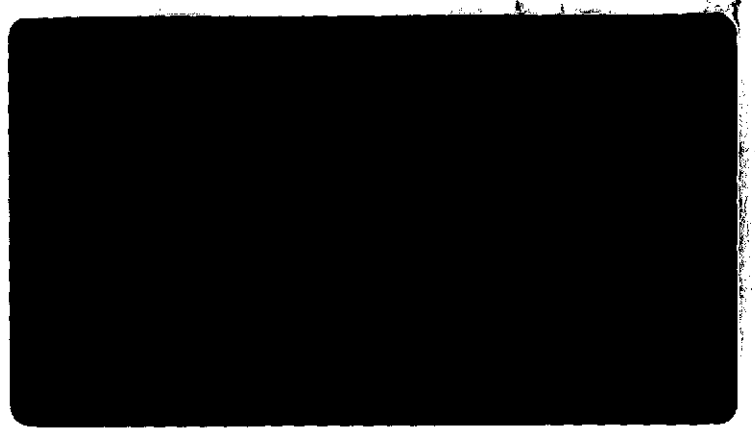

Mechanical Engineering Department
College of Engineering
Clemson University
Clemson, South Carolina

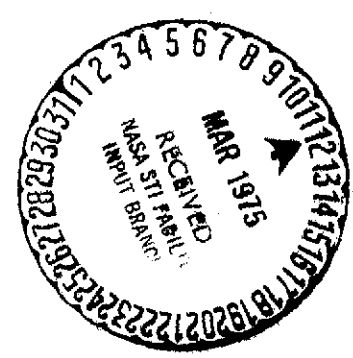

A CURVE FITTING METHOD FOR SOLVING THE FLUTTER EQUATION

by

Jerry Lynn Cooper

NASA CR- 132629

A CURVE FITTING METHOD FOR SOLVING THE FLUTTER EQUATION

by

Jerry Lynn Cooper

Approved C.S. Rudisill — In Charge of Major — 11/29/72 — Date

Approved J.C. Hunt — Head of Major Department — 12/6/72 — Date

Approved R. Elling — Committee Member — 11/29/72 — Date

Approved Eugene Park — Committee Member — 11/29/72 — Date

Mechanical Engineering Department
College of Engineering
Clemson University
Clemson, SC

NASA Grant NGR 41-001-027

A Report
Submitted to the
Faculty of Clemson University
in Partial Fulfillment of the Requirements
for the Degree of Master of Science in the Department
of Mechanical Engineering

December 1972

TABLE OF CONTENTS

LIST OF TABLES

Table

LIST OF FIGURES

ACKNOWLEDGMENTS

The author wishes to express his sincere gratitude to his major advisor, Dr. Carl S. Rudisill, for his continuous help and guidance throughout the author's master of science work. The author can not express in words the gratitude owed to his parents. Hopefully, a period of seventeen months can soon be repaid to my wife, Sallie, during which she had to show much patience and understanding for the many lost evenings at home.

Many thanks are also due to the Department of Mechanical Engineering, Clemson University, and the National Aeronautics and Space Administration for financial support during the author's studies. The NASA support was provided by Dr. Carl S. Rudisill from NASA research grant NGR-41-001-027.

A CURVE FITTING METHOD FOR SOLVING THE FLUTTER EQUATION

CHAPTER I

INTRODUCTION

In the optimization of a complex structure such as an airplane, one of the usual design constraints is that of flutter. Flutter is a hazardous phenomenon, for which the physics is not fully understood, in which an elastic body in an airstream, e.g. an airplane wing, becomes dynamically unstable. The first flutter investigation occurred about 1915, but an accurate theory of aircraft structure flutter was not formulated until 1935. Engineers in the recent past were able to design flutter free airplanes with the existing established techniques, but these methods without the digital computer meant long cumbersome hand calculations. As always time consumption meant money consumption, and with the age of new computers automated methods of flutter analysis were needed. Automated methods have now been applied to the different methods of flutter analysis, but these are basically iterative techniques that could be time consuming and therefore costly.

It is the objective of the author, not to extend the theory of flutter, but to present a flutter velocity extraction technique which is relatively fast with respect to digital computational time and is very simple. The flutter analysis presented here is a part of a large optimization computer program that optimizes a simple three bay cantilevered box beam (Figure 9) for minimum mass subject to the flutter velocity constraint. The box beam was used since many airplane wings resemble a box beam structure. Two examples are presented. Case I is

the system resulting from what will be defined as the minimum variable parameters (P(I) = PMIN(I)). Case 2 is the system resulting from a set of variable parameters which are six times the minimum parameters (P(I) = PMIN(I) x 6). These variable parameters (cross sectional areas, thicknesses, etc.) are listed in Table III of the Appendix.

Before explaining this method of flutter analysis a better understanding of the overall problem of flutter should first be developed. The following chapter contains a discussion of flutter for a system with single degree of freedom followed by the broader concept of flutter for a system with many degrees of freedom. The formulation of the basic flutter equation is also presented in this chapter. The classical or established methods of flutter analysis, recent work in the area of flutter, and the statement of the problem are given in Chapter III. Chapter IV presents the derivatives of the eigenvalues λ with respect to the reduced frequency k, which could have been derived directly from a paper by Rudisill and Bhatia (11), but which are given in detail since some of the complexity and understanding might be taken from the problem. These derivatives make possible the computerized flutter technique explained in Chapter V. The results and conclusions of this technique are also given at the end of Chapter V.

CHAPTER II

FLUTTER AND THE FORMULATION OF THE FLUTTER EQUATION

As defined in the Introduction, flutter is a hazardous phenomenon in which an elastic body in an airstream becomes dynamically unstable. The elastic bending of the wing is such that energy is added to the structure faster than it can be dissipated. The flutter speed V_f and the frequency ω_f are the lowest airspeed and the corresponding circular frequency of oscillation, respectively, at which a given structure flying under given atmospheric conditions will exhibit sustained simple harmonic oscillations (1, p. 5). Flight at velocities above the flutter airspeed will cause divergent oscillations or damage to the structure, while airspeeds below V_f represent stable conditions. The flutter speed is therefore a condition of neutral stability for the system.

Theoretical flutter analysis many times consists of assuming in advance that all dependent variables are porportional to $e^{i\omega t}$ where ω is a real frequency and $i = (-1)^{1/2}$. Combinations of the velocity V and the frequency ω for which this occurs must be found. This double combination thus leads to a complex or double eigenvalue problem, with two characteristic numbers determining the airspeed and the frequency. The simpler analogous situation is the free vibration of a linear structure in a vacuum, which is a real or single eigenvalue problem.

In the past, flutter predictions have been made by many different methods. Some of the methods used were analog simulation, scaled dynamic models in wind tunnels and flight testing of full scale models

by pilots. The last method requires that the airplane be flown at the predicted flutter velocity. The excitation of the structure at this speed sometimes causes divergent oscillations which could mean death to the pilot.

Single Degree of Freedom

The flutter problem discussed in this paper is one for a structure with many degrees of freedom; therefore, a simple system will first be explained. Bisplinghoff (2) considers the example of a rigid two dimensional airfoil in Figure 1. The airfoil is hinged at its leading edge so that it is elastically restrained from rotating about its leading edge due to the torsional spring with a spring constant equal to K_α ft-lb/rad. The unstretched position of the spring corresponds to a zero angle of attack α. The equation of motion for this single degree of freedom system is

$$I_\alpha \ddot{\alpha} + K_\alpha \alpha = M_y \qquad 2\text{-}1$$

where

I_α = moment of inertia about the leading edge

M_y = aerodynamic moment due to $\alpha(t)$

α = angle of attack and

K_α = spring constant.

In order to produce flutter for this simple problem, some unrealistic assumptions must be made. These assumptions are that the air density ρ will be very small and the air foil will be heavily

weighted. First solve for the flutter condition by assuming as a solution for equation (2-1) the following,

$$\alpha = \bar{\alpha}_0 e^{i\omega t} \qquad 2\text{-}2$$

where $\bar{\alpha}_0$ is a constant angular amplitude displacement. Substituting equation (2-2) into equation (2-1) yields,

$$I_\alpha(\bar{\alpha}_0 i^2 \omega^2 e^{i\omega t}) + K_\alpha(\bar{\alpha}_o e^{i\omega t}) = M_y. \qquad 2\text{-}3$$

Upon dividing equation (2-3) by $\pi\rho b^4 \omega^2 \bar{\alpha}_o e^{i\omega t}$, where b is the reference semichord, the result is

$$\frac{I_\alpha}{\pi\rho b^4}\left[1 - \left(\frac{\omega_\alpha}{\omega}\right)^2\right] + m_y = 0, \qquad 2\text{-}4$$

where $\omega_\alpha = \left(\frac{K_\alpha}{I_\alpha}\right)^{\frac{1}{2}}$ is the natural frequency of torsional vibration in a vacuum and $m_y = M_y/\pi\rho b^4 \omega^2 \bar{\alpha}_o e^{i\omega t}$ represents the dimensionless aerodynamic coefficients. For a thin airfoil with small harmonic motion in two dimensional flow m_y may be written as

$$m_y = M_\alpha + 1/2(L_\alpha + 1/2) + 1/4(L_h) \qquad 2\text{-}5$$

where M_α, L_α, and L_h are complex functions of the reduced frequency k. The quantity is therefore a complex function and can be split into real and imaginary parts,

$$\mathrm{Re}(m_y) = \frac{I_\alpha}{\pi\rho b^4}\left[\left(\frac{\omega_\alpha}{\omega}\right)^2 - 1\right] \qquad 2\text{-}6$$

$$\mathrm{Im}(m_y) = 0. \qquad 2\text{-}7$$

From equations (2-6) and (2-7) flutter occurs for the value of the reduced frequency k for which the out-of-phase component of the

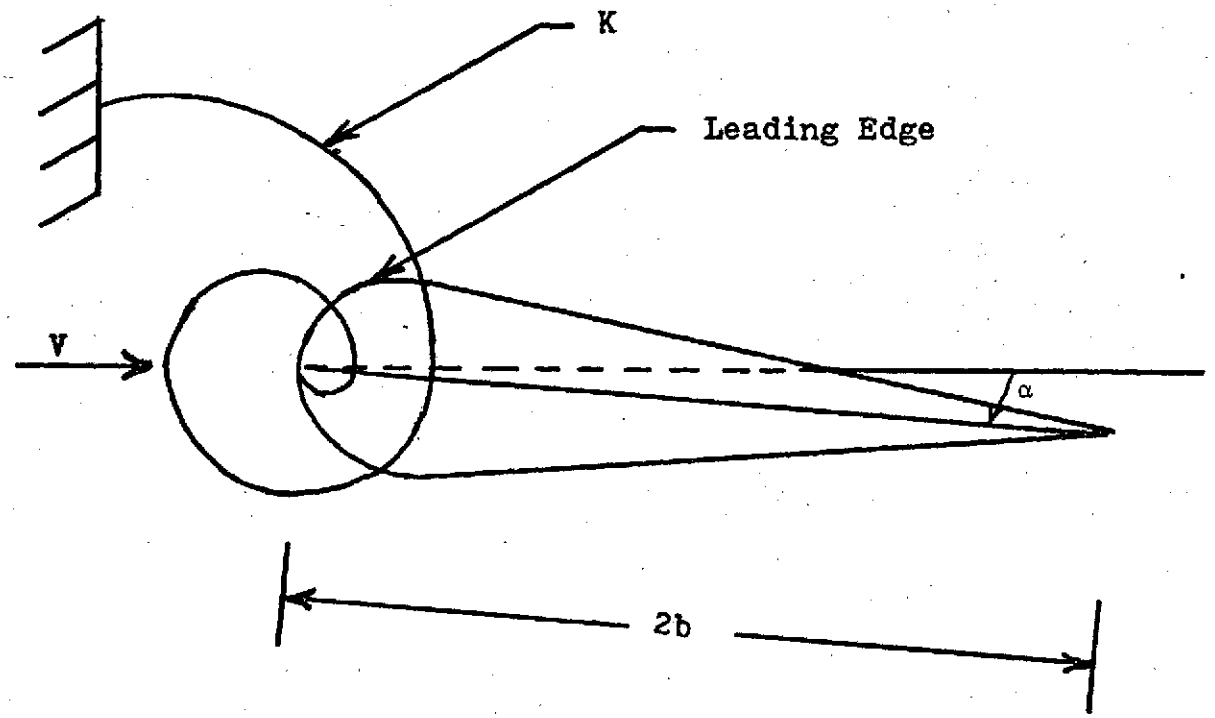

K = spring constant of torsional spring
b = semichord
α = angle of attack
V = velocity of airstream

Figure 1. Rigid Two-Dimensional Airfoil Restrained about its Leading Edge.

aerodynamic moment $Im(m_y)$, will vanish, provided that the corresponding in-phase part, $Re(m_y)$, is of such magnitude that equation (2-6) yields a pure real flutter frequency. The out-of-phase component $Im(m_y)$ is the only damping or instability for the airfoil. For $Im(m_y)$ less than zero or an m_y which lags the simple harmonic motion, energy is removed from the oscillations, resulting in damping of the airfoil. If $Im(m_y)$ is greater than zero then divergent oscillations result with energy added to the airfoil.

A System of Many Degrees of Freedom

By the finite element method a complex structure with many degrees of freedom is described as an assembly of structural elements connected by discrete or continuous attachments, and the displacements at nodes, including angular displacements, are represented as the actual displacements on the continuous structure. The interaction forces, including bending moments and torques between the discrete attachments, are represented as discrete joint forces. Figure 2 shows how a cantilevered beam would be represented using the finite element method. The applied forces P_1, P_2, the reaction force P_r, the applied moments M_1, M_2, and the reaction moment M_r are replaced by discrete forces, M_1, Y_1, M_2, Y_2, M_3, Y_3, M_4, Y_4, and nodal displacements v_1, θ_1, v_2, θ_2, v_3, θ_3, v_4, θ_4 at nodes (1), (2), and (3).

For the system with many degrees of freedom and therefore many elements the elastic and inertia properties of these elements are determined in matrix form. It is from these properties that the

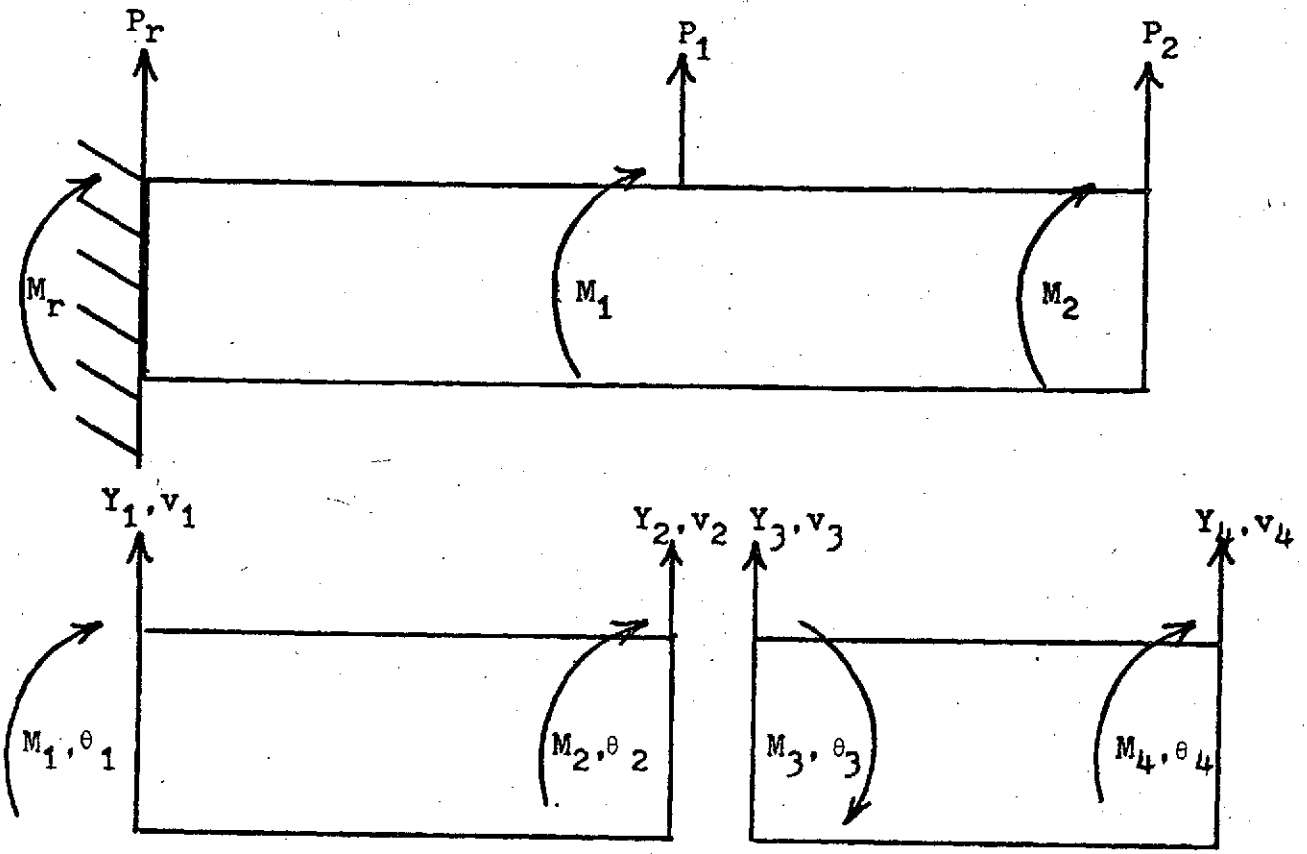

Figure 2. Discrete Element Representation of a Cantilevered Beam.

matrix equations for static or dynamic equilibrium are derived. The motion of a discrete and linearly elastic system can be expressed in the form (11)

$$[M]\{\ddot{U}\} + [K]\{U\} = \{P\} \qquad 2\text{-}8$$

where,

$\{U\}$ = n x 1 vector representing nodal displacements for the assembled structure, referred to a global coordinate system,

$\{\ddot{U}\} = d^2\{U\}/dt^2$ = n x 1 vector representing nodal accelerations,

$[K]$ = n x n stiffness matrix for the complete structure corresponding to displacements $\{U\}$,

$\{P\}$ = n x 1 vector representing the total applied forces at the nodes, corresponding to the nodes by $\{U\}$, and

n = the number of degrees of freedom for the structure.

As with the single degree of freedom system the theoretical flutter analysis for many degrees of freedom consists of finding combinations of the airspeed V and the circular frequency of oscillation ω for which the out-of-phase component of the imaginary part of the aerodynamic moment vanishes, producing simple harmonic motion. Based on the assumption of simple harmonic motion, the displacement vector $\{U\}$ and the acceleration vector $\{\ddot{U}\}$ may be expressed in terms of a constant amplitude vector $\{U_0\}$ as

$$\{U\} = \{U_0\}\, e^{i\omega t} \qquad 2\text{-}9$$

and

$$\{\ddot{U}\} = -\omega^2 \{U_0\}\, e^{i\omega t}$$

The applied loads, P(t), may be expressed as

$$P(t) = \omega^2 \rho b^4 \, L \, [A]\{U\} \qquad 2\text{-}11$$

where ρ, b, [A], and L are the air density, semichord, air force matrix, and span length respectively. Substitution of equations (2-10) and (2-11) into equation (2-8) yields,

$$-\omega^2 \, e^{i\omega t}[M]\{U_0\} + [K]\{U\} = \omega^2 \rho b^4 \, L \, [A]\{U\} \qquad 2\text{-}12$$

Equation (2-12) may be written as

$$-\omega^2[M]\{U\} + [K]\{U\} = \omega^2 \rho b^4 \, L \, [A]\{U\} \qquad 2\text{-}13$$

Finally equation (2-13) may be written as,

$$[[K] - \lambda([M] + c[A])]\{U\} = \{0\} \qquad 2\text{-}14$$

where $c = \rho b^4 \, L$ and $\lambda = \omega^2$. Here λ is referred to as the eigenvalue of equation (2-14). Equation (2-14) is the fundamental equation of flutter.

The stiffness matrix K and the inertia matrix M are functions of the variable parameters (cross sectional areas, thicknesses, diameters squared, etc.). The air force matrix A is a complex function of the reduced frequency k, the air density, the mach number, and the semichord b. The reduced frequency k is defined by the relation,

$$k = b\omega/V_f$$

where V_f is the flutter velocity. The matrices K and M are symmetric while matrix A is not.

For a nontrivial solution of equation (2-14) the flutter determinant $|[K] - \lambda([M] + c[A])|$ must be equal to zero. The known quantities of the determinant are matrices K and M which are determined

from the variable parameters of the structure and therefore the above determinant yields a polynomial in λ ($=\omega^2$) with unknown complex coefficients which are in general functions of the reduced frequency k and mach number. The theory used for formulation of the air force matrix A for this paper is that of Theodorsen for subsonic incompressible flow. The use of this particular theory yields a polynomial from the flutter determinant which is a function of the reduced frequency k only.

Real values of the reduced frequency k are assumed and the corresponding values of the eigenvalues are computed for which the flutter determinant is zero. A system with n degrees of freedom will have n distinct complex values of λ corresponding to an assumed value of the reduced frequency k, if there are no repeated roots. Repeated roots are seldom encountered in a structural system. The flutter velocity analysis consists of finding values of the reduced frequency for which the imaginary part of the eigenvalues will equal zero. The flutter velocity is then computed from the following relation

$$V_f = b\omega/k \qquad 2\text{-}15$$

It is seen from equation (2-15) that although a value of 1/k may yield a real value for the eigenvalue λ, it may not be the lowest flutter velocity, since V_f is also a function of the circular frequency of oscillation ω. The semichord b will be a constant. Thus, the lowest of the flutter velocities must be found for the system. In practice the lowest flutter velocity is usually found by checking only

the first three to five flutter velocities for increasing values of 1/k. No proof that this is always the case has ever been presented in the flutter literature, however.

CHAPTER III

WORK BY OTHERS

Lawrence and Jackson (5) discuss the flutter analysis methods classified as the American approach, the British approach, and the Richardson approach. In their paper they have shown the results of the three methods, compared them, and given their conclusions. It is the purpose of the author to discuss in this chapter what may be considered the classical techniques of flutter analysis and then briefly summarize the recent state of the art. The American and British techniques will be considered as the classical methods of analysis. The different methods of flutter analysis commonly used agree in regard to critical flutter airspeeds, provided the same basic data are used, but give different results for the stability decay rates at other airspeeds.

British Approach

In the United Kingdom the flutter equation is written in the form,

$$M \frac{d^2\{U\}}{d\tau^2} + [\bar{V}[D_a] + [D_s]] \frac{d\{U\}}{d\tau} + [\bar{V}^2[K_a] + [K_s]] \{U\}=0 \qquad 3\text{-}1$$

where

[M] = structural and aerodynamic inertia matrix,

{U} = eigenvectors or column matrix of generalized coordinates,

V = airspeed

V_0 = reference airspeed,

$\bar{V}$ = V/V_0,

L = span length,

τ = $V_0 t/L$,

$[D_a]$ = aerodynamic damping matrix,

$[D_s]$ = structural damping matrix,

$[K_a]$ = aerodynamic stiffness matrix, and

$[K_s]$ = structural stiffness matrix.

A solution of the form $\{U\} = \{\bar{U}\} e^{\lambda t}$ is assumed where $\{\bar{U}\}$ is a constant amplitude vector and λ_j are the resulting complex eigenvalues of the form

$$\lambda_j = \mu_j + i\omega_j$$

where μ is the exponential growth rate and ω is the circular frequency of oscillation. The system is stable if μ is greater than zero and the state of flutter occurs when $\mu = 0$, or $\lambda = i\omega$, or the eigenvalue is purely imaginary. Equation (3-1) holds only for simple harmonic motion.

The aerodynamic stiffness matrix K_a, and the aerodynamic damping matrix D_a are functions of the frequency $\bar{\nu} = \omega/\bar{V}$, and usually the mach number. The structural damping matrix D_s is frequently set equal to zero since it is negligible compared with damping matrix D_a due to the aerodynamic forces. Solutions of equation (3-1) are found by assuming a value of $\bar{\nu}$ for the calculation of matrices D_a and K_a, and then solving for the eigenvalues λ_j from equation (3-1). The eigenvalues in general are not purely imaginary, and in general the computed value

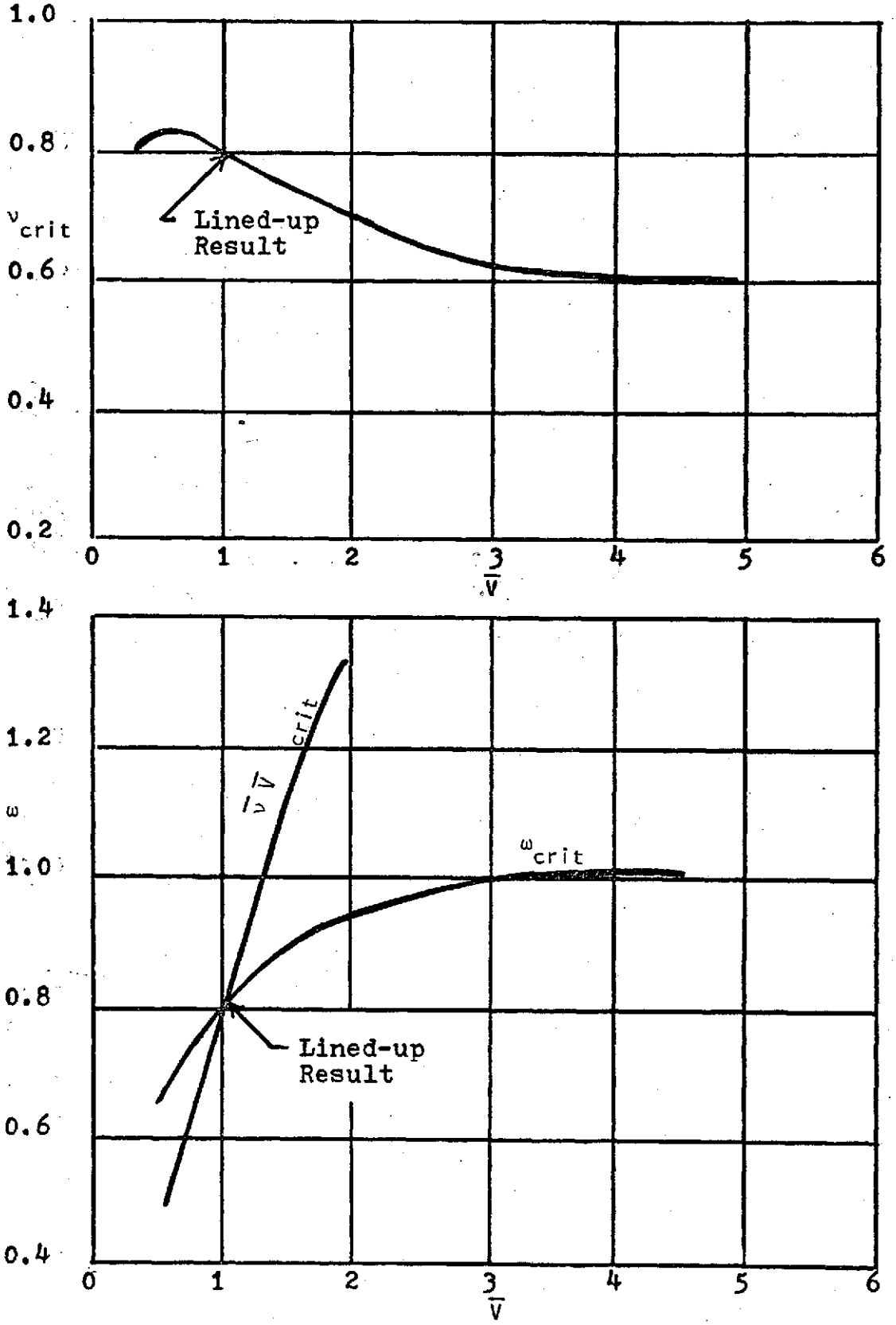

Figure 3. British Method.

of $\bar{\nu} = \omega/\bar{V}$, where ω comes from the imaginary part of the computed complex eigenvalue, do not line up or equal each other. When the computed eigenvalue is pure imaginary ($\mu = 0$), then the assumed $\bar{\nu}$ and the computed $\bar{\nu}$ will line up.

In order to find the lined-up values of $\bar{\nu}$ a graph is plotted of ω obtained from the eigenvalues against $\bar{V}$, and the intersections of each curve with the line $\omega = \bar{\nu}\bar{V}$, where $\bar{\nu}$ is the assumed value of the frequency which was used originally to compute matrices D_a and K_a, give the lined-up values of frequency ω and airspeed V. This method is graphically represented in Figure 3. The lowest critical velocity from the lined-up values will be the flutter velocity.

The main disadvantage of this method is that the eigenvalues for a large range of assumed frequency $\bar{\nu}$ values must be calculated before lined-up values can be found. Therefore, the British method will in general be time consuming and costly for application on the computer.

American Approach

The American method of analysis, commonly referred to as the V-g method, is quite different from that of the United Kingdom. The flutter equation is formulated as follows,

$$\left[[M] - \frac{i\bar{V}[D_a]}{\omega} - \left(\frac{\bar{V}}{\omega}\right)^2 [K_a] - \frac{1 + ig}{\omega^2}[K_s]\right] \{\bar{U}\} = 0 \qquad 3\text{-}2$$

where $1/\bar{\nu} = \bar{V}/\omega$. It is seen from equation (3-2) that the structural damping matrix D_s is completely ignored and g, a fictitious structural

damping is introduced. The structural damping will actually be represented by $(g/\omega)[K_s]$ and is supposedly just sufficient to maintain simple harmonic motion. The solution $\{U\} = \{\bar{U}\}\, e^{i\omega\tau}$ is postulated leading to an eigenvalue problem to determine the complex eigenvalues.

Once again an assumed value of $\bar{\nu}$ which is used for calculating the aerodynamic damping matrix D_a and the aerodynamic stiffness matrix K_a yields in general the complex eigenvalues from equation (3-2). By separation of the real and imaginary parts of the eigenvalue λ, g and ω may be obtained. The corresponding velocity V is obtained from the relation $\bar{V} = \bar{\nu}/\omega$. A negative value of g means that the system is damped and therefore, stable. The critical flutter airspeed occurs when $g = 0$. Figure 4 shows a graphical representation of the American method. It is seen from Figure 4 that the solutions for a particular value of ω/V lie on a straight line through the origin of the ω-V plane. It is also seen that lined-up values of $\bar{\nu}$ play no part in this method as compared to the British method. Further comparison with the British method shows that all computed values of the frequency $\bar{\nu}$ correspond exactly with the assumed values of $\bar{\nu}$. Once again the American approach calls for an iterative method varying $\bar{\nu}$ to find eigenvalues which will yield $g = 0$. From the American formulation of the flutter equation a plotting process to find zero values of g would be time consuming and costly, but the American approach does have the advantage of not having to find the lined-up values of $\bar{\nu}$.

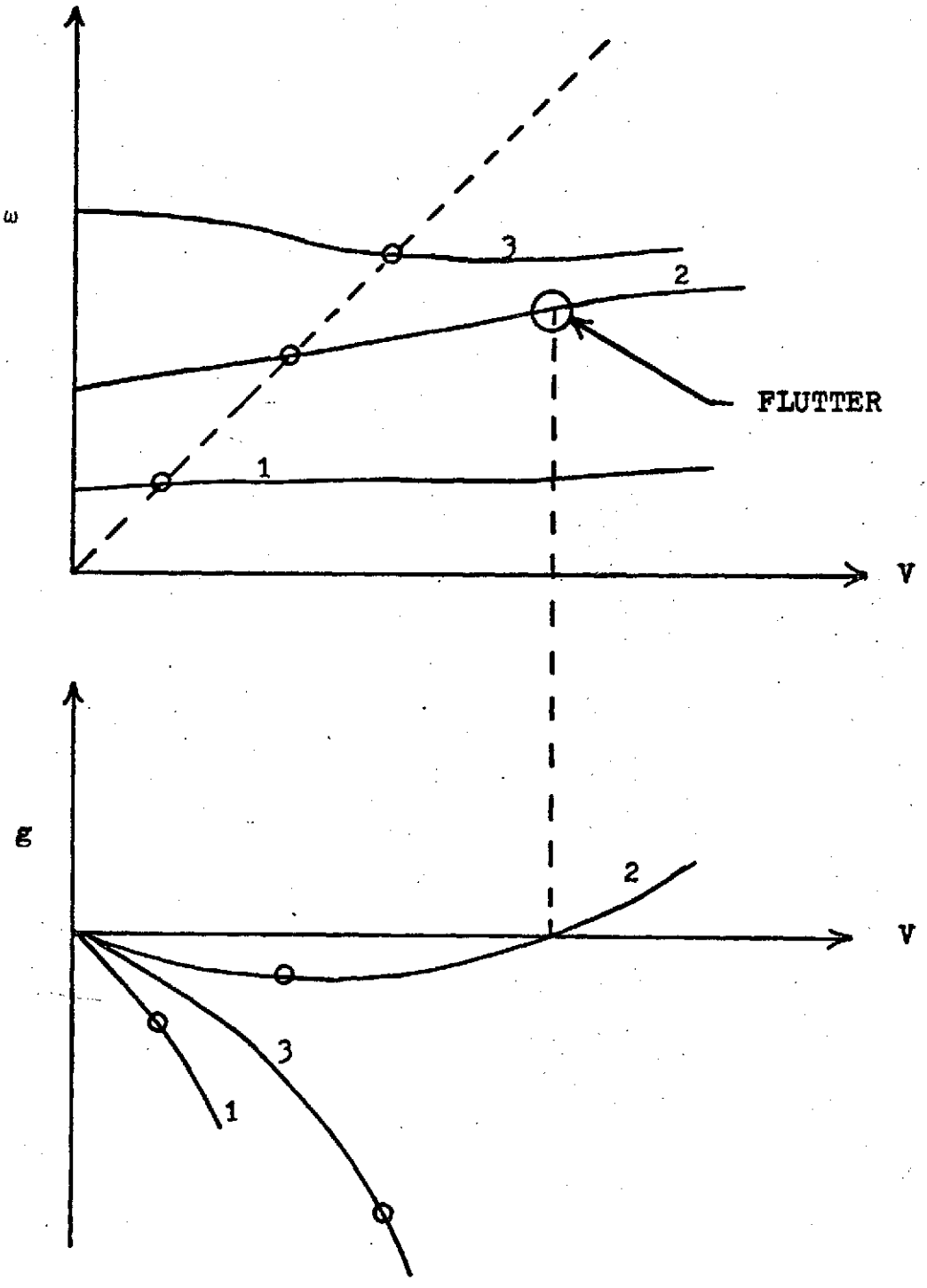

Figure 4. American Method.

Recent Work

Richardson's method is basically an extension of flutter theory to give correct subcritical decay rates for a system with many degrees of freedom and multidimensional compressible aerodynamic forces. Richardson (8) formulates the general motion of a system as follows:

$$[[M] - [M_1]] \frac{d^2\{U\}}{d\tau^2} + [K_s]\{U\} = \overline{V}^2 \int_o^\tau [A(\tau - \tau_o)] \frac{d\{U(\tau)\}}{d\tau_o} d\tau_o \quad 3\text{-}3$$

where the matrix $A(\tau)$ is the indicial aerodynamic matrix, and is related to the aerodynamic damping matrix D_a, the aerodynamic stiffness matrix K_a, and the aerodynamic inertia matrix M_1. The indicial aerodynamic matrix $A(\tau)$ is approximated by a power series expansion which was a main point by Richardson in this approach.

The solution of equation (3-3) by Richardson results in m coefficients of the matrices D_a and K_a, which represent the unsteady state of the growth of lift functions for an airplane travelling at speed V in air or the coefficients resulting from unsteady aerodynamic forces. The solution of equation (3-3) results in $n(m + 1)$ roots instead of the usual n complex roots corresponding to n degrees of freedom encountered in the American and British methods. The n roots represent the usual decayed oscillations and the nm roots are negative real roots representing exponential decays. The Richardson method, like the British and American methods, gives accurate critical airspeeds for the same basic data, but below the critical airspeed

the British and American methods are not as accurate as the Richardson method for computation of the decay rate. Of the three methods the American method must be considered the simplest to use for prediction of the flutter velocity.

Others that have recently worked with flutter are Hassig (3) and Phoa (7). Hassig applies a determinant iteration method to the British method of solution. In his formulation of the flutter equation he includes transfer functions for application to hydraulic controls and automatic controls systems. The method is an iterative automatic search procedure for the flutter velocity. Phoa uses Nyquisit's technique for his computerized technique. His approach shows the applicability to systems which include feedback control systems. Although automated, the method is also an iterative procedure.

Statement of the Problem

Although automated techniques (Hassig, Phoa) have been applied to the various methods of flutter calculation, these methods are iterative procedures that could be time consuming and therefore, costly. Hassig's determinant method, however, must be considered as a more direct method of solution than the method used by Phoa.

It is the objective of the author, not to extend the theory of flutter, but to find a direct method of solution for the flutter velocity that is fast and simple, and apply this method to the optimization of a cantilevered box beam for minimum mass due to a flutter velocity constraint.

Rudisill and Bhatia (11) have derived the second derivatives of the flutter velocity from the basic flutter equation (2-14). From their work and this formulation of the flutter equation (2-14) the first and second derivatives of the eigenvalues with respect to the reduced frequency ($d\lambda_j/dk$, $d^2\lambda_j/dk^2$) can easily be derived. With these derivatives it is the objective of the author to apply a curve fitting technique for which the flutter velocity could be found directly and simply. The expressions for the first and second derivatives of the eigenvalues with respect to the reduced frequency could simply be written down, but the author believes that some of the understanding and difficulty would be taken from the problem. Therefore, these expressions are derived in the following chapter.

CHAPTER IV

FIRST AND SECOND DERIVATIVES OF THE EIGENVALUES

In Chapter II it was seen that the fundamental flutter equation was written as,

$$[[K] - \lambda([M] + c[A])]\{U\} = 0 \qquad 2\text{-}15$$

For future derivation equation (2-15) will be written as,

$$[[K] - \lambda_j([M] + [A])]\{U_j\} = 0 \qquad 4\text{-}1$$

where the notation [A] has replaced c[A] since $c = \rho b^4 L$ is a constant coefficient of matrix A. The subscript j indicates there will be n eigenvalues λ_j and n corresponding eigenvectors U_j for a single solution of the flutter equation (4-1) where n is the order of matrices K, M, and A.

From equation (4-1) it is seen that $[[K] - \lambda_j([M] + [A])]$ is actually a composite matrix of the stiffness, mass, and air force matrices. Transposing this matrix yields

$$[[K] - \lambda_j([M] + [A])]^T = [[K]^T - \lambda_j([M]^T + [A]^T)] \qquad 4\text{-}2$$

Since the stiffness and mass matrices are symmetric,

$$[K]^T = [K] \text{ and } [M]^T = [M].$$

The resulting eigenvectors from the transposed matrix (4-2) will be denoted as V_j. The flutter equation may now be written as,

$$[[K] - \lambda_j([M] + [A]^T)]\{V_j\} = 0$$

Transposing this equation gives,

$$\{V_j\}^T[[K] - \lambda_j([M] + [A])] = 0 \qquad 4\text{-}3$$

For a linearly elastic structure such as the box beam, the displacement at a node δ_i can be related to the applied forces by the following relation,

$$\delta_i = c_{i1}F_1 + c_{i2}F_2 + \ldots + c_{in}F_n \qquad 4\text{-}4$$

The coefficients c_{in} are known as the deflection influence coefficients. In matrix notation equation (4-4) becomes

$$\{\delta\} = [C]\{F\} \qquad 4\text{-}5$$

Matrix C is known as the matrix of deflection influence coefficients or is many times referred to as the overall structure flexibility matrix. If the inverse of matrix C exists then the applied forces may be found in terms of the displacements. In matrix equation form this becomes

$$\{F\} = [C]^{-1}\{\delta\} \qquad 4\text{-}6$$

If $[C]^{-1}$ exists then $[C]^{-1} = [K]$ is the stiffness matrix. This relation is also true for the flutter equation (4-1).

Premultiplying equation (4-1) by the flexibility matrix C yields,

$$[[I] - \lambda_j[C]([M] + [A])]\{U_j\} = 0 \qquad 4\text{-}7$$

In order to get equation (4-7) in a form used for later differentiation define,

$$\bar{\lambda}_j = 1/\lambda_j = 1/\omega^2 \qquad 4\text{-}8$$

Multiplying equation (4-7) by $-\bar{\lambda}_j$ yields,

$$[-\bar{\lambda}_j[I] + [C]([M] + [A])]\{U_j\} = 0 \qquad 4\text{-}9$$

Rearranging the terms of equation (4-9) yields,

$$[[C]([M] + [A]) - \bar{\lambda}_j [I]]\{U_j\} = 0 \qquad 4\text{-}10$$

which will be the form of the flutter equation to be differentiated. For digital computational purposes this formulation of the flutter equation was found to be the fastest and the simplest. Thus, the following equation develops from equation (4-10),

$$\{V_j\}^T[[C]([M] + [A]) - \bar{\lambda}_j [I]] = 0 \qquad 4\text{-}11$$

With reference to equation (4-11) let

$$[F_j] = [[C]([M] + [A]) - \bar{\lambda}_j [I]] \qquad 4\text{-}12$$

From equation (4-12) the flutter equation may be written as

$$[F_j]\{U_j\} = 0 \qquad 4\text{-}13$$

and

$$\{V_j\}^T[F_j] = 0 \qquad 4\text{-}14$$

Differentiating equation (4-13) with respect to the reduced frequency k the resulting equation is,

$$\frac{d[F_j]}{dk}\{U_j\} + [F_j]\frac{d\{U_j\}}{dk} = 0 \qquad 4\text{-}15$$

Premultiplying equation (4-15) by $\{V_j\}^T$ yields

$$\{V_j\}^T\frac{d[F_j]}{dk}\{U_j\} + \{V_j\}^T[F_j]\frac{d\{U_j\}}{dk} = 0 \qquad 4\text{-}16$$

From equation (4-14) it is seen that the second term of equation (4-16) vanishes. The result is,

$$\{V_j\}^T\frac{d[F_j]}{dk}\{U_j\} = 0 \qquad 4\text{-}17$$

The flexibility matrix C and the inertia matrix M are functions of the variable parameters only and not the reduced frequency k. The air force matrix A and the eigenvalues $\overline{\lambda_j}$ are however functions of the reduced frequency. Differentiation of equation (4-12) with respect to the reduced frequency k will therefore yield

$$d[F_j]/dk = [C] \frac{d[A]}{dk} - \frac{d\overline{\lambda_j}}{dk} [I] \qquad 4\text{-}18$$

Substituting this result into equation (4-17), the following result is obtained,

$$\{V_j\}^T[C] \frac{d[A]}{dk} \{U_j\} - \{V_j\}^T \frac{d\lambda_j}{dk} [I] \{U_j\} = 0 \qquad 4\text{-}19$$

Solving equation (4-19) for the first derivative of the eigenvalues with respect to the reduced frequency, $\frac{d\overline{\lambda_j}}{dk}$, gives

$$\frac{d\lambda_j}{dk} = \frac{\{V_j\}^T[C] \frac{d[A]}{dk} \{U_j\}}{\{V_j\}^T[I]\{U_j\}} \qquad 4\text{-}20$$

Since $\{V_j\}^T[I]\{U_j\} = \{V_j\}^T\{U_j\}$, equation (4-20) may be rewritten as

$$\frac{d\lambda_j}{dk} = \frac{\{V_j\}^T[C] \frac{d[A]}{dk} \{U_j\}}{\{V_j\}^T\{U_j\}} \qquad 4\text{-}21$$

The expression for the first derivative may further be simplified by making the associated row vector V_j^T orthonormal with respect to the eigenvectors U_j or

$$\{\overline{V}_j\}^T\{U_j\} = 1 \qquad 4\text{-}22$$

where $\{\overline{V}_j\}^T$ is orthonormal. The orthonormalization will be explained in the following manipulations.

Consider the following equations,

$$\{V_j\}^T[[C]([M] + [A]) - \overline{\lambda_j}\,[I]] = 0 \qquad 4\text{-}23$$

and

$$[[C]([M] + [A]) - \overline{\lambda_i}\,[I]]\{U_j\} = 0 \qquad 4\text{-}24$$

where $\overline{\lambda}_j$ and $\overline{\lambda}_i$ are eigenvalues of the respective equations. Post-multiplying equation (4-23) by $\{U_i\}$ and premultiplying equation (4-24) by $\{V_j\}^T$ yields,

$$\{V_j\}^T[[C]([M] + [A]) - \overline{\lambda}_j[I]]\{U_i\} = 0 \qquad 4\text{-}25$$

$$\{V_j\}^T[[C]([M] + [A]) - \overline{\lambda}_i[I]]\{U_i\} = 0 \qquad 4\text{-}26$$

Subtracting equation (4-25 from equation (4-26),

$$\{V_j\}^T(\overline{\lambda}_j - \overline{\lambda}_i)[I]\{U_i\} = 0 \qquad 4\text{-}27$$

is obtained. From equation (4-27) if $\overline{\lambda}_j$ and $\overline{\lambda}_i$ are distinct ($i \neq j$), then

$$\{V_j\}^T\{U_i\} = 0 \qquad 4\text{-}28$$

If $\overline{\lambda}_i = \overline{\lambda}_j$ then for the nontrivial solution

$$\{V_j\}^T\{U_j\} = d \qquad 4\text{-}29$$

where d is a constant. Dividing both sides of equation (4-29) by d yields,

$$\{\overline{V}_j\}^T\{U_j\} = 1 \qquad 4\text{-}30$$

where $\bar{V}_j^T$ is the orthonormal associated row vector of $\{U_j\}$ with respect to $\{U_j\}$. Using this result and applying it to equation (4-21) the first derivative of the eigenvalues with respect to the reduced frequency becomes,

$$\frac{d\bar{\lambda}_j}{dk} = \{\bar{V}_j\}^T[C]\frac{d[A]}{dk}\{U_j\} \qquad 4\text{-}31$$

Second Derivative of the Eigenvalue With Respect to the Reduced Frequency

The starting point for the second derivative will be equation (4-15) which is,

$$\frac{d[F_j]}{dk}\{U_j\} + [F_j]\frac{d\{U_j\}}{dk} = 0 \qquad 4\text{-}15$$

Differentiating equation (4-15) with respect to the reduced frequency k,

$$\frac{d^2[F_j]}{dk^2}\{U_j\} + \frac{d[F_j]}{dk}\frac{d\{U_j\}}{dk} + \frac{d[F_j]}{dk}\frac{d\{U_j\}}{dk} + [F_j]\frac{d^2\{U_j\}}{dk^2} = 0 \qquad 4\text{-}32$$

is obtained. Premultiplying equation (4-32) by $\{\bar{V}_j\}^T$ yields,

$$\{\bar{V}_j\}^T\frac{d^2[F_j]}{dk^2}\{U_j\} + \{\bar{V}_j\}^T\frac{d[F_j]}{dk}\frac{d\{U_j\}}{dk} + \{\bar{V}_j\}^T\frac{d[F_j]}{dk}\frac{d\{U_j\}}{dk}$$

$$+ \{\bar{V}_j\}^T[F_j]\frac{d^2\{U_j\}}{dk^2} = 0 \qquad 4\text{-}33$$

It was previously shown from equation (4-14) that

$$\{V_j\}^T[F_j] = 0 \qquad 4\text{-}14$$

It is therefore also true that,

$$\{\bar{V}_j\}^T[F_j] = 0 \qquad 4\text{-}34$$

Grouping terms and using equation (4-34), equation (4-33) reduces to the following,

$$\{\bar{V}_j\}^T \frac{d^2[F_j]}{dk^2}\{U_j\} + 2\{\bar{V}_j\}^T \frac{d[F_j]}{dk}\frac{d\{U_j\}}{dk} = 0 \qquad 4\text{-}35$$

F_j was defined as;

$$[F_j] = [[C]([M] + [A]) - \bar{\lambda}_j[I]] \qquad 4\text{-}12$$

Differentiating F_j with respect to the reduced frequency k, yields,

$$\frac{d[F_j]}{dk} = [C]\frac{d[A]}{dk} - \frac{d\bar{\lambda}_j}{dk}[I] \qquad 4\text{-}36$$

and

$$\frac{d^2[F_j]}{dk^2} = [C]\frac{d^2[A]}{dk^2} - \frac{d^2\bar{\lambda}_j}{dk^2}[I] \qquad 4\text{-}37$$

Substituting $d[F_j]/dk$ and $d^2[F_j]/dk^2$ into equation (4-35) yields,

$$\{\bar{V}_j\}^T[[C]\frac{d^2[A]}{dk^2} - \frac{d^2\bar{\lambda}_j}{dk^2}[I]]\{U_j\} + 2\{\bar{V}_j\}^T[[C]\frac{d[A]}{dk} - \frac{d\bar{\lambda}_j}{dk}[I]]\frac{d\{U_j\}}{dk} = 0 \qquad 4\text{-}38$$

Solving equation (4-38) for $d^2\bar{\lambda}_j/dk^2$, the resulting expression is,

$$\frac{d^2\bar{\lambda}_j}{dk^2} = \frac{2\{\bar{V}_j\}^T[[C]\frac{d[A]}{dk} - \frac{d\bar{\lambda}_j}{dk}[I]]\frac{d\{U_j\}}{dk} + \{\bar{V}_j\}^T[C]\frac{d^2[A]}{dk}\{U_j\}}{\{\bar{V}_j\}^T[I]\{U_j\}} \qquad 4\text{-}39$$

Since the denominator is unity the expression for the second derivative becomes,

$$\frac{d^2\bar{\lambda}_j}{dk^2} = 2\{\bar{V}_j\}^T[[C]\frac{d[A]}{dk} - \frac{d\bar{\lambda}_j}{dk}[I]]\frac{d\{U_j\}}{dk} + \{\bar{V}_j\}^T[C]\frac{d^2[A]}{dk^2}\{U_j\} \qquad 4\text{-}40$$

The only unknown of equation (4-40) is $d\{U_j\}/dk$, which may be written as a linear combination of vectors U_h,

$$\frac{d\{U_j\}}{dk} = \sum_{h=1}^{n} a_{jkh}\{U_h\} \qquad 4\text{-}41$$

where a_{jkh} is a scalar quantity and U_h are eigenvectors of the n eigenvectors which form a complete set of vectors in a n vector space. Substitution of equation (4-41) into equation (4-15) yields,

$$\frac{d[F_j]}{dk}\{U_j\} + [F_j]\sum_{h=1}^{n} a_{jkh}\{U_h\} = 0 \qquad 4\text{-}42$$

Premultiplying equation (4-42) by $\{\bar{V}_i\}^T$ where $i \neq j$ yields,

$$\{\bar{V}_i\}^T\frac{d[F_j]}{dk}\{U_j\} + \{\bar{V}_i\}^T[F_j]\sum_{h=1}^{n} a_{jkh}\{U_h\} = 0 \qquad 4\text{-}43$$

From equation (4-43)

$$\{\bar{V}_i\}^T[F_j] = \{\bar{V}_i\}^T[[C]([M] + [A]) - \bar{\lambda}_j[I]] \qquad 4\text{-}44$$

is obtained. Postmultiplication by $\{U_h\}$ yields,

$$\{\bar{V}_i\}^T[F_j]\{U_h\} = \{\bar{V}_i\}^T[[C]([M] + [A]) - \bar{\lambda}_j[I]]\{U_h\} \qquad 4\text{-}45$$

From the basic flutter equation (4-10) the following relation may be written,

$$[[C]([M] + [A])]\{U_j\} = \bar{\lambda}_j[I]\{U_j\} \qquad 4\text{-}46$$

Premultiplication by $\{\bar{V}_j\}^T$ of equation (4-46) yields,

$$\{\bar{V}_j\}^T[[C]([M] + [A])]\{U_j\} = \{V_j\}^T\bar{\lambda}_j[I]\{U_j\}, \qquad 4\text{-}47$$

but the quantity on the right side of equation (4-47) yields,

$$\{\bar{V}_j\}^T\bar{\lambda}_j[I]\{U_j\} = \bar{\lambda}_j$$

from the orthonormality of $\{\bar{V}_j\}^T$ with respect to $\{U_j\}$. Thus, it is seen that,

$$\{\bar{V}_j\}^T[[C]([M] + [A]) - \bar{\lambda}_i[I]]\{U_j\} = \{\bar{V}_j\}^T[[C]([M] + [A])]\{U_j\} - \{\bar{V}_j\}^T\bar{\lambda}_i[I]\{U_j\} \qquad 4\text{-}48$$

or,

$$\{\bar{V}_j\}^T[F_i]\{U_j\} = \bar{\lambda}_j - \bar{\lambda}_i \qquad 4\text{-}49$$

Applying the above relation to equation (4-43) gives

$$\{\bar{V}_i\}^T \frac{d[F_j]}{dk}\{U_j\} + a_{jki}(\bar{\lambda}_i - \bar{\lambda}_j) = 0$$

for $h = i$, since $\{\bar{V}_i\}^T[F_j]\{U_h\} = 0$ for $h \neq i$. Solving for a_{jki} yields,

$$a_{jki} = \frac{-\{\bar{V}_i\}^T \frac{d[F_j]}{dk}\{U_j\}}{\bar{\lambda}_i - \bar{\lambda}_j} \qquad 4\text{-}50$$

where $i \neq j$. The following relations are shown to give the case when $i = j$ or the expression for a_{jkj}, even though these coefficients will be seen to vanish in later derivations.

It was shown previously in equation (4-30) that $\{\bar{V}_j\}^T\{U_j\} = 1$. It can also be shown in a similar manner that $\{U_j\}$ can be normalized so that

$$\{U_j\}^T\{U_j\} = 1, \tag{4-51}$$

and that

$$\{U_j\}^T\{U_h\} = \text{constant} = b_{jh}. \tag{4-52}$$

Differentiating equation (4-51) with respect to the reduced frequency k yields,

$$\frac{d\{U_j\}^T}{dk}\{U_j\} + \{U_j\}^T\frac{d\{U_j\}}{dk} = 0 \tag{4-53}$$

From equation (4-41) it was seen that $d\{U_j\}/dk$ could be written as linear combination of vectors $\{U_h\}$, thus the following relation for $d\{U_j\}^T/dk$ is,

$$\frac{d\{U_j\}^T}{dk} = \sum_{h=1}^{n} a_{jkh}\{U_h\}^T \tag{4-54}$$

Substituting equations (4-41) and (4-54) into equation (4-53) yields,

$$\sum_{h=1}^{n} a_{jkh}\{U_h\}^T\{U_j\} + \sum_{h=1}^{n} a_{jkh}\{U_j\}^T\{U_h\} = 0 \tag{4-55}$$

Factoring out the a_{jkj} coefficients from this equation the result is

$$\sum_{\substack{h=1\\h\neq j}}^{n} a_{jkh}\{U_h\}^T\{U_j\} + \sum_{\substack{h=1\\h\neq j}}^{n} a_{jkh}\{U_j\}^T\{U_h\} + 2a_{jkj} = 0 \tag{4-56}$$

Since $\{U_h\}^T\{U_j\} = b_{hj}$ and $\{U_j\}^T\{U_h\} = b_{jh}$, the expression for a_{jkj} is,

$$a_{jkj} = -\frac{1}{2}\left(\sum_{\substack{h=1\\h\neq j}}^{n} a_{jkh}(b_{hj} + b_{jh})\right) \tag{4-57}$$

The second derivative of the eigenvalues with respect to the reduced frequency was expressed as,

$$\frac{d^2\bar{\lambda}_j}{dk^2} = 2\{\bar{V}_j\}^T[[C]\frac{d[A]}{dk} - \frac{d\bar{\lambda}_j}{dk}[I]]\frac{d\{U_j\}}{dk} + \{\bar{V}_j\}^T[C]\frac{d^2[A]}{dk^2}\{U_j\} \qquad 4\text{-}40$$

Let us focus attention to the terms containing $\frac{d\{U_j\}}{dk}$ of equation (4-40),

$$2\{\bar{V}_j\}^T[[C]\frac{d[A]}{dk} - \frac{d\bar{\lambda}_j}{dk}[I]]\frac{d\{U_j\}}{dk} = 2\{\bar{V}_j\}^T\frac{d[F_j]}{dk}\frac{d\{U_j\}}{dk} \qquad 4\text{-}62$$

Substitution of the expression for the first derivative of the eigenvalues with respect to the reduced frequency into equation (4-62) yields,

$$2\{\bar{V}_j\}^T\frac{d[F_j]}{dk}\frac{d\{U_j\}}{dk} = 2\{\bar{V}_j\}^T[[C]\frac{d[A]}{dk} - \{\bar{V}_j\}^T[C]\frac{d[A]}{dk}\{U_j\}[I]]\frac{d\{U_j\}}{dk} \qquad 4\text{-}63$$

where $\{\bar{V}_j\}^T[C]\frac{d[A]}{dk}\{U_j\}$ is a scalar.

Since $\{\bar{V}_j\}^T[C]\frac{d[A]}{dk}\{U_j\}$ is a scalar, equation (4-63) may be written as

$$2\{\bar{V}_j\}^T\frac{d[F_j]}{dk}\frac{d\{U_j\}}{dk} = 2\{\bar{V}_j\}^T[C]\frac{d[A]}{dk}\{\frac{d\{U_j\}}{dk}\cdot 1 - \{U_j\}\{\bar{V}_j\}^T\frac{d\{U_j\}}{dk}\} \qquad 4\text{-}64$$

It was shown previously that $\{\bar{V}_j\}^T\{U_j\} = 1$ from equation (4-30).

Taking the transpose of equation (4-30) yields

$$\{U_j\}^T\{\bar{V}_j\} = 1 \qquad 4\text{-}65$$

It is also, therefore, true that,

$$\{\bar{V}_j\}^T\frac{d\{U_j\}}{dk} = \frac{d\{U_j\}^T}{dk}\{\bar{V}_j\} \qquad 4\text{-}66$$

With this result $\frac{d\{U_j\}}{dk}$ may be written as

$$\frac{d\{U_j\}}{dk} = \sum_{\substack{h=1 \\ h\neq j}}^{n} a_{jkh}\{U_h\} + a_{jkj}\{U_j\} \qquad 4\text{-}58$$

or substituting the expressions for a_{jkh} and a_{jkj} yields,

$$\frac{d\{U_j\}}{dk} = -\sum_{\substack{h=1 \\ h\neq j}}^{n} \frac{\{\bar{V}_h\}^T \frac{d[F_j]}{dk}\{U_j\}\{U_h\}}{\bar{\lambda}_h - \bar{\lambda}_j} - \frac{1}{2}\left(\sum_{\substack{h=1 \\ h\neq j}}^{n} a_{jkh}(b_{hj} + b_{jh})\right)\{U_j\} \qquad 4\text{-}59$$

In a similar manner $\frac{d\{U_j\}^T}{dk}$ may be written as,

$$\frac{d\{U_j\}^T}{dk} = -\sum_{\substack{h=1 \\ h\neq j}}^{n} \frac{\{\bar{V}_h\}^T \frac{d[F_j]}{dk}\{U_j\}^T\{U_h\}^T}{\bar{\lambda}_h - \bar{\lambda}_j} - \frac{1}{2}\left(\sum_{\substack{h=1 \\ h\neq j}}^{n} a_{jkh}(b_{hj} + b_{jh})\right)\{U_j\}^T. \qquad 4\text{-}60$$

Postmultiplying equation (4-59) by $\{U_j\}^T$ and premultiplying equation (4-60) by $\{U_j\}$ and subtracting the two equations the result is,

$$\frac{d\{U_j\}}{dk}\{U_j\}^T - \{U_j\}\frac{d\{U_j\}^T}{dk} = -\sum_{\substack{h=1 \\ h\neq j}}^{n} \frac{\{\bar{V}_h\}^T \frac{d[F_j]}{dk}\{U_j\}\{U_h\}\{U_j\}^T}{\bar{\lambda}_h - \bar{\lambda}_j} \qquad 4\text{-}61$$

$$+ \sum_{\substack{h=1 \\ h\neq j}}^{n} \frac{\{\bar{V}_h\}^T \frac{d[F_j]}{dk}\{U_j\}\{U_j\}^T\{U_h\}^T}{\bar{\lambda}_h - \bar{\lambda}_j}$$

From equation (4-61) it is seen that the coefficients a_{jkj} have vanished from further manipulations.

Substitution of $\{U_j\}^T\{\bar{V}_j\}$ for "1" and the expression for $\{\bar{V}_j\}^T d\{U_j\}/dk$, equation (4-64) becomes,

$$2\{\bar{V}_j\}^T\frac{d[F_j]}{dk}\frac{d\{U_j\}}{dk} = 2\{\bar{V}_j\}^T[C]\frac{d[A]}{dk}\{\frac{d\{U_j\}}{dk}\{U_j\}^T\{\bar{V}_j\} - \{U_j\}\frac{d\{U_j\}^T}{dk}\{\bar{V}_j\}\} \qquad 4\text{-}67$$

Factoring out $\{\bar{V}_j\}$, equation (4-67) may be written as,

$$2\{\bar{V}_j\}^T\frac{d[F_j]}{dk}\frac{d\{U_j\}}{dk} = 2\{\bar{V}_j\}^T[C]\frac{d[A]}{dk}\{\frac{d\{U_j\}}{dk}\{U_j\}^T - \{U_j\}\frac{d\{U_j\}^T}{dk}\}\{\bar{V}_j\} \qquad 4\text{-}68$$

Equation (4-61) gives the expression for $\{\frac{d\{U_j\}}{dk}\{U_j\}^T - \{U_j\}\frac{d\{U_j\}^T}{dk}\}$. Substitution of this equation into equation (4-68) yields,

$$2\{\bar{V}_j\}^T\frac{d[F_j]}{dk}\frac{d\{U_j\}}{dk} = 2\{\bar{V}_j\}^T[C]\frac{d[A]}{dk}\{-\sum_{\substack{h=1\\h\neq j}}^{n}\frac{\{\bar{V}_h\}^T\frac{d[F_j]}{dk}\{U_j\}\{U_h\}\{U_j\}^T}{\bar{\lambda}_h - \bar{\lambda}_j} + \sum_{\substack{h=1\\h\neq j}}^{n}\frac{\{V_h\}^T\frac{d[F_j]}{dk}\{U_j\}\{U_j\}^T\{U_h\}^T}{\bar{\lambda}_h - \bar{\lambda}_j}\}\{\bar{V}_j\} \qquad 4\text{-}69$$

It was previously shown that $\{\bar{V}_j\}^T\{U_i\} = 0$, where $i \neq j$. Thus

$$\{U_h\}^T\{\bar{V}_j\} = 0 \qquad 4\text{-}70$$

where $h \neq j$. Equation (4-70) causes the second term of equation (4-69) to vanish. The resulting equation is,

$$2\{\bar{V}_j\}^T\frac{d[F_j]}{dk}\frac{d\{U_j\}}{dk} = 2\{\bar{V}_j\}^T[C]\frac{d[A]}{dk}\{-\sum_{\substack{h=1\\h\neq j}}^{n}\frac{\{\bar{V}_h\}^T\frac{d[F_j]}{dk}\{U_j\}\{U_h\}}{\bar{\lambda}_h - \bar{\lambda}_j}\} \qquad 4\text{-}71$$

From equation (4-18) it can be shown that,

$$\{\bar{V}_h\}^T \frac{d[F_j]}{dk} \{U_j\} = \{\bar{V}_h\}^T [C] \frac{d[A]}{dk} \{U_j\} \qquad 4\text{-}72$$

From the result of equation (4-72), equation (4-71) may be written as,

$$2\{\bar{V}_j\}^T \frac{d[F_j]}{dk} \frac{d\{U_j\}}{dk} = 2 \sum_{\substack{h=1 \\ h\neq j}}^{n} \frac{(\{\bar{V}_j\}^T [C] \frac{d[A]}{dk} \{U_h\})(\{\bar{V}_h\}^T [C] \frac{d[A]}{dk} \{U_j\})}{\bar{\lambda}_j - \bar{\lambda}_h} \qquad 4\text{-}73$$

Substitution of equation (4-73) into equation (4-40) yields the expression for the second derivative of the eigenvalue with respect to the reduced frequency as,

$$\frac{d^2\bar{\lambda}_j}{dk^2} = \{\bar{V}_j\}^T [C] \frac{d^2[A]}{dk^2} \{U_j\} + 2 \sum_{\substack{h=1 \\ h\neq j}}^{n} \frac{(\{\bar{V}_j\}^T [C] \frac{d[A]}{dk} \{U_h\})(\{\bar{V}_h\}^T [C] \frac{d[A]}{dk} \{U_j\})}{\bar{\lambda}_j - \bar{\lambda}_h} \qquad 4\text{-}74$$

The following chapter explains the author's method of finding the critical flutter velocity. Without the first and second derivatives of the eigenvalues with respect to the reduced frequency the method used would be impossible.

CHAPTER V

A COMPUTERIZED CURVE FITTING FLUTTER ANALYSIS

From Chapter IV it was seen that the flutter equation could be written as,

$$[[C]([M] + [A]) - \bar{\lambda}_j[I]]\{U_j\} = 0 \qquad 4\text{-}10$$

where C, M, and A were defined as the flexibility, inertia, and air force matrices, respectively. $\{U_j\}$ were defined as the eigenvectors or a column vector of generalized coordinates. The solution of equation (4-10) for an assumed value of the reduced frequency k yielded j complex eigenvalues of the form

$$\bar{\lambda}_j = 1/\lambda_j = \chi_j + \psi_j i \qquad 5\text{-}1$$

where $\chi_j = \frac{1}{\omega_j^2}$, $i = (-1)^{1/2}$, and ψ_j represents the imaginary part of the eigenvalue. The values of ψ_j are labeled in descending order of χ_j. Each j subscript corresponds to a mode of oscillation.

The eigenvalues $\bar{\lambda}_j$ are a function of the reduced frequency k, which is a function of the semichord b, the circular frequency of oscillation ω, and the velocity V by the relation,

$$\frac{k}{b} = \frac{\omega}{V} .$$

The eigenvalues can then be said to be a function of b/k or V/ω. If the imaginary part of the eigenvalues ψ_j are plotted against ν_j, where $\nu_j = V_j/\omega_j$ a set of typical curves might like the curves of Figures 5 and 6. Figure 7 gives a representation of a set of typical χ_j curves. It is seen from Figures 5 and 6 that modes 2, 4, and 6

produce ψ_j curves that cross the ν axis. At these points where $\bar{\lambda}_j$ is pure real or ψ_j is zero, flutter will occur. The lowest velocity corresponding to a pure real $\bar{\lambda}_j$ will be the critical flutter velocity for the system, where the flutter velocity is computed from the relation,

$$V_f = (\chi_j)^{-1/2} \nu_j \qquad 5\text{-}2$$

From a structural synthesis point of view it is computationally inefficient to make plots of ψ_j versus ν_j for each flutter analysis. Instead of using the plotting procedure, the crossings of ψ_j may be approximated by fitting cubic or quadratic equations to ψ_j from computed values of ψ_j, $d\psi_j/d\nu$, and $d^2\psi_j/d^2\nu$. The first and second derivatives of the eigenvalues with respect to the reduced frequency were derived in Chapter IV. In order to use the curve fitting technique, the first and second derivatives of the eigenvalues with respect to ν must be derived.

Let $D = b/k$, where b is the reference semichord and k is the reduced frequency. Then,

$$dD = -\frac{b}{k^2}\, dk \qquad 5\text{-}3$$

or,

$$\frac{d(\frac{b}{k})}{dk} = -\frac{b}{k^2} \qquad 5\text{-}4$$

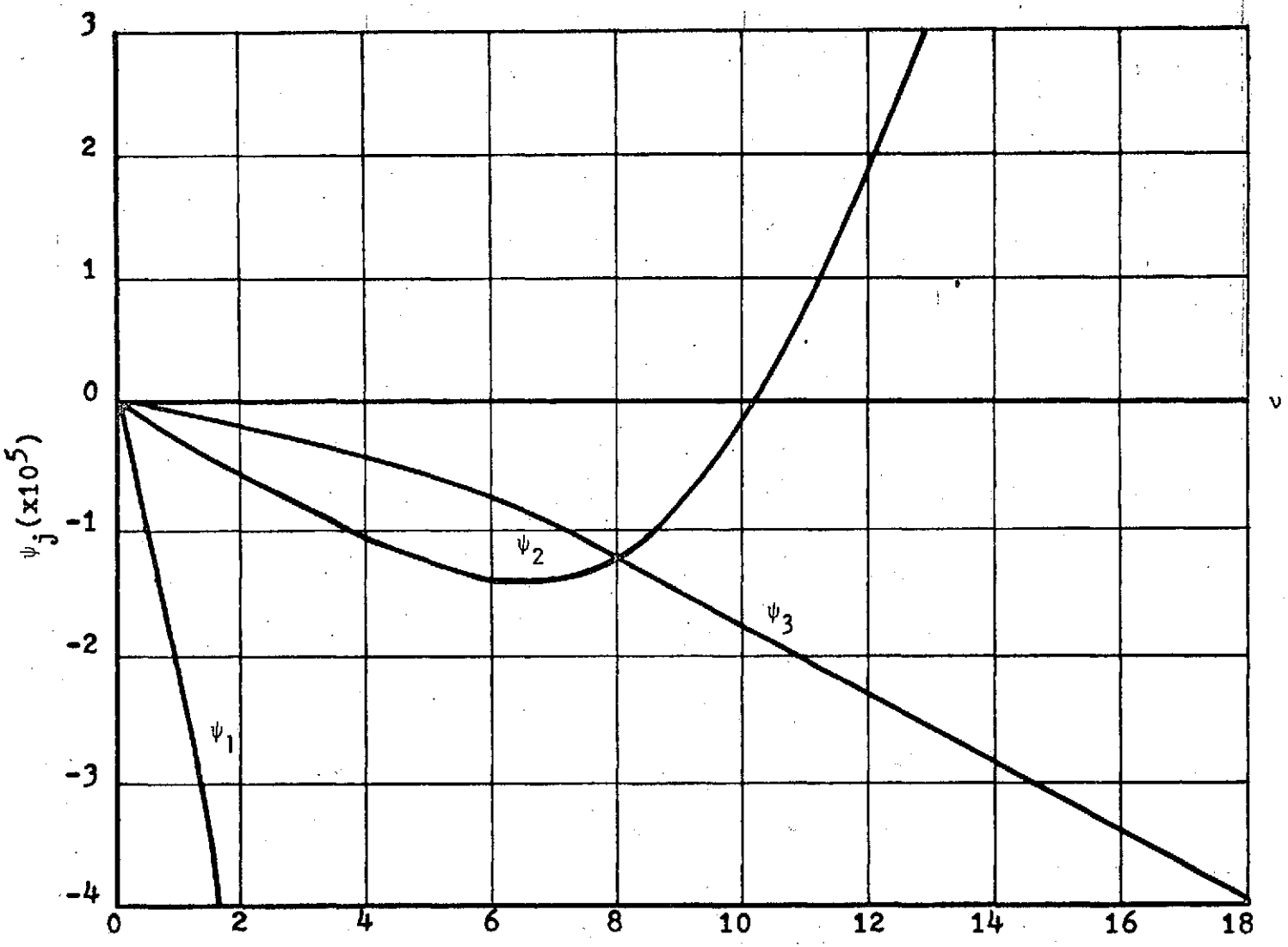

Figure 5. Imaginary Part of the Eigenvalues, Modes 1, 2, 3.

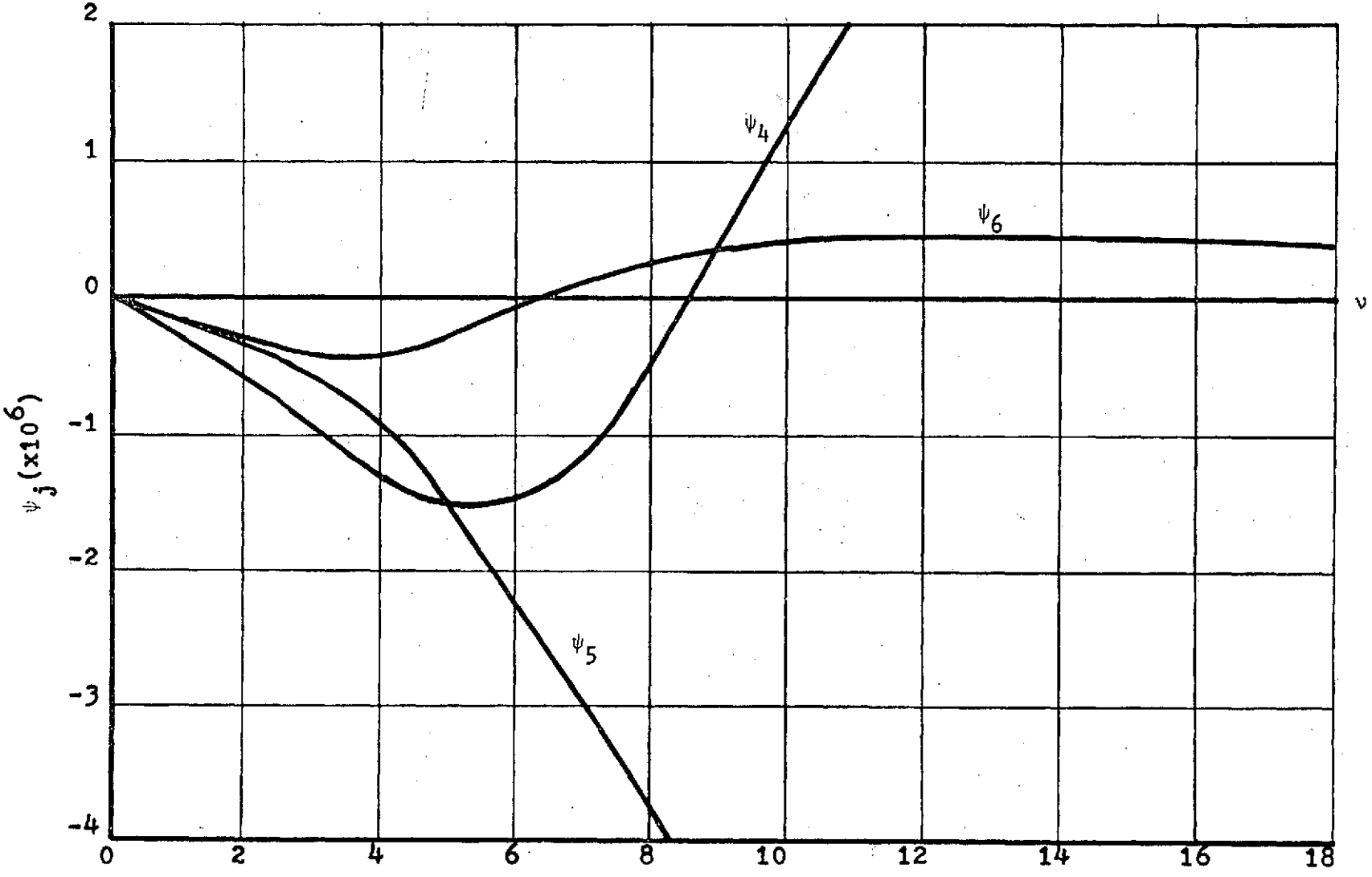

Figure 6. Imaginary Part of the Eigenvalues, Modes 4, 5, 6.

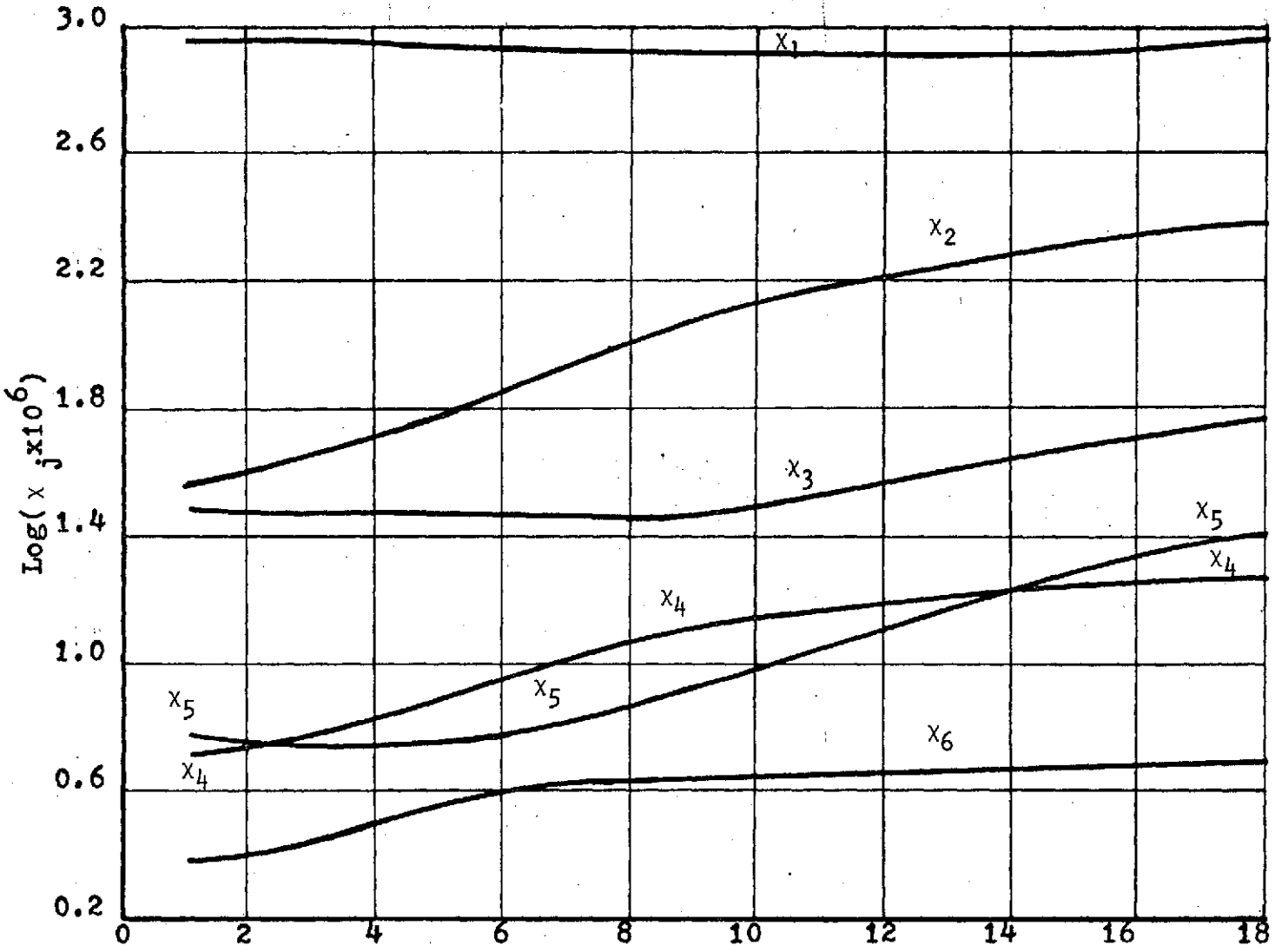

Figure 7. Real Part of the Eigenvalues, Modes 1-6.

The first derivative of the eigenvalue with respect to b/k may be expressed as,

$$\frac{d\bar{\lambda}_j}{d\frac{b}{k}} = \frac{d\bar{\lambda}_j}{dk}\frac{dk}{d\frac{b}{k}} \qquad 5\text{-}5$$

where,

$$\frac{d\bar{\lambda}_j}{dk} = \{\bar{V}_j\}^T[C]\frac{d[A]}{dk}\{U_j\} \qquad 4\text{-}31$$

Since $b/k = V/\omega = v$, the expression for the first derivative of the eigenvalue with respect to v may be written as,

$$\frac{d\bar{\lambda}_j}{dv} = -\frac{k^2}{b}\{\bar{V}_j\}^T[C]\frac{d[A]}{dk}\{U_j\} \qquad 5\text{-}6$$

Differentiating equation (5-5) with respect to b/k yields,

$$\frac{d^2\bar{\lambda}_j}{d(\frac{b}{k})^2} = \frac{d^2\bar{\lambda}_j}{dv^2} = \frac{d^2\bar{\lambda}_j}{dk^2}\left(\frac{dk}{d(\frac{b}{k})}\right)^2 + \frac{d\bar{\lambda}_j}{dk}\frac{d^2k}{d(\frac{b}{k})^2} \qquad 5\text{-}7$$

where $dk/d(b/k) = -k^2/b$ and $d^2k/d(b/k)^2 = 2k^3/b^2$. Substitution of the relations for $d\bar{\lambda}_j/dk$ and $d^2\bar{\lambda}_j/dk^2$ into equation (5-7) yields,

$$\frac{d^2\bar{\lambda}_j}{dv^2} = \frac{2k^3}{b^2}\{\bar{V}_j\}^T[C]\frac{d[A]}{dk}\{U_j\}$$

$$+ \left(-\frac{k^2}{b}\right)^2\{\bar{V}_j\}^T[C]\frac{d^2[A]}{dk^2}\{U_j\}$$

$$+ 2\sum_{\substack{h=1\\h\neq j}}^{n}\frac{\{\bar{V}_j\}^T[C]\frac{d[A]}{dk}\{U_h\}\{\bar{V}_h\}^T[C]\frac{d[A]}{dk}\{U_j\}}{\bar{\lambda}_j - \bar{\lambda}_h} \qquad 5\text{-}8$$

Curve Fitting Technique

The ψ_j curves are approximated by cubic equations of the form,

$$\psi_j = A_j\nu + B_j\nu^2 + C_j\nu^3 \qquad 5\text{-}9$$

The graph of cubic equations (5-9) pass through the origin and the coefficients A_j, B_j, and C_j are evaluated such that the curves of equation (5-9) pass through the points (ν_o, ψ_j^o) and $(\bar{\nu}, \bar{\psi}_j)$. The first derivative of ψ_j with respect to ν is,

$$\frac{d\psi_j}{d\nu} = A_j + 2B_j\nu + 3C_j\nu^2 \qquad 5\text{-}10$$

The curves of equation (5-10) pass through the point $(\nu_o, d\psi_j^o/d\nu)$ where ψ_j^o and $d\psi_j^o/d\nu$ denote values of ψ_j and $d\psi_j/d\nu$ evaluated at $\nu = \nu_o$ respectively, and $\bar{\psi}_j$ denotes ψ_j evaluated at $\bar{\nu} = \nu_o/M$, where M is some large number, say 10 or 100. ν_o is an assumed trial value of ν.

The coefficients A_j, B_j, and C_j are calculated from the following equations,

$$\psi_j^o = A_j\nu_o + B_j\nu_o^2 + C_j\nu_o^3 \qquad 5\text{-}11$$

$$d\psi_j^o/d\nu = A_j + 2B_j\nu_o + 3C_j\nu_o^2 \qquad 5\text{-}12$$

and,

$$\bar{\psi}_j = A_j\bar{\nu} + B_j\bar{\nu}^2 + C_j\bar{\nu}^3 \qquad 5\text{-}13$$

Using Cramer's rule the coefficients of equation (5-9) may be expressed in the forms,

$$A_j = \{\bar{\psi}_j \nu_o^4 + \psi_j^o(2\bar{\nu}^3\nu_o - 3\bar{\nu}^2\nu_o^2) + d\psi_j^o/d\nu(\bar{\nu}^2\nu_o^3 - \bar{\nu}\nu_o^3)\}/D \qquad 5\text{-}14$$

$$B_j = \{-2\bar{\psi}_j \nu_o^3 + \psi_j^o(3\bar{\nu}\nu_o^2 - \bar{\nu}^3) + d\psi_j^o/d\nu(\bar{\nu}^3\nu_o - \bar{\nu}\nu_o^3)\}/D \qquad 5\text{-}15$$

$$C_j = \{\bar{\psi}_j \nu_o^2 + \psi_j^o(\bar{\nu}^2 - 2\bar{\nu}\nu_o) + d\psi_j^o/d\nu(\bar{\nu}\nu_o^2 - \bar{\nu}^2\nu_o)\}/D \qquad 5\text{-}16$$

and,

$$D = \bar{\nu}\nu_o^4 - 2\bar{\nu}^2\nu^3 + \bar{\nu}^3\nu_o^2 \qquad 5\text{-}17$$

Since ψ_j is zero at $\nu = 0$, then the other two crossings of ψ_j may be found by setting ψ_j in equation (5-9) equal to zero, thus

$$A_j + B_j\nu + C_j\nu^2 = 0 \qquad 5\text{-}18$$

From the quadratic formula the roots may be expressed as,

$$\nu = \{-B_j \pm (B_j^2 - 4A_jC_j)^{1/2}\}/2C_j \qquad 5\text{-}19$$

provided C_j is not zero and $(B_j^2 - 4A_jC_j)$ is greater than or equal to zero. If ν from equation (5-19) is not pure real and positive then curve fitting by the use of a quadratic equation of the same form as equation (5-18) may prove successful.

The coefficients (A_j, B_j, C_j) of the quadratic equation,

$$\psi_j = A_j + B_j\nu + C_j\nu^2 \qquad 5\text{-}20$$

are computed for curves which pass through points (ν_o, ψ_j^o) and have first and second derivatives which pass through points $(\nu_o, \frac{d\psi_j^o}{d\nu})$

and $(\nu_o, d^2\psi_j/d\nu^2)$, respectively, may be found from the following equations,

$$\psi_j^o = A_j + B_j\nu_o + C_j\nu_o^2 \qquad 5\text{-}21$$

$$d\psi_j^o/d\nu = B_j + 2C_j\nu_o \qquad \text{and,} \qquad 5\text{-}22$$

$$d^2\psi_j^o/d\nu^2 = 2C_j \qquad 5\text{-}23$$

From equations (5-21) through (5-23) the coefficients may be expressed as,

$$2C_j = d^2\psi_j^o/d\nu^2 \qquad 5\text{-}24$$

$$B_j = d\psi_j^o/d\nu - 2C_j\nu_o \qquad 5\text{-}25$$

and,

$$A_j = \psi_j^o - B_j\nu_o - C_j\nu_o^2 \qquad 5\text{-}26$$

Substitution of these coefficients into equation (5-19) yields the roots of equation (5-20).

If the roots of a mode are not real and positive, then the curve fit for that mode fails. If one of the C_j for the cubic equation is zero then the approximate crossing for that mode may be found by using the Newton-Raphson's method for finding the root, provided $d\psi_j^o/d\nu$ is not also zero, then,

$$\nu = \nu_o - \psi_j^o(d\psi_j^o/d\nu) \qquad 5\text{-}27$$

It was noted previously that the flutter velocity is computed from the relation,

$$V_f = (\chi_j)^{-1/2}\nu_j \qquad 5\text{-}2$$

Since the flutter velocity is computed from the predicted root ν_j, then the flutter velocity will be correct only if the corresponding χ_j value is used. The values of $\chi_j = 1/\omega_j^2$ at the crossings may be estimated from the first three terms of the Taylor expansion of χ_j, then

$$\chi_j = \chi_j^o + (\nu-\nu_o)d\chi_j^o/d\nu + 0.5(\nu-\nu_o)^2 d^2\chi_j^o/d\nu^2 \qquad 5\text{-}28$$

From the cubic and quadratic fit only the positive roots which also have positive slope $d\psi_j/d\nu$ at the crossings, will approximate the lowest flutter velocity.

A simplified flow diagram for the curve fitting flutter analysis is shown in Figure 8. Following Figure 8 it is seen that an initial value of $\nu = \nu_o$, M, and some tolerance ε are assigned. The quantity $\bar{\nu} = \nu_o/M$ is then calculated which will cause the cubic fit to have a negative slope near the origin. The imaginary parts of the eigenvalues $\bar{\psi}_j$ are then computed at $\bar{\nu}$ for all n modes. $V_f = 10^{30}$ and $\nu^* = 0$ are the upper and lower limits of the flutter velocity and the ν value, respectively. It should be noted that each mode of oscillation n is checked for a crossing of ψ_j and a critical velocity is computed for each crossing. The velocities which are computed from the predicted crossings and the approximate value of χ_j (from Taylor's expansion) are compared to find the smallest velocity, which is then set as the new upper limit V_f. The flutter velocity V_f predicted from the initial assumed value ν_o is then compared with the velocity

$$V_o = \nu_o\omega_j^o \qquad 5\text{-}29$$

If the absolute value of $(V_f - V_o)/V_o$ is greater than some small number ε, then the computations are repeated with ν_o set equal to the predicted crossover value of ν^* which corresponds to the lowest critical velocity V_f computed. If a positive crossing with positive slope $d\psi_j/d\nu$ is not predicted then $\nu^* = 0$ will terminate computations. Also if the number of flutter iterations, for which there is no convergence, exceeds some number (e.g. 5), then computations are terminated.

Examples

The data for equation (4-10) were generated for the cantilevered box beam (Figure 9) where the design parameters were those listed in Table III. A digital computer program was written which implemented the flutter velocity solution previously explained.

Case 1 will be considered as the minimum set of parameters (P(I) = PMIN(I)) and Case 2 as the minimum set of parameters times six (P(I) = PMIN(I) x 6). For the minimum set of parameters an initial value of $\nu_o = 1$ was assumed and the program found a flutter velocity of 715.6 feet per second at $\nu = 7.907$ feet per radian, and for ε equal to 0.05. The computations of the flutter velocity were repeated for values of $\nu_o = 2, 3, 4, \ldots, 20$. In each case the program converged to a flutter velocity between 715.6 and 716.3 feet per second. The total time for the twenty flutter velocity calculations was 245.53 seconds or an average of 12.276 seconds per flutter velocity

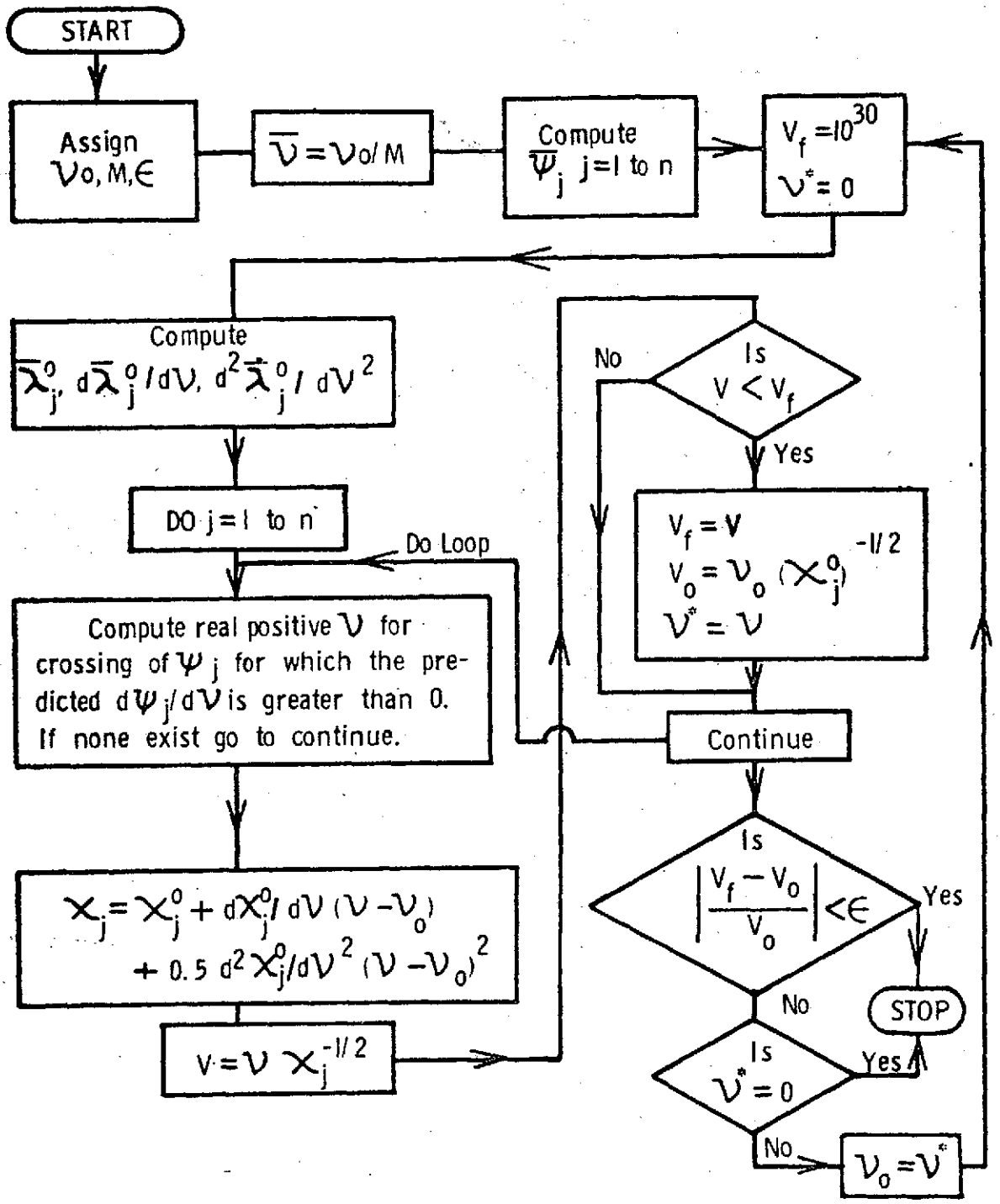

Figure 8. Simplified Flow Diagram for Curve Fitting Analysis.

computation. From Table I it is seen that the maximum number of iterations to find the flutter velocity is five. For initial values of ν_o equal to 7.0 and 8.0 the algorithm converged to an answer in two and one iterations respectively.

The flutter velocity analyses were repeated for design parameters of Case 2 in a similar manner. The total time for twenty flutter calculations was 210.83 seconds, or an average of 10.54 seconds per flutter velocity analysis. From Table II it is seen that for assumed ν_o values of 9, 10, and 11 that the algorithm converged to the answer on the first attempt. The average time for a flutter velocity analysis iteration for Cases1 and 2 was 3.91 seconds. All computations were performed by an IBM 360, Model 50 digital computer.

Figures 12-35 show the actual computed ψ_j versus ν curves and the approximation of each curve as generated from the algorithm. The assumed values of $\nu_o = 5.0$ and $\nu_o = 9.0$ were used for Case 1 and Case 2 respectively. These values (ν_o) were chosen since they lay between the crossings of different modes. Also, individual graphs are shown since in many cases the cubic or quadratic fit would lie on top of the computed curve for the majority of ν values given. Tables V-VII give the numerical values of the plotted curves and the computed airspeed V for the reader to see a numerical comparison between the computed curve and the approximation.

Table I. Convergence for Twenty Assumed Values of ν_o for Case L.

Assumed Value ν_o	Predicted Root ν^*	Predicted Velocity V_f	Predicted Mode n
1.0	9.278	869.2	2
	7.762	701.5	3
	7.907	715.6	2
2.0	6.097	554.2	2
	7.416	659.0	2
	7.911	714.8	2
	7.906	715.6	2
3.0	5.641	500.7	2
	7.089	627.0	2
	7.885	710.2	2
	7.906	715.6	2
4.0	5.952	523.9	2
	7.326	649.7	2
	7.911	714.4	2
	7.906	715.6	2
5.0	6.611	582.3	2
	7.742	692.5	2
	7.908	715.7	2
6.0	7.374	654.1	2
	7.916	715.1	2
	7.906	715.6	2

Assumed Value ν_o	Predicted Root ν^*	Predicted Velocity V_f	Predicted Mode n
7.0	7.886	709.3	2
	7.906	715.6	2
8.0	7.907	715.6	2
9.0	9.000	1328.0	3
	8.006	724.9	2
	7.907	715.6	2
10.0	7.596	689.0	3
	7.915	716.0	2
11.0	7.268	664.5	3
	7.928	715.5	2
	7.906	715.6	2
	7.080	653.7	3
	7.926	713.7	2
	7.906	715.6	2
13.0	7.060	658.7	3
	7.931	723.9	2
	7.906	715.6	2
14.0	7.168	675.4	3
	7.941	715.9	2
	7.906	715.6	2
15.0	7.367	700.3	3
	7.937	717.0	2
	7.906	715.6	2

Assumed Value ν_o	Predicted Root ν^*	Predicted Velocity V_f	Predicted Mode n
16.0	7.628	730.9	3
	7.917	716.3	2
17.0	4.827	471.7	4
	6.569	575.9	2
	7.861	701.5	2
	7.906	715.6	2
18.0	5.009	494.3	4
	6.725	589.6	2
	7.933	709.8	2
	7.906	715.6	2
19.0	5.209	518.8	4
	6.094	605.4	2
	7.979	716.2	2
	7.907	715.6	2
20.0	5.422	544.8	4
	7.099	623.1	2
	7.987	719.2	2
	7.907	715.7	2

Table II. Convergence for Twenty Assumed Values of ν_o for Case 2.

Assumed Value ν_o	Predicted Root ν^*	Predicted Velocity V_f	Predicted Mode n
1.0	33.17	9836.0	5
	4.39	352.4	2
	13.63	1180.0	2
	8.99	793.7	2
	10.15	870.4	2
2.0	7.28	2633.0	5
	10.34	892.2	2
	10.16	870.1	2
3.0	28.96	2126.0	2
	4.28	373.3	2
	13.74	1195.0	2
	8.91	787.7	2
	10.15	870.5	2
4.0	14.63	1270.0	2
	8.04	755.2	2
	10.19	876.7	2
	10.16	870.1	2
5.0	11.94	1049.0	2
	9.95	857.3	2
	10.16	870.1	2

Assumed Value ν_o	Predicted Root ν^*	Predicted Velocity V_f	Predicted Mode n
6.0	10.87	948.9	2
	10.14	868.8	2
7.0	10.38	899.2	2
	10.16	870.0	2
8.0	10.18	876.9	2
	10.16	870.1	2
9.0	10.14	870.2	2
10.0	10.16	870.1	2
11.0	10.12	868.2	2
12.0	9.93	856.0	2
	10.16	870.0	2
13.0	9.47	826.0	2
	10.15	869.8	2
14.0	8.75	774.7	2
	10.14	870.8	2
	10.16	870.1	2
15.0	7.89	708.9	2
	10.17	877.7	2
	10.16	870.1	2
16.0	7.12	644.0	2
	10.28	892.9	2
	10.16	870.1	2

Assumed Value ν_o	Predicted Root ν^*	Predicted Velocity V_f	Predicted Mode n
17.0	6.57	591.9	2
	10.42	911.6	2
	10.16	870.0	2
18.0	6.21	555.2	2
	10.54	927.6	2
	10.15	869.8	2
19.0	6.00	531.4	2
	10.62	938.3	2
	10.15	869.6	2
20.0	5.90	517.4	2
	10.65	943.6	2
	10.15	869.5	2

Conclusions

For the two examples presented here the flutter velocity analysis program always converged to an answer for values of ν_o chosen between 1 and 20 and did not show any tendency to diverge from the solution, however, this does not guarantee that the method will be reliable for all systems. It may be possible that some other type of fit besides a cubic or quadratic equation would give more accurate results, but the former was used because of simplicity. The value of M = 10 was used for the cases presented, but for some systems this number may be either too large or too small and might yield a negative slope from the origin.

It should be noted that the second derivatives of ψ_j are not needed unless the cubic equation fails to give a real positive value of ν, however, the computer program computed all of the second derivatives even if they were not needed. Some computational time may be saved by computing only those values of $d^2\psi_j/d\nu^2$ which are needed. For the cases shown the cubic was used for four of the six modes.

One problem that did not effect convergence for the cases explained was that of "switching of the modes" for the ψ_j values. The subroutine which computes the eigenvalues arranges the eigenvalues $\overline{\lambda}_j$ in descending magnitude of the real part of the eigenvalue χ_j. This is done since the χ_j values for a particular mode vary only slightly as can be seen from Figure 10 or 11. The imaginary part of

the eigenvalues ψ_j, however, for a mode may change from point to point by a considerable amount. The ordering of the eigenvalues by χ_j, therefore, may cause the ψ_j value computed from ν_o not to correspond with the $\bar{\psi}_j$ value computed from $\nu = \bar{\nu}$ thus resulting in a bad fit for the actual shape of that mode. From Figure 11 switching is seen to occur for values of $\nu = 3.0$ and $\nu = 14.0$.

It is the belief of the author that the flutter technique presented here is a basically simple and efficient method for finding the flutter velocity. For the designer with a feeling for the range of ν_o values to try, this method should be quite successful.

BIBLIOGRAPHY

BIBLIOGRAPHY

1. Bhatia, K. G. "Optimization of Structures to Satisfy Aeroelastic Constraints." Ph.D. Dissertation. Dept. of Mechanical Engineering, Clemson University, December, 1971.

2. Bisplinghoff, R. L., H. Ashley and R. L. Halfman. Aeroelasticity. Reading, Mass.: Addison-Wesley Publishing Co., Inc. 1955.

3. Hassig, H. J. "Determinant Iteration Applied to the P-K Method of Solving the Flutter Equation," Aerospace Flutter and Dynamics Council Meeting. December, 1968.

4. Irwin, C. A. K. and P. R. Guyett. "The Subcritical Response and Flutter of a Swept Wing Mode." Great Britain Aeronautical Research Council, Reports and Memoranda No. 3497. August, 1965.

5. Lawrence, A. J. and P. Jackson. "Comparison of Different Methods of Assessing the Free Oscillatory Characteristics of Aeroelastic Systems." Aeronautical Research Council, Current Paper, C. P. No. 1084. December, 1968.

6. Martin, H. C. Introduction to Matrix Methods of Structural Analysis. New York: McGraw-Hill, Inc. 1966.

7. Phoa, Y. T. "A Computerized Flutter Solution Procedure." Presented at the National Symposium on Computerized Structural Analysis and Design. March, 1972.

8. Richardson, G. R. "A More Realistic Method for Routine Flutter Calculations." AIAA Symposium of Structural Dynamics and Aeroelasticity. 1965.

9. Rudisill, C. S. Personal Communication, Clemson University, Clemson, South Carolina. 1972.

10. Rudisill, C. S. and K. G. Bhatia. "Optimization of Complex Structures to Satisfy Flutter Requirements." AIAA Journal, Vol. 9, No. 8: 1487-1491. August, 1971.

11. Rudisill, C. S. and K. G. Bhatia. "Second Derivatives of the Flutter Velocity and the Optimization of Aircraft Structures." AIAA Journal, Log. No. J6121.

12. Scanlan, R. H. and R. Rosenbaum. Aircraft Vibration and Flutter. New York: Dover Publications, Inc. 1968.

13. Turner, M. J. "Optimization of Structures to Satisfy Flutter Requirements." AIAA Journal, Vol. 7, No. 5: 945-951. May, 1969.

APPENDIX A

Box Beam and Variable Parameters

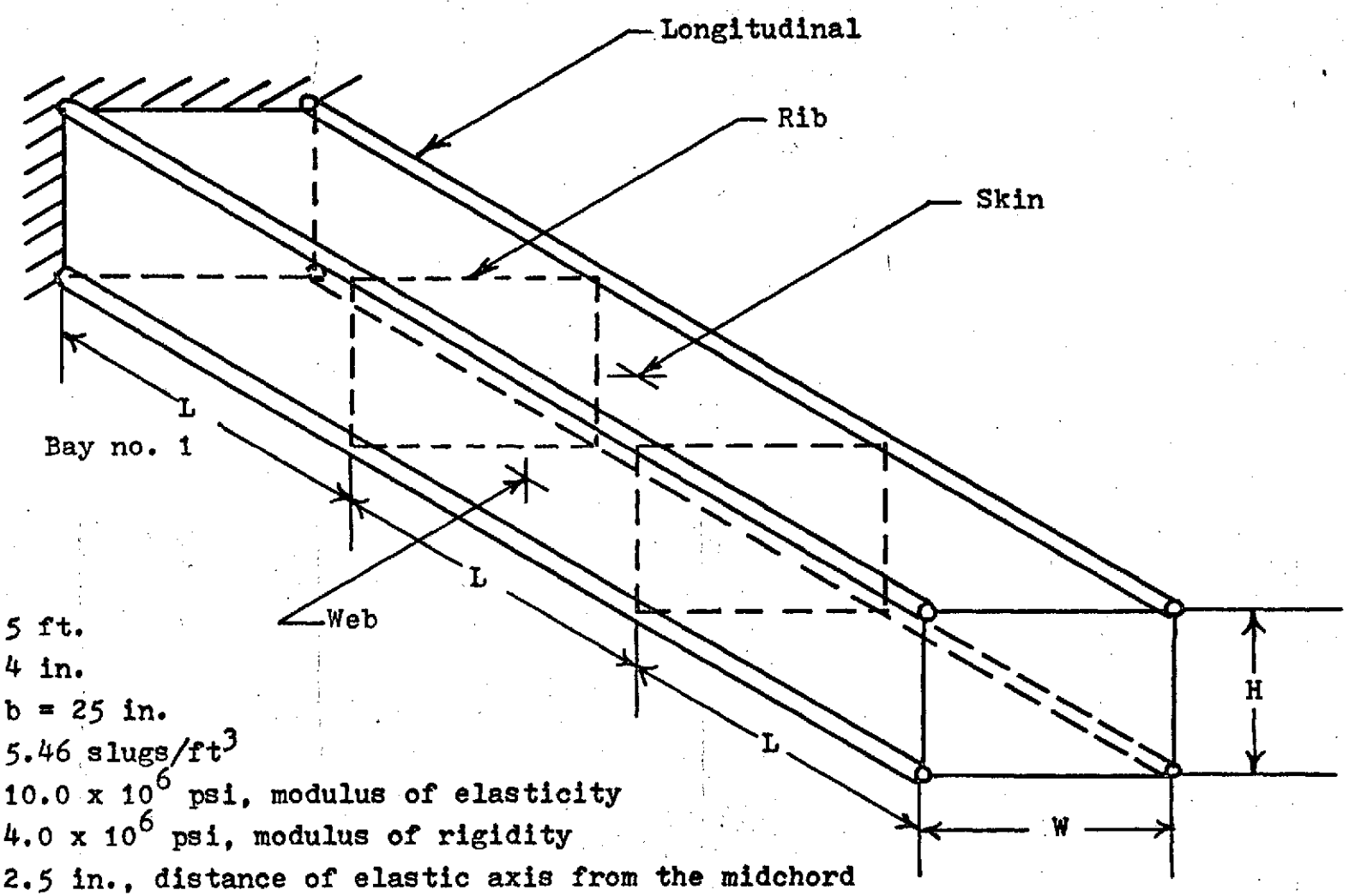

L = 5 ft.
H = 4 in.
W = b = 25 in.
ρ = 5.46 slugs/ft^3
E = 10.0 x 10^6 psi, modulus of elasticity
G = 4.0 x 10^6 psi, modulus of rigidity
a = 2.5 in., distance of elastic axis from the midchord

Figure 9. Rectangular Box Beam and Properties

Table III. Variable Parameters of Box Beam.

Case 1, P(I) = PMIN(I).

Bay No.	Areas of Longitudinals (ft^2)	Front and Back Web Thicknesses (ft)	Top and Bottom Skin Thicknesses (ft)	Rib Thicknesses (ft)
1	0.002315	0.001111	0.0005555	0.0005555
2	0.002315	0.001111	0.0005555	0.0005555
3	0.002315	0.001111	0.0005555	0.0005555

Case 2, P(I) = PMIN(I) x 6.

Bay No.	Areas of Longitudinals (ft^2)	Front and Back Web Thicknesses (ft)	Top and Bottom Skin Thicknesses (ft)	Rib Thicknesses (ft)
1	0.01389	0.006667	0.003333	0.003333
2	0.01389	0.006667	0.003333	0.003333
3	0.01389	0.006667	0.003333	0.003333

APPENDIX B

Plots and Corresponding Tables of Computed Curves and Cubic or Quadratic Fit

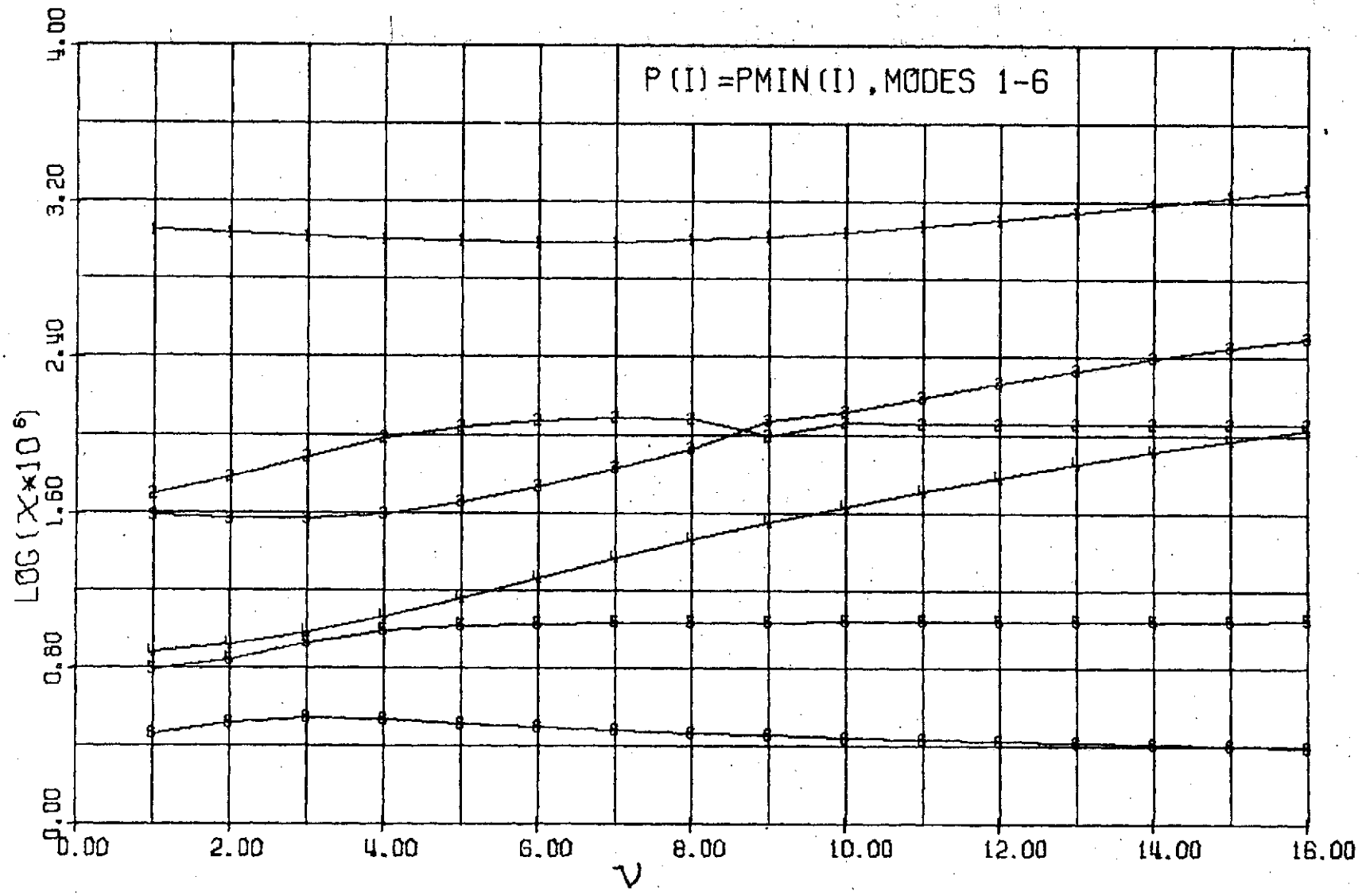

Figure 10. Real Part of Eigenvalues for Case 1.

Table IV. Real Part of the Eigenvalues for Case 1.

ν ft/rad	MODE 1 ($\times 10^3$)	MODE 2 ($\times 10^4$)	MODE 3 ($\times 10^5$)
1.0	1.13	0.50	0.38
2.0	1.09	0.62	0.37
3.0	1.05	0.78	0.37
4.0	1.01	0.96	0.40
5.0	0.98	1.11	0.46
6.0	0.97	1.19	0.55
7.0	0.98	1.23	0.68
8.0	1.01	1.22	0.86
9.0	1.05	0.99	1.19
10.0	1.11	1.17	1.32
11.0	1.19	1.15	1.57
12.0	1.29	1.14	1.85
13.0	1.49	1.14	2.15
14.0	1.54	1.14	2.47
15.0	1.69	1.14	2.82
16.0	1.86	1.14	3.19

Table IV. Real Part of the Eigenvalues for Case 1.

ν ft/rad	MODE 4 ($\times 10^5$)	MODE 5 ($\times 10^5$)	MODE 6 ($\times 10^6$)
1.0	0.76	0.62	2.96
2.0	0.86	0.70	3.35
3.0	0.97	0.85	3.50
4.0	1.17	0.98	3.44
5.0	1.47	1.04	3.31
6.0	1.86	1.07	3.19
7.0	2.35	1.08	3.07
8.0	2.92	1.09	2.96
9.0	3.58	1.09	2.86
10.0	4.34	1.10	2.79
11.0	5.19	1.10	2.72
12.0	6.14	1.10	2.66
13.0	7.18	1.11	2.61
14.0	8.32	1.11	2.57
15.0	9.57	1.11	2.53
16.0	10.90	1.12	2.50

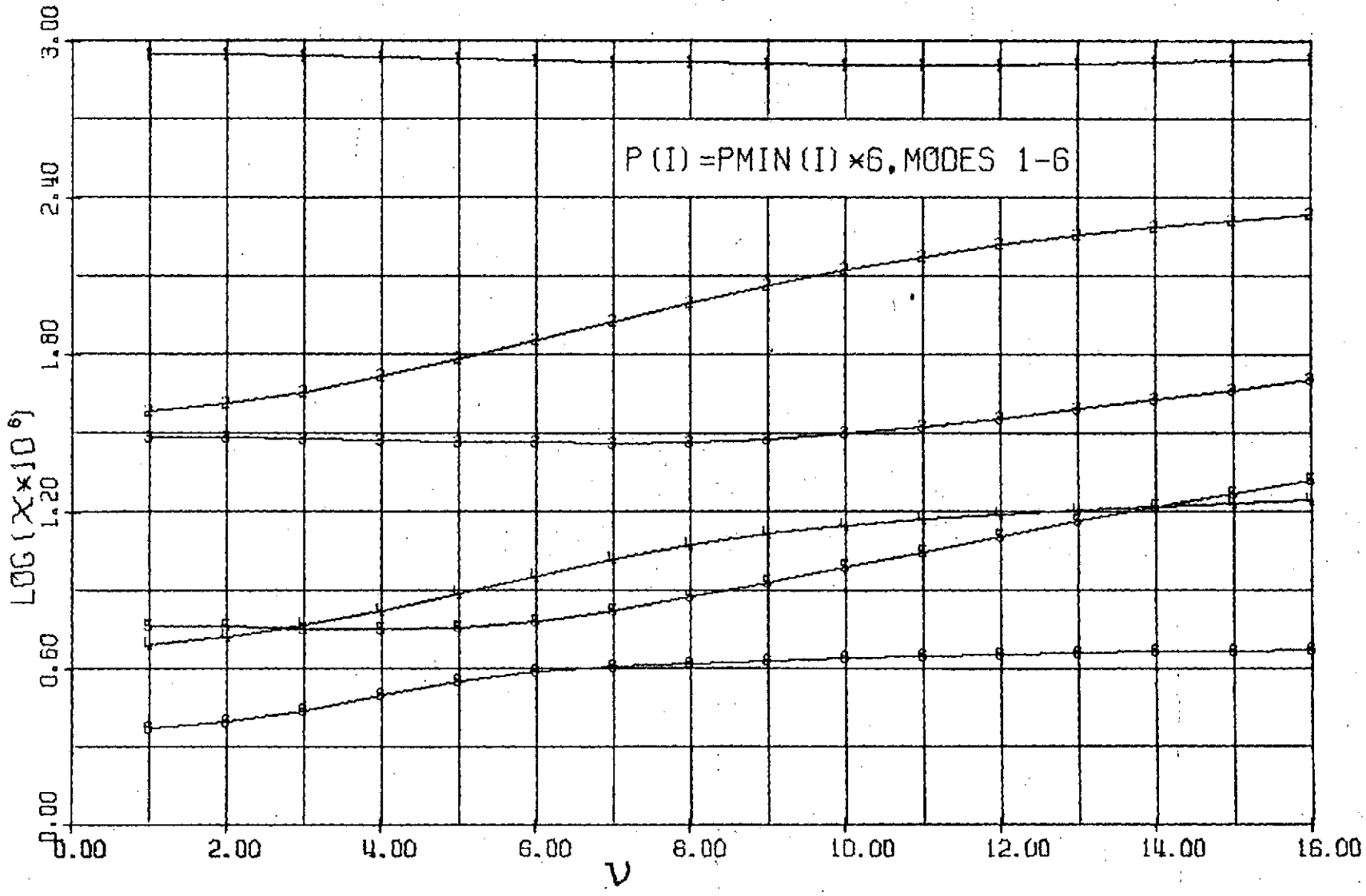

Figure 11. Real Part of the Eigenvalues for Case 2.

Table V. Real Part of the Eigenvalues for Case 2.

ν ft/rad	MODE 1 ($\times 10^4$)	MODE 2 ($\times 10^4$)	MODE 3 ($\times 10^5$)
1.0	8.91	0.39	3.07
2.0	8.85	0.41	3.04
3.0	8.76	0.46	3.01
4.0	8.66	0.52	2.98
5.0	8.55	0.61	2.94
6.0	8.45	0.72	2.92
7.0	8.34	0.85	2.90
8.0	8.25	1.00	2.93
9.0	8.17	1.17	3.02
10.0	8.11	1.34	3.17
11.0	8.09	1.50	3.37
12.0	8.10	1.66	3.63
13.0	8.16	1.81	3.92
14.0	8.26	1.94	4.26
15.0	8.41	2.06	4.64
16.0	8.59	2.18	5.06

Table V. Real Part of the Eigenvalues for Case 2.

ν ft/rad	MODE 4 ($\times 10^5$)	MODE 5 ($\times 10^5$)	MODE 6 ($\times 10^6$)
1.0	0.49	0.58	2.36
2.0	0.53	0.58	2.51
3.0	0.59	0.57	2.77
4.0	0.67	0.56	3.16
5.0	0.77	0.57	3.59
6.0	0.91	0.61	3.88
7.0	1.06	0.67	4.06
8.0	1.20	0.76	4.19
9.0	1.32	0.86	4.29
10.0	1.41	0.98	4.39
11.0	1.49	1.12	4.47
12.0	1.56	1.28	4.54
13.0	1.61	1.46	4.60
14.0	1.66	1.67	4.65
15.0	1.72	1.87	4.69
16.0	1.77	2.10	4.72

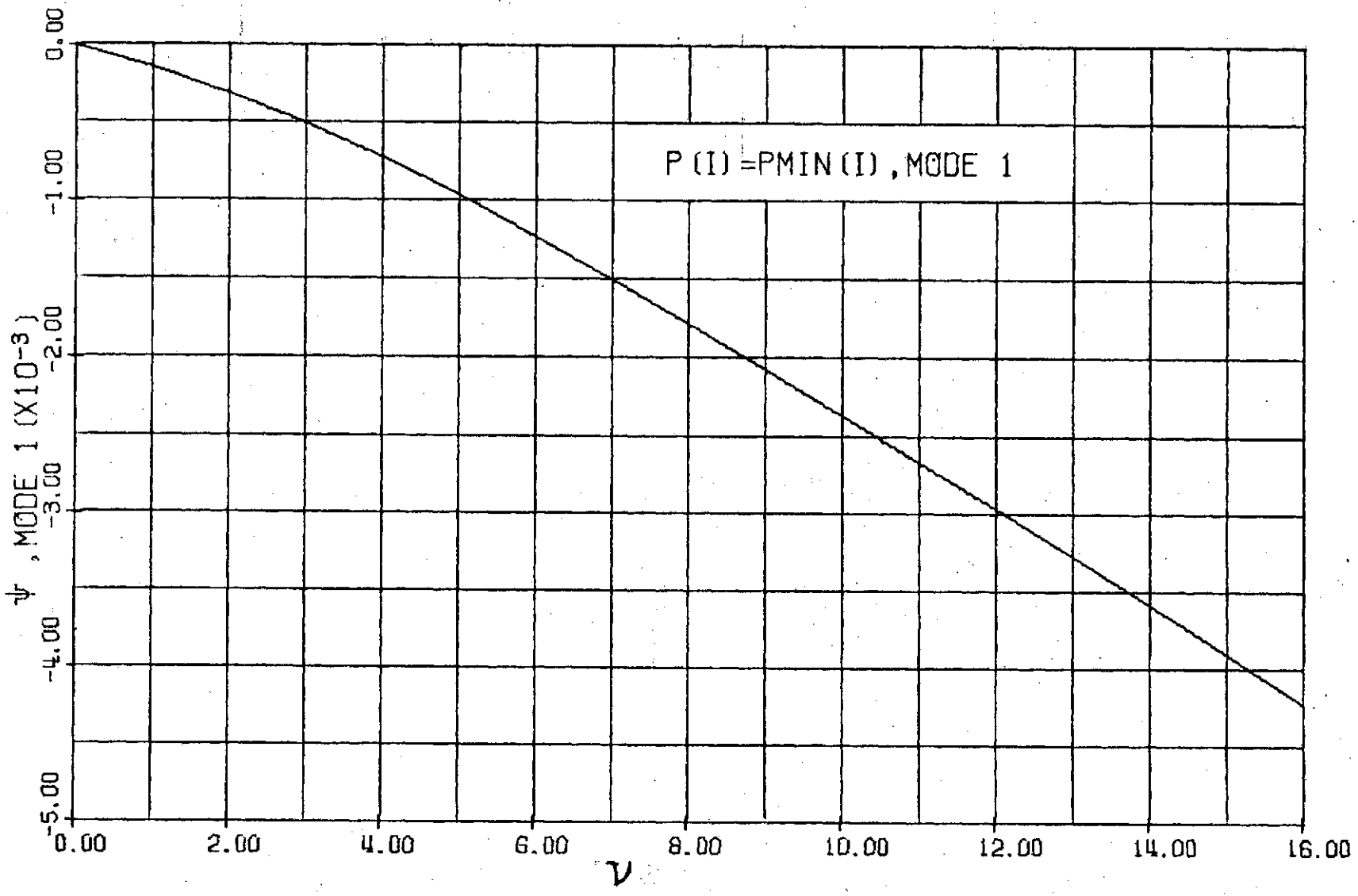

Figure 12. ψ_1 versus ν for Case 1.

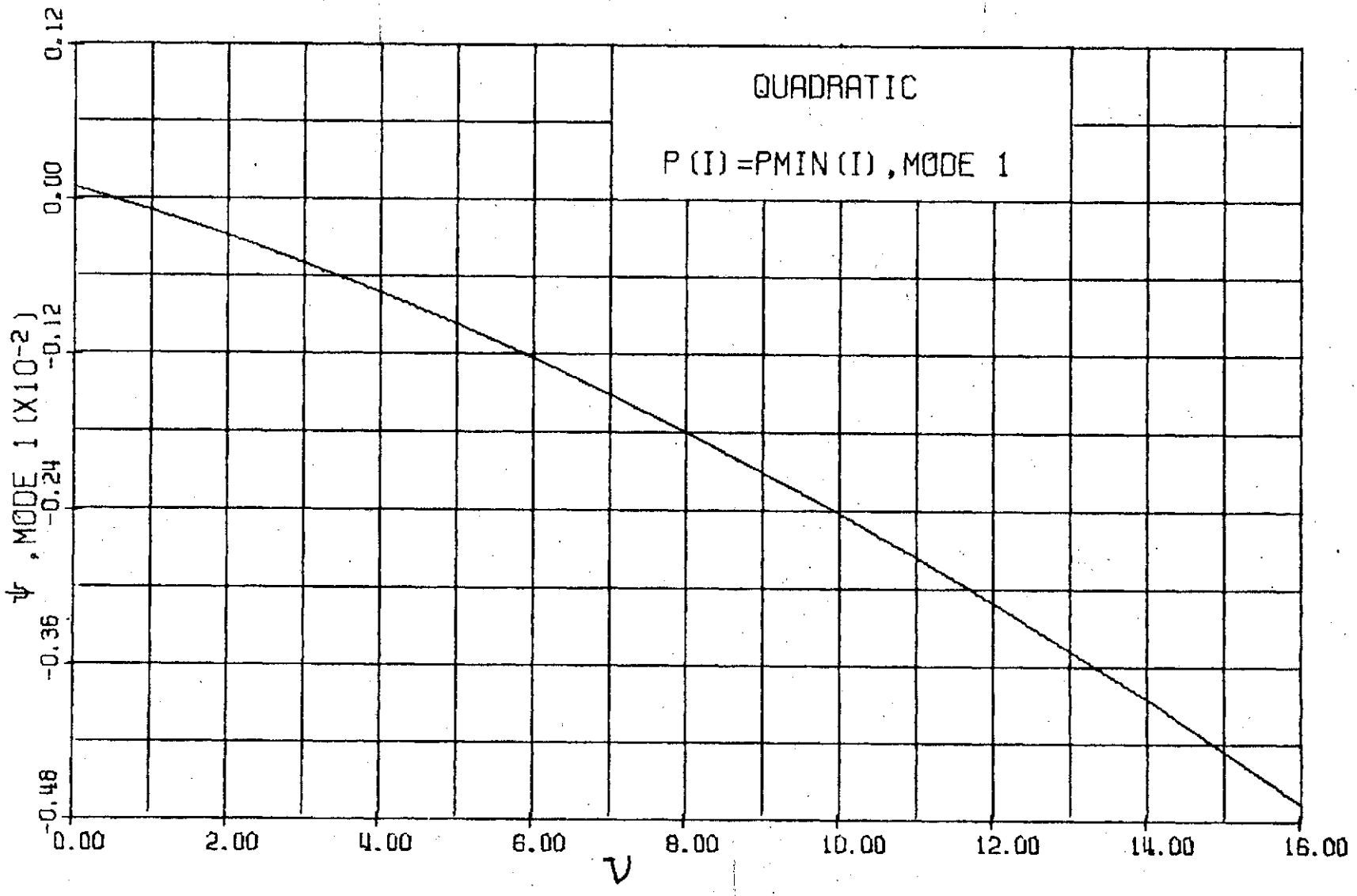

Figure 13. Quadratic Approximation of ψ_1 for $\nu_o = 5.0$, Case 1.

Table VI. Computed ψ_1 and Quadratic Fit for Case 1 and $\nu_o = 5.0$.

ν ft/rad	COMPUTED CURVE ($\times 10^3$)	QUADRATIC $\nu_o = 5.0$ ($\times 10^3$)	COMPUTED AIRSPEED ft/sec
0.0	0.0	+0.09	0.0
1.0	-0.15	-0.09	29.7
2.0	-0.32	-0.29	60.6
3.0	-0.51	-0.50	92.6
4.0	-0.73	-0.73	126.0
5.0	-0.97	-0.97	160.0
6.0	-1.23	-1.23	192.0
7.0	-1.50	-1.50	223.0
8.0	-1.78	-1.79	252.0
9.0	-2.07	-2.10	278.0
10.0	-2.36	-2.42	300.0
11.0	-2.66	-2.75	319.0
12.0	-2.96	-3.10	334.0
13.0	-3.27	-3.47	346.0
14.0	-3.58	-3.85	357.0
15.0	-3.90	-4.25	365.0
16.0	-4.22	-4.66	371.0

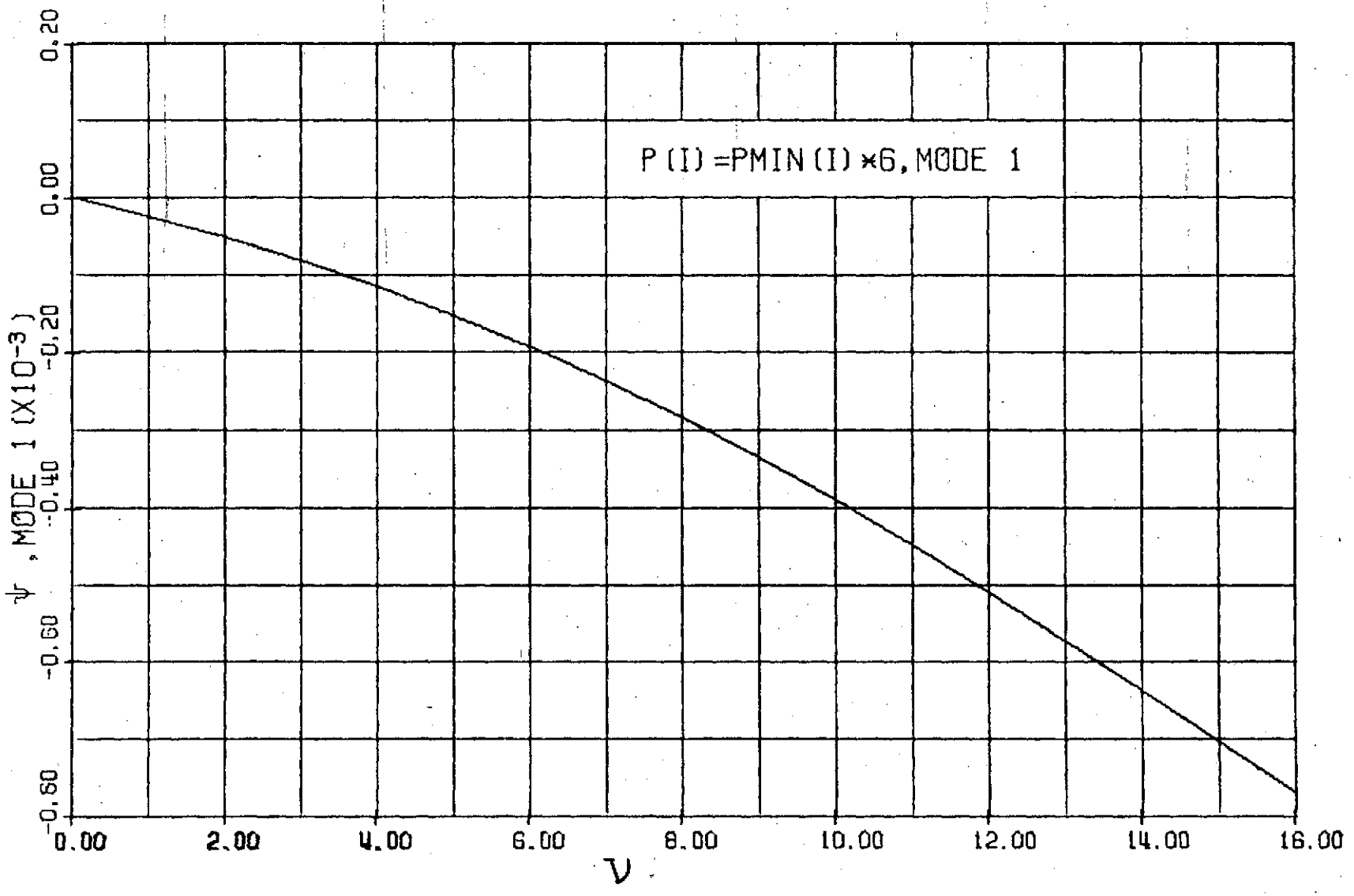

Figure 14. ψ_1 versus ν for Case 2.

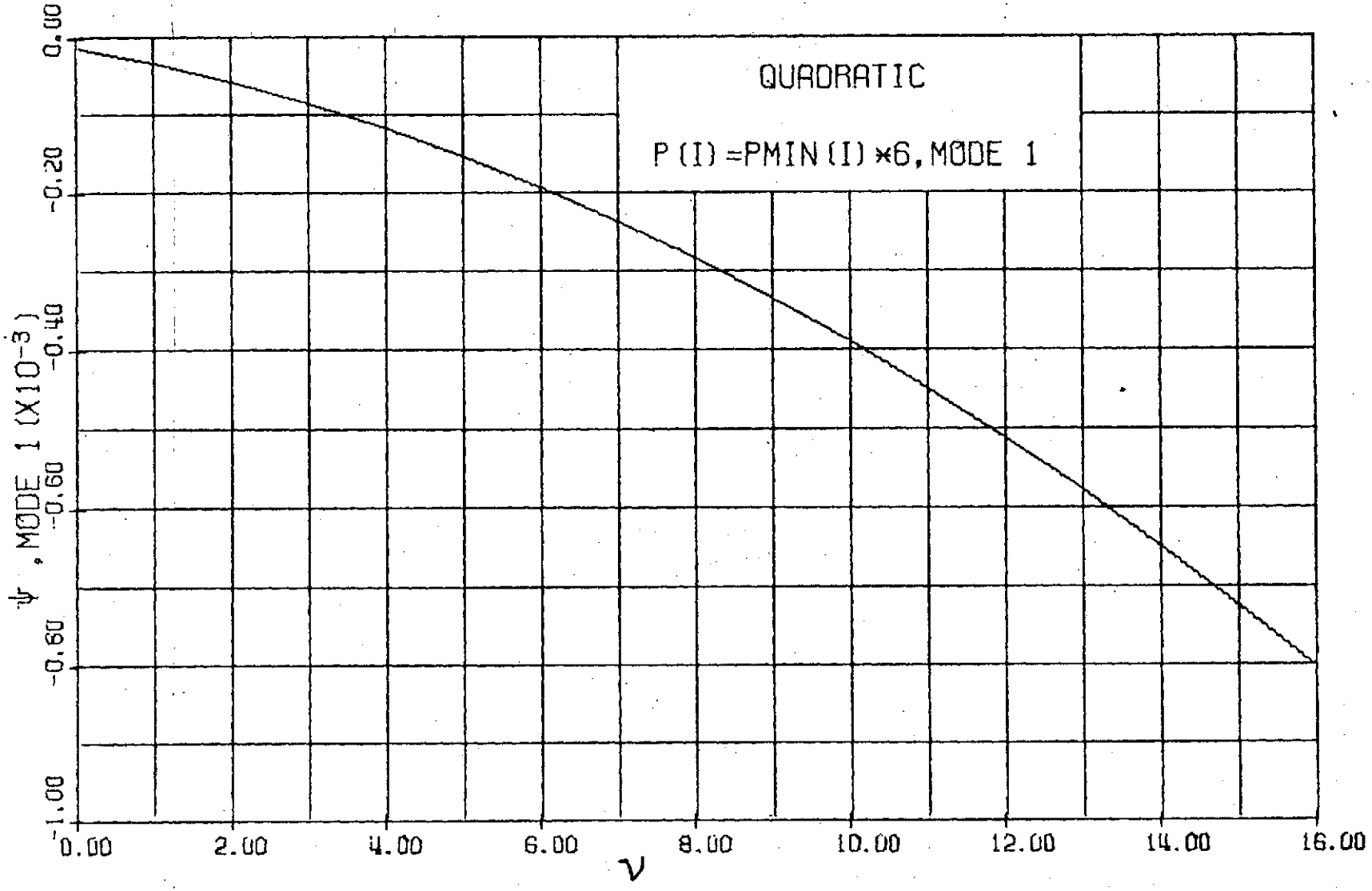

Figure 15. Quadratic Approximation of ψ_1 for $\nu_o = 9.0$, Case 2.

Table VII. Computed ψ_1 and Quadratic Fit Values for Case 2 and $\nu_o = 9.0$.

ν ft/rad	COMPUTED CURVE ($\times 10^4$)	QUADRATIC $\nu_o = 9.0$ ($\times 10^4$)	COMPUTED AIRSPEED ft/sec
0.0	0.0	-0.13	0.0
1.0	-0.25	-0.34	33.5
2.0	-0.51	-0.57	67.2
3.0	-0.82	-0.85	101.0
4.0	-1.15	-1.17	136.0
5.0	-1.52	-1.53	171.0
6.0	-1.92	-1.92	206.0
7.0	-2.36	-2.36	242.0
8.0	-2.83	-2.83	279.0
9.0	-3.34	-3.34	315.0
10.0	-3.89	-3.89	351.0
11.0	-4.47	-4.48	387.0
12.0	-5.09	-5.11	422.0
13.0	-5.72	-5.77	455.0
14.0	-6.37	-6.48	487.0
15.0	-7.03	-7.22	517.0
16.0	-7.69	-8.01	546.0

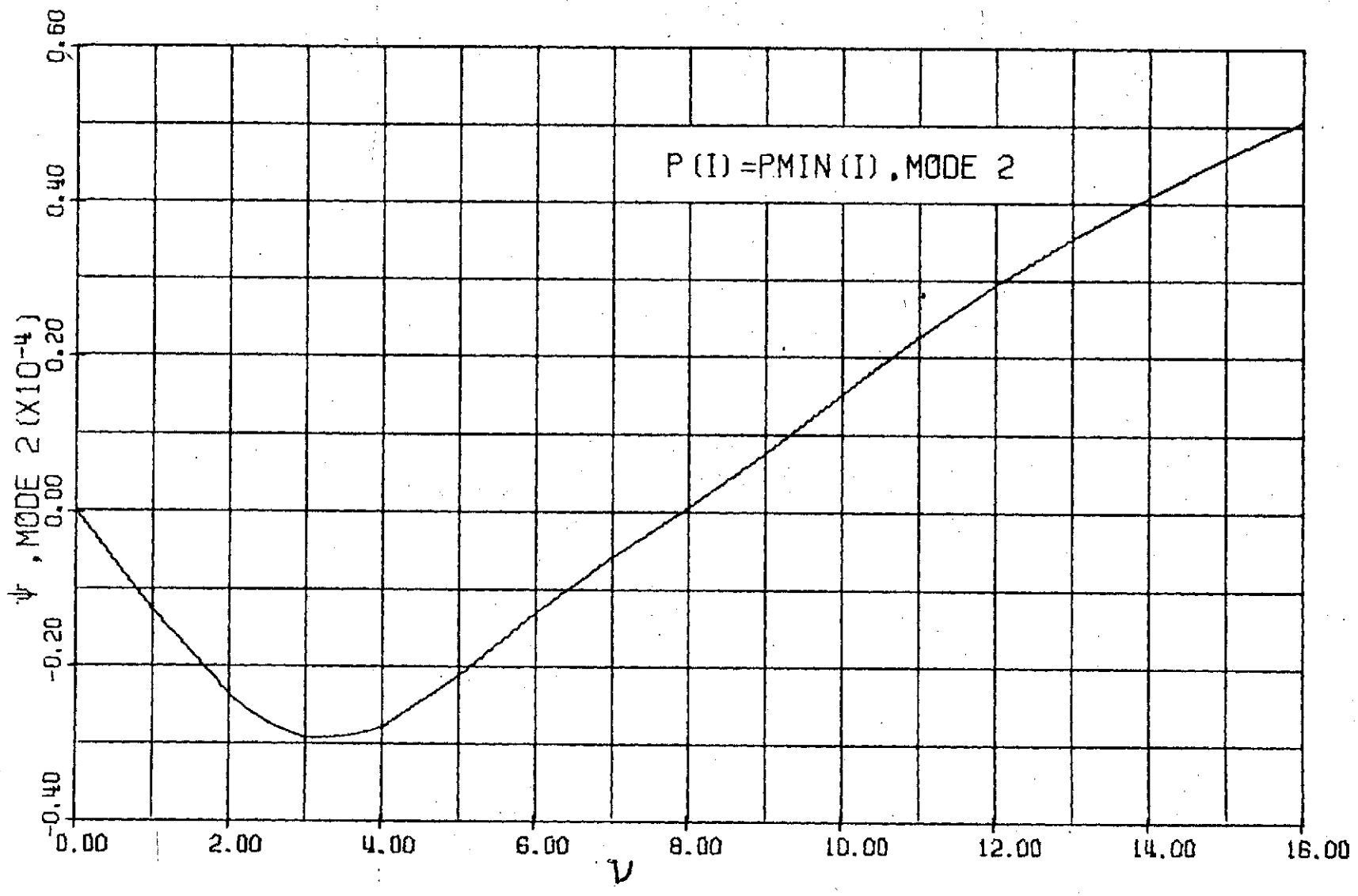

Figure 16. ψ_2 versus ν for Case 1.

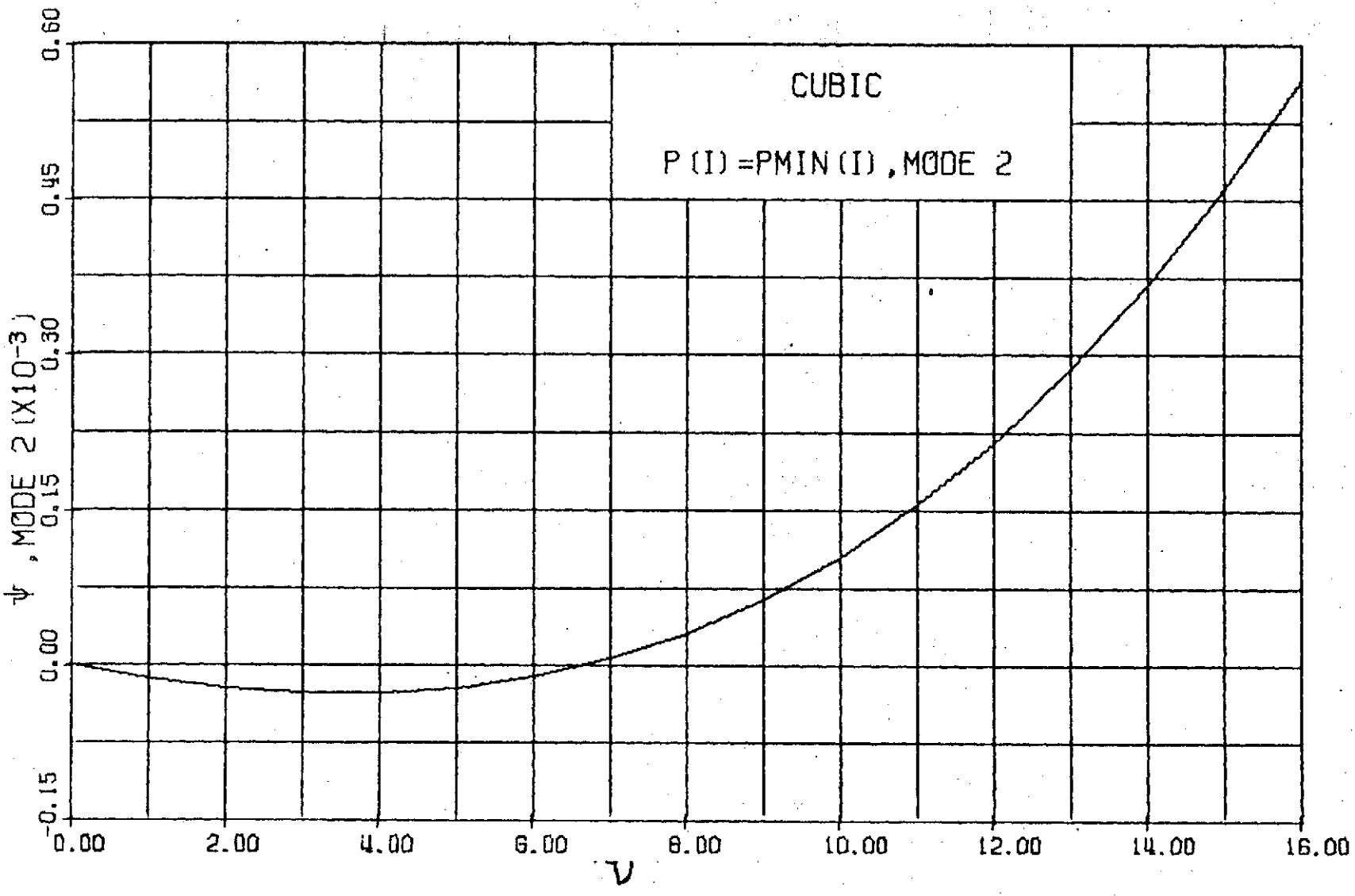

Figure 17. Cubic Approximation of ψ_2 for Case 1.

Table VIII. Computed ψ_2 and Cubic Fit Values for Case 1 and $\nu_o = 5.0$.

ν ft/rad	COMPUTED CURVE ($\times 10^4$)	QUADRATIC $\nu_o = 5.0$ ($\times 10^4$)	COMPUTED AIRSPEED ft/sec
0.0	0.0	0.0	0
1.0	-0.13	-0.13	141
2.0	-0.23	-0.21	255
3.0	-0.29	-0.26	339
4.0	-0.28	-0.26	407
5.0	-0.21	-0.21	475
6.0	-0.13	-0.10	550
7.0	-0.06	+0.08	631
8.0	+0.01	0.33	724
9.0	0.08	0.65	906
10.0	0.15	1.06	925
11.0	0.23	1.57	1030
12.0	0.29	2.16	1120
13.0	0.35	2.87	1220
14.0	0.41	3.68	1310
15.0	0.46	4.61	1400
16.0	0.51	5.66	1500

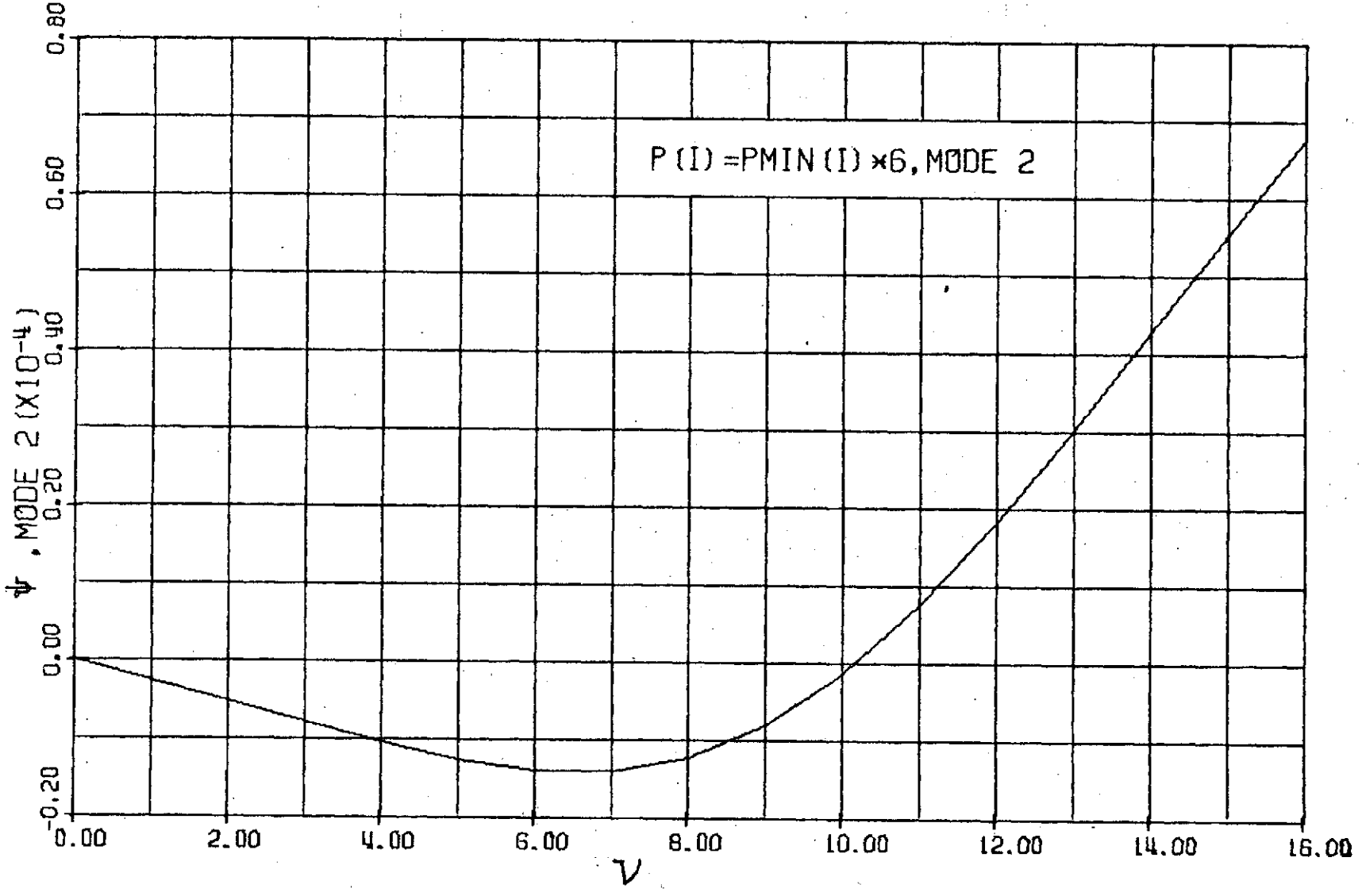

Figure 18. ψ_2 versus ν for Case 2.

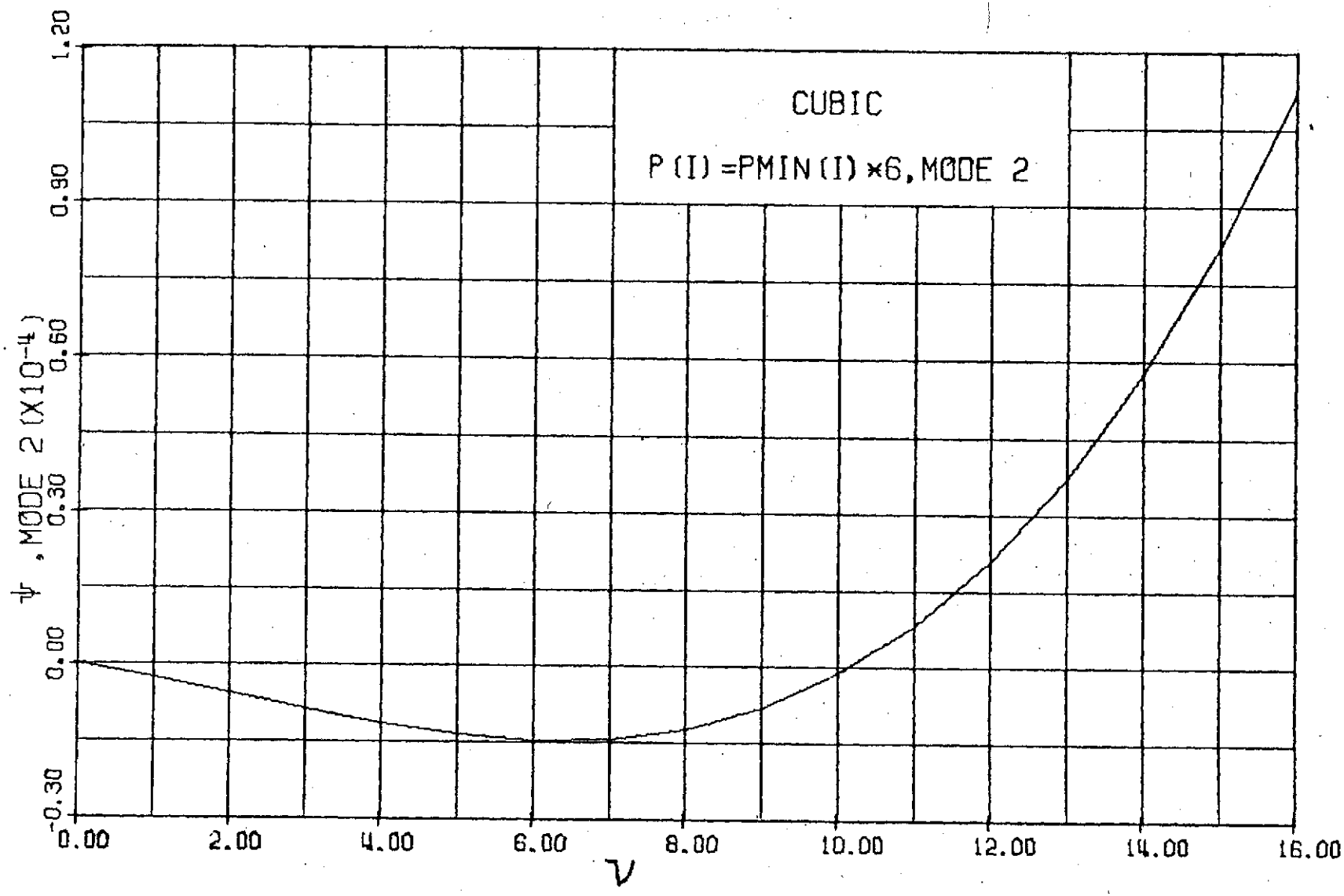

Figure 19. Cubic Approximation of ψ_2 for Case 2.

Table IX. Computed ψ_2 and Cubic Fit Values for Case 2 and $\nu_o = 9.0$.

ν ft/rad	COMPUTED CURVE ($\times 10^5$)	CUBIC FIT $\nu_o = 9.0$ ($\times 10^5$)	COMPUTED AIRSPEED ft/sec
0.0	0.0	0.0	0
1.0	-0.24	-0.25	161
2.0	-0.50	-0.54	311
3.0	-0.77	-0.84	444
4.0	-1.03	-1.11	554
5.0	-1.25	-1.33	641
6.0	-1.39	-1.44	708
7.0	-1.38	-1.41	759
8.0	-1.20	-1.20	800
9.0	-0.78	-0.78	832
10.0	-0.13	-0.12	864
11.0	+0.76	+0.83	898
12.0	1.83	2.11	931
13.0	3.03	3.74	966
14.0	4.28	5.78	1010
15.0	5.54	8.24	1050
16.0	6.77	1.12	1080

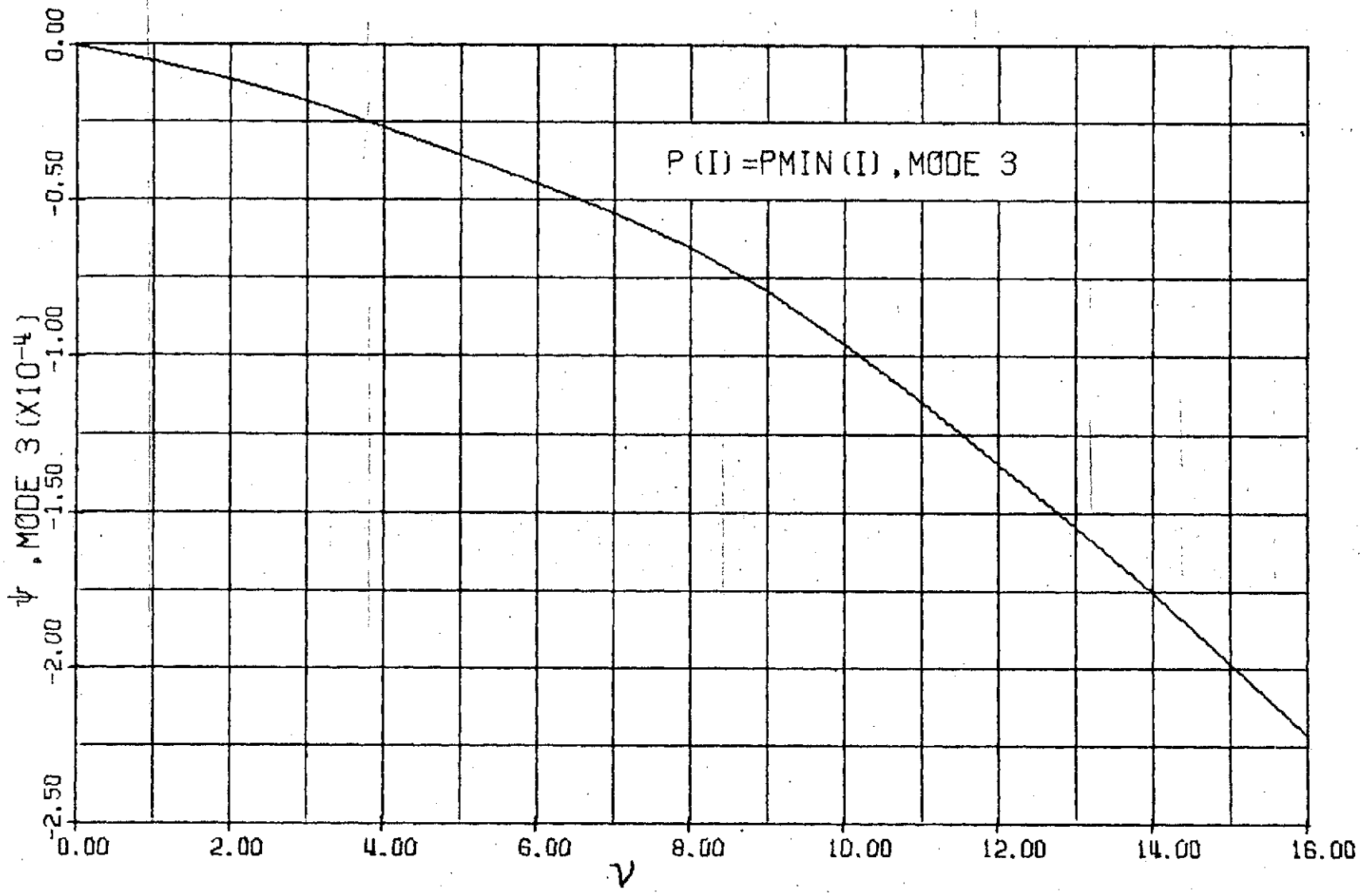

Figure 20. ψ_3 versus ν for Case 1.

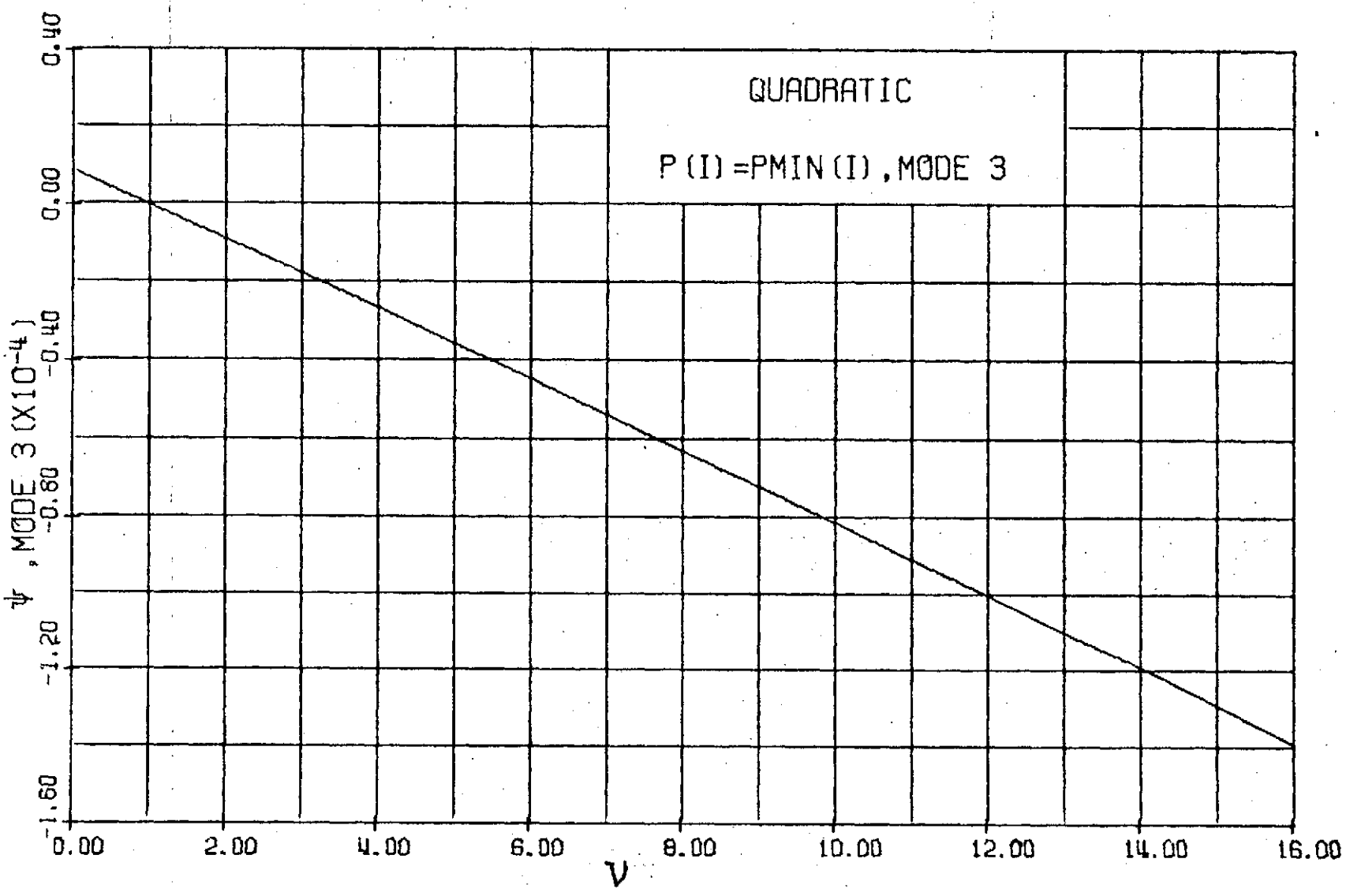

Figure 21. Quadratic Approximation of ψ_3 for Case 1.

Table X. Computed ψ_3 and Quadratic Fit Values for Case 13 and $\nu_o = 5.0$.

ν ft/rad	COMPUTED CURVE ($\times 10^4$)	QUADRATIC $\nu_o = 5.0$ ($\times 10^4$)	COMPUTED AIRSPEED ft/sec
0.0	0.0	+0.08	0
1.0	-0.05	-0.002	161
2.0	-0.11	-0.09	327
3.0	-0.18	-0.18	491
4.0	-0.27	-0.27	634
5.0	-0.36	-0.36	741
6.0	-0.45	-0.45	811
7.0	-0.54	-0.54	849
8.0	-0.65	-0.63	863
9.0	-0.92	-0.72	825
10.0	-0.96	-0.82	870
11.0	-1.14	-0.91	878
12.0	-1.34	-1.00	882
13.0	-1.54	-1.10	887
14.0	-1.75	-1.19	891
15.0	-1.98	-1.29	893
16.0	-2.21	-1.39	896

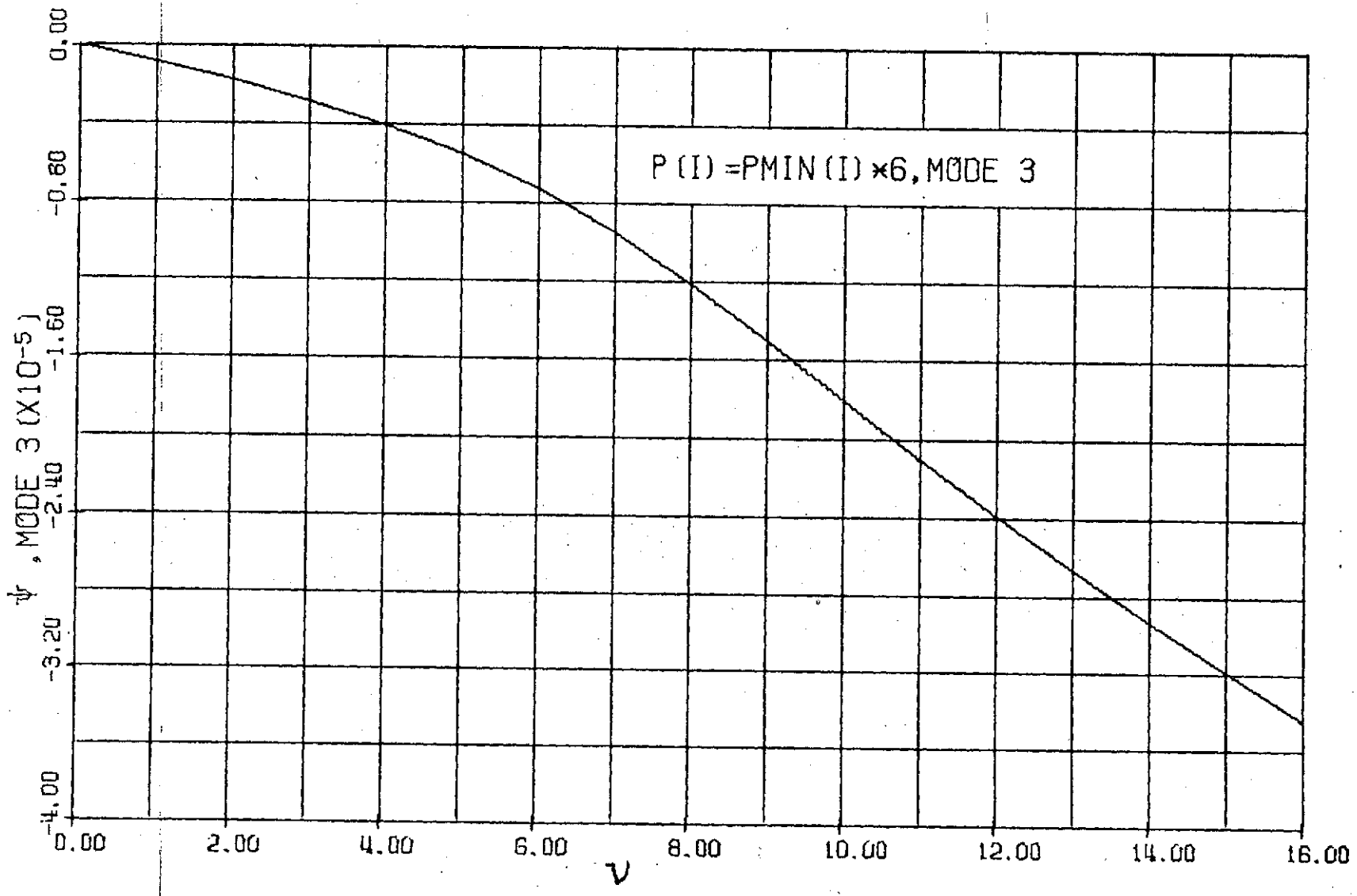

Figure 22. ψ_3 versus ν for Case 2.

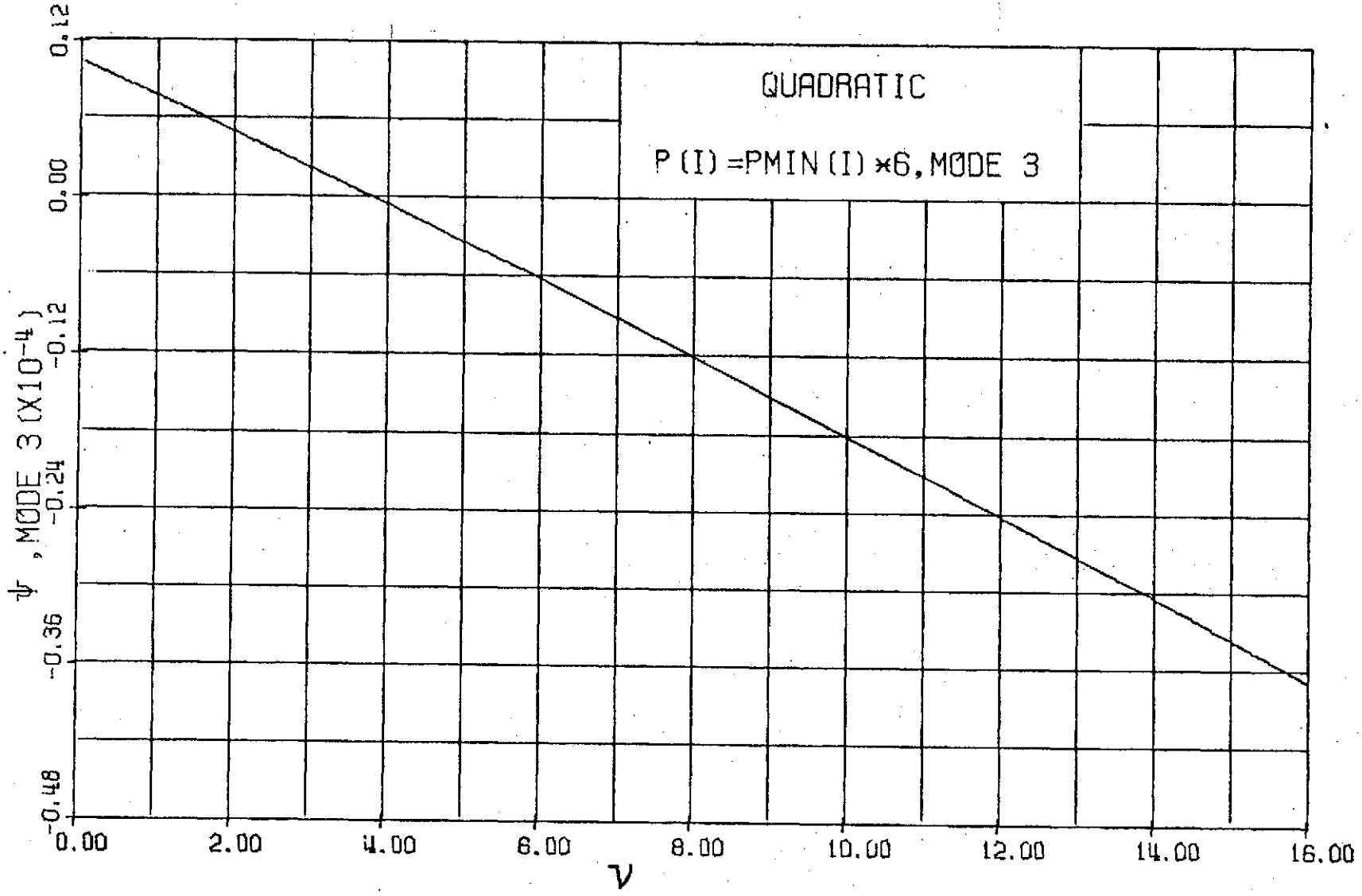

Figure 23. Quadratic Approximation of ψ_3 for Case 2.

Table XI. Computed ψ_3 and Quadratic Fit Values for Case 2 and $\nu_o = 9.0$.

ν ft/rad	COMPUTED CURVE ($\times 10^5$)	QUADRATIC $\nu_o = 9.0$ ($\times 10^5$)	COMPUTED AIRSPEED ft/sec
0.0	0.0	1.04	0
1.0	-0.08	0.78	180
2.0	-0.18	0.50	363
3.0	-0.28	0.23	547
4.0	-0.40	-0.05	733
5.0	-0.55	-0.34	922
6.0	-0.73	-0.63	1110
7.0	-0.95	-0.91	1300
8.0	-1.21	-1.21	1480
9.0	-1.50	-1.50	1640
10.0	-1.80	-1.81	1780
11.0	-2.10	-2.11	1890
12.0	-2.39	-2.42	1990
13.0	-2.66	-2.73	2080
14.0	-2.93	-3.04	2140
15.0	-3.19	-3.36	2200
16.0	-3.44	-3.69	2250

-2

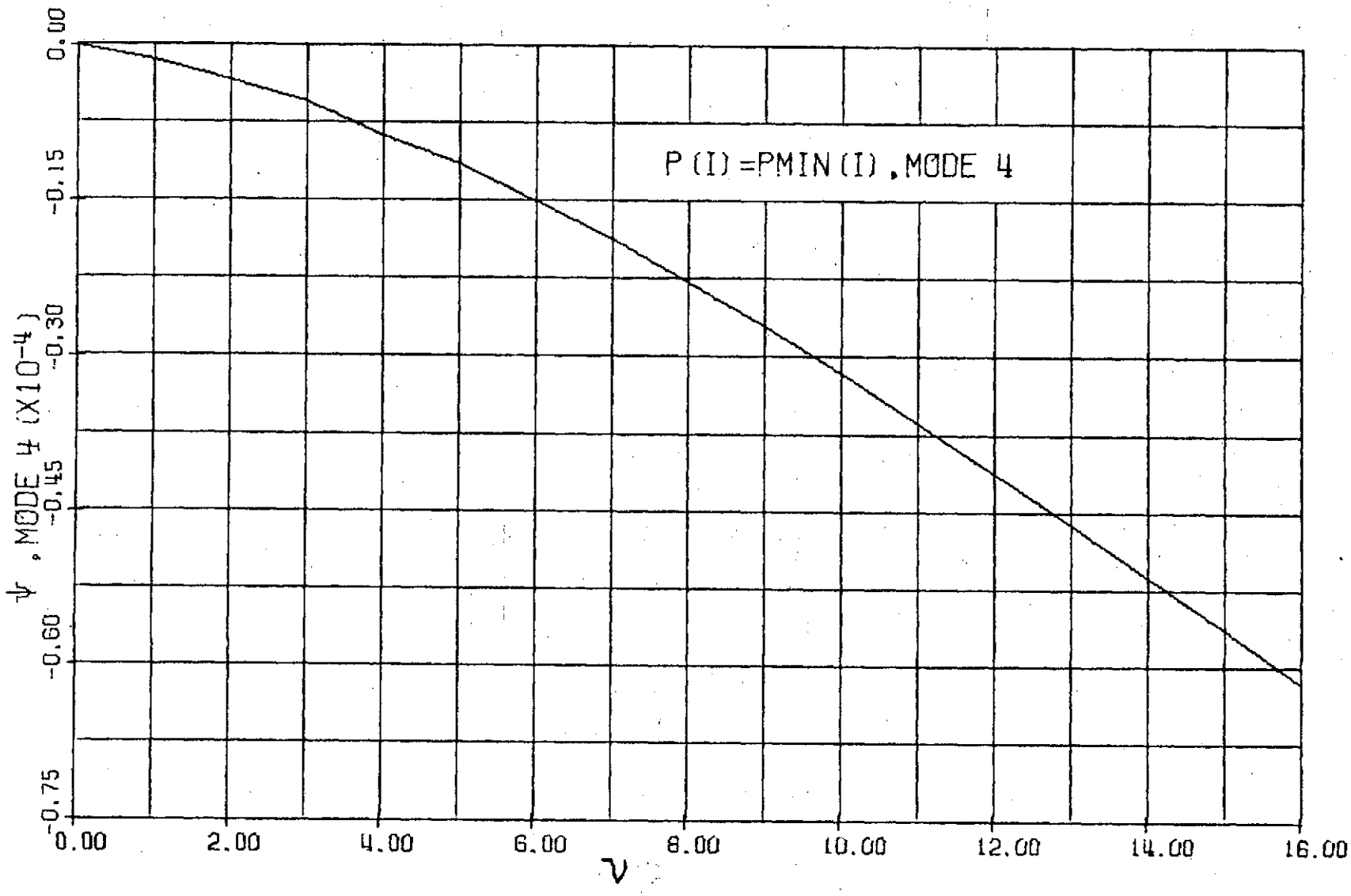

Figure 24. ψ_4 versus ν for Case 1.

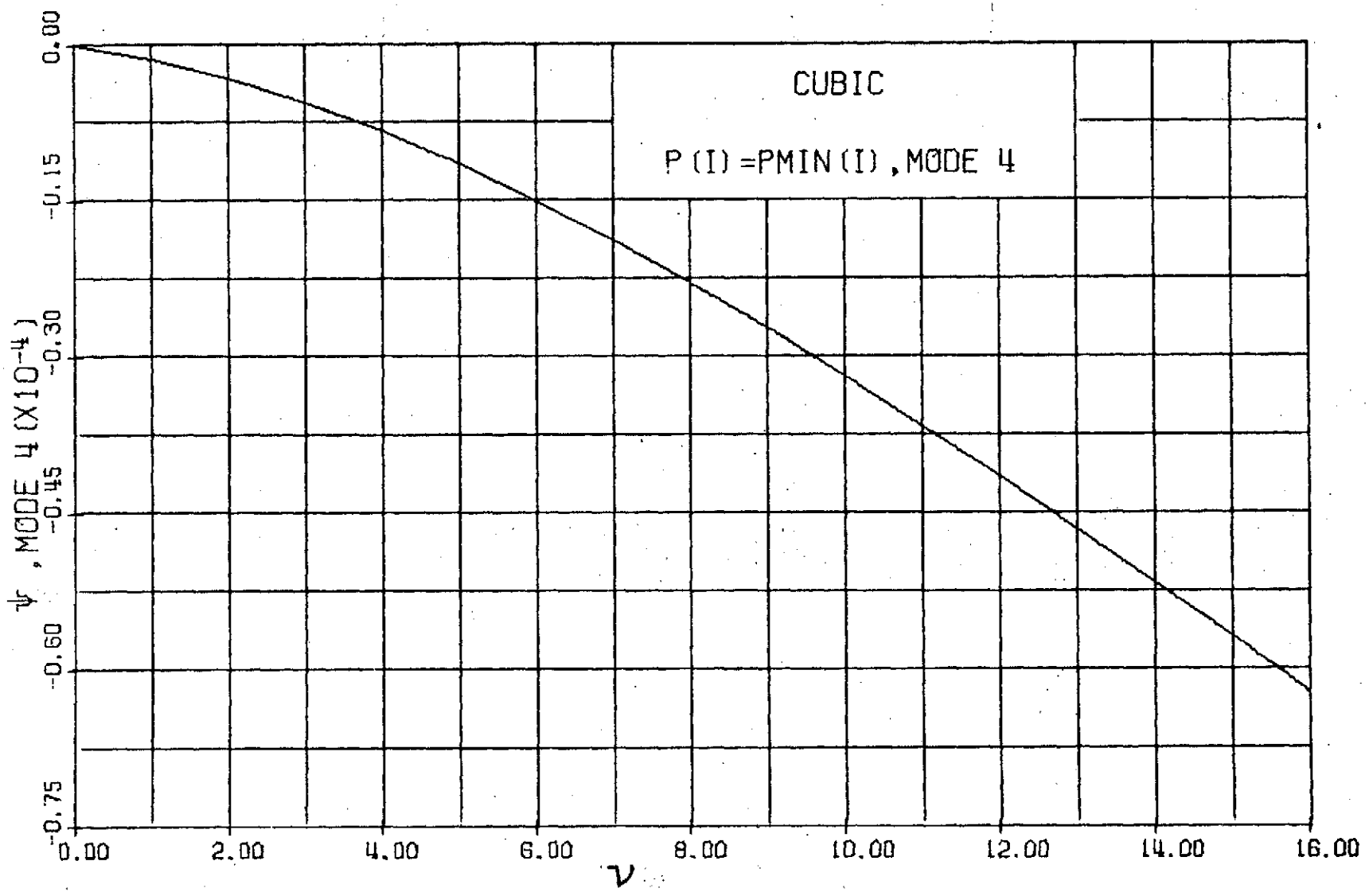

Figure 25. Cubic Approximation of ψ_4 for Case 1.

Table XII. Computed ψ_4 and Cubic Fit Values for Case 1 and $\nu_o = 5.0$.

ν ft/rad	COMPUTED CURVE ($\times 10^5$)	CUBIC FIT $\nu_o = 5.0$ ($\times 10^5$)	COMPUTED AIRSPEED ft/sec
0.0	0.0	0.0	0
1.0	-0.14	-0.14	362
2.0	-0.34	-0.33	690
3.0	-0.55	-0.56	964
4.0	-0.83	-0.84	1170
5.0	-1.15	-1.15	1300
6.0	-1.50	-1.50	1390
7.0	-1.87	-1.88	1440
8.0	-2.28	-2.29	1480
9.0	-2.70	-2.72	1500
10.0	-3.16	-3.18	1520
11.0	-3.63	-3.66	1530
12.0	-4.11	-4.15	1530
13.0	-4.61	-4.65	1530
14.0	-5.12	-5.17	1530
15.0	-5.63	-5.68	1530
16.0	-6.16	-6.21	1530

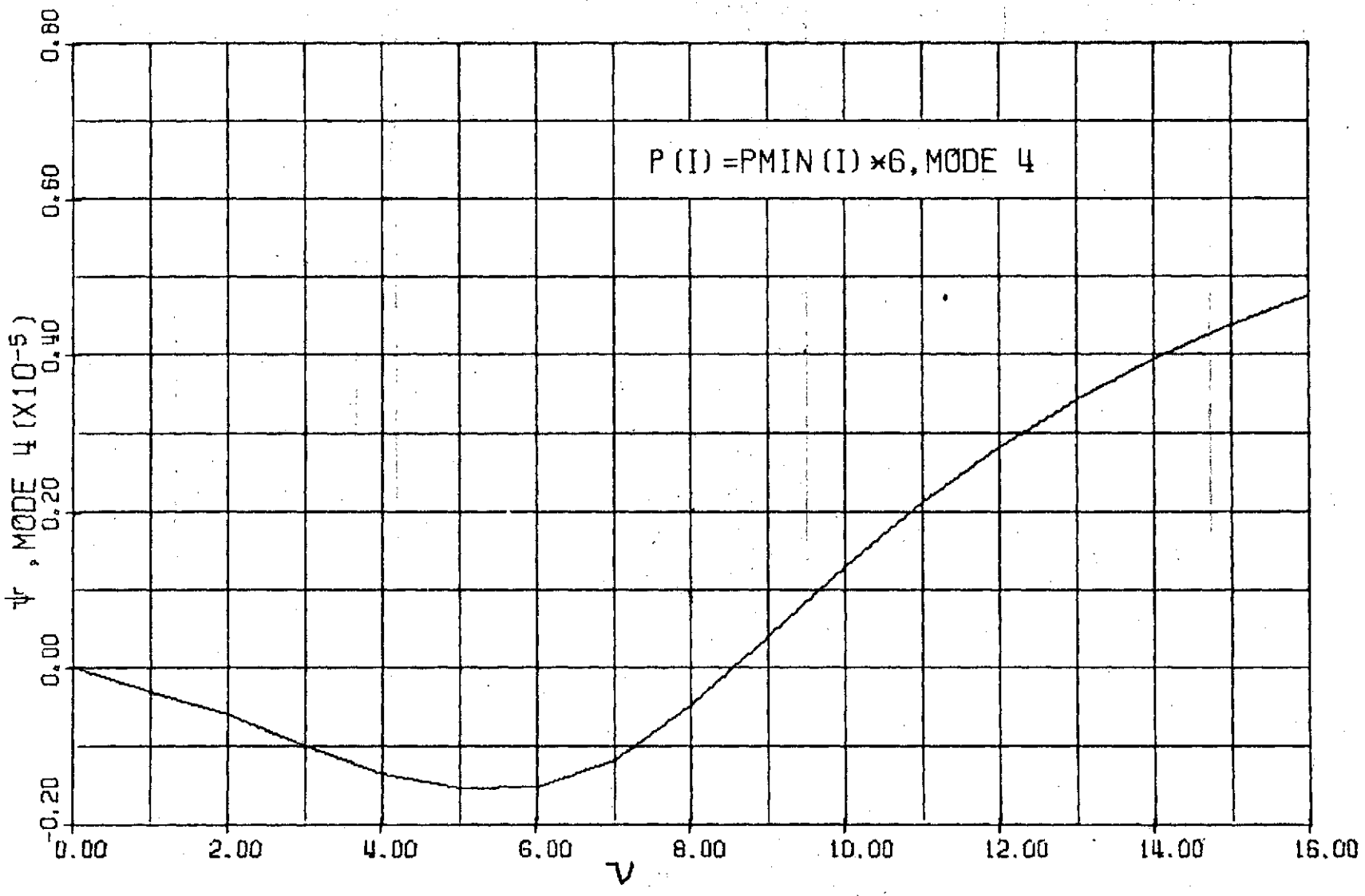

Figure 26. ψ_4 versus ν for Case 2.

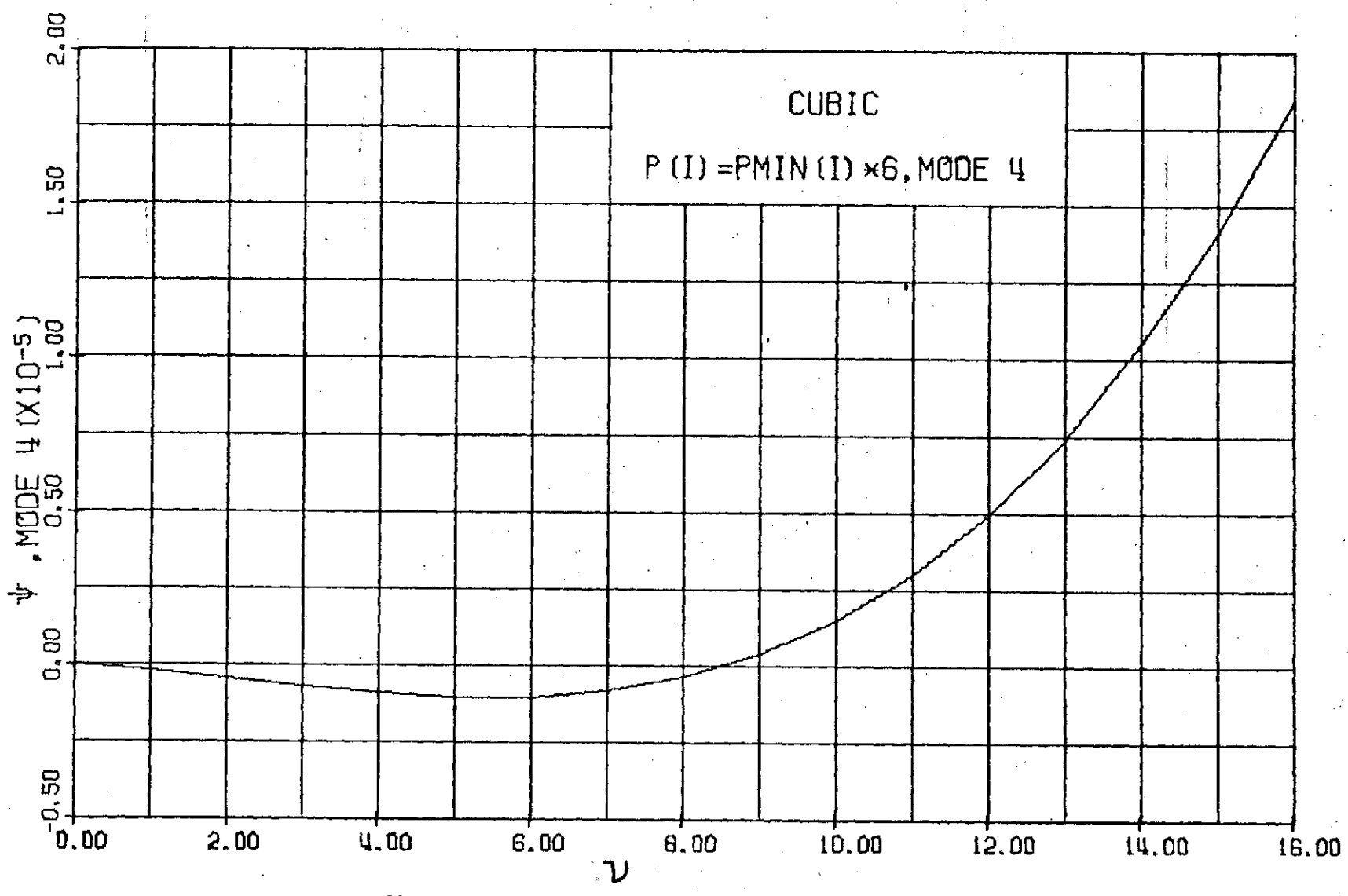

Figure 27. Cubic Approximation of ψ_4 for Case 2.

Table XIII. Computed ψ_4 and Cubic Fit Values for Case 2 and $\nu_0 = 9.0$.

ν ft/rad	COMPUTED CURVE ($\times 10^6$)	CUBIC FIT $\nu_o = 9.0$ ($\times 10^6$)	COMPUTED AIRSPEED ft/sec
0.0	0.0	0.0	0
1.0	-0.30	-0.18	450
2.0	-0.59	-0.43	872
3.0	-0.99	-0.68	1230
4.0	-1.34	-0.90	1559
5.0	-1.52	-1.02	1800
6.0	-1.50	-1.01	1990
7.0	-1.16	-0.80	2150
8.0	-0.48	-0.34	2310
9.0	+0.41	+0.41	2480
10.0	1.31	1.51	2660
11.0	2.12	3.02	2850
12.0	2.83	4.97	3040
13.0	3.43	7.44	3240
14.0	3.95	10.45	3440
15.0	4.39	14.08	3620
16.0	4.76	18.37	3800

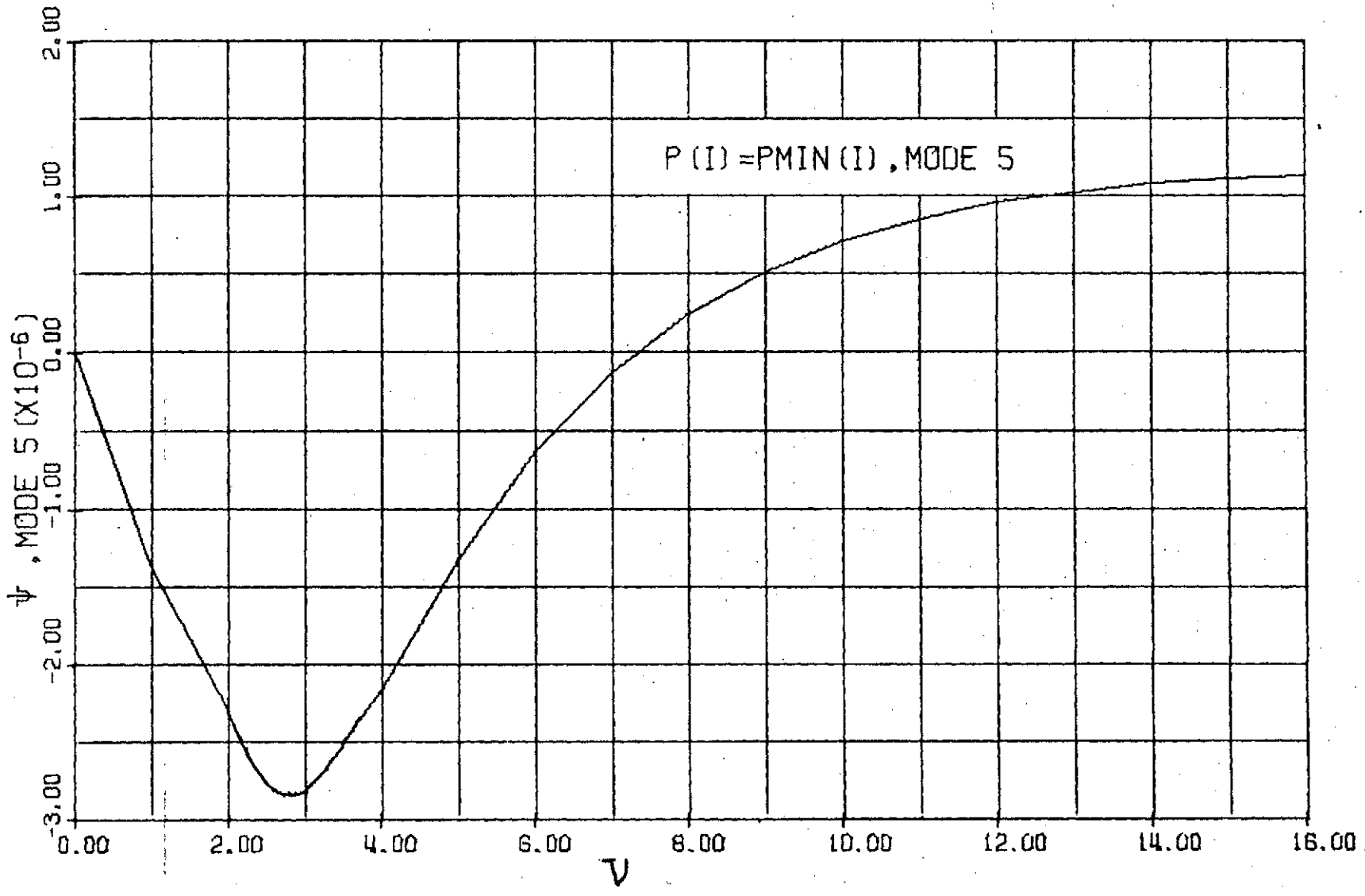

Figure 28. ψ_5 versus ν for Case 1.

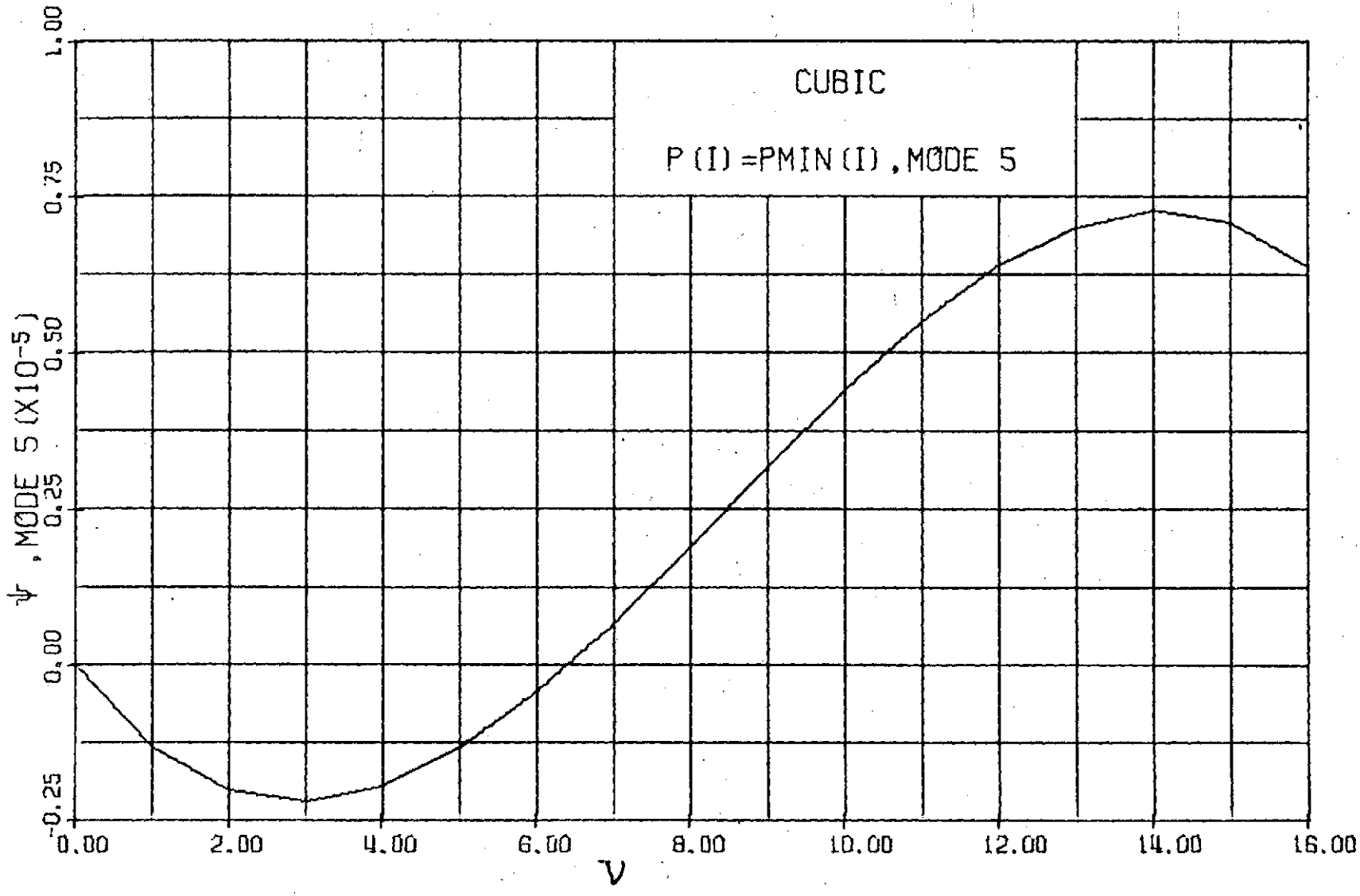

Figure 29. Cubic Approximation of ψ_5 for Case 1.

Table XIV. Computed ψ_5 and Cubic Fit Values for Case 1 and $\nu_o = 5.0$.

ν ft/rad	COMPUTED CURVE ($\times 10^6$)	CUBIC FIT $\nu_o = 5.0$ ($\times 10^6$)	COMPUTED AIRSPEED ft/sec
0.0	0.0	0.0	0
1.0	-1.37	-1.31	400
2.0	-2.29	-2.01	755
3.0	-2.81	-2.19	1030
4.0	-2.15	-1.93	1280
5.0	-1.31	-1.31	1550
6.0	-0.63	-0.41	1830
7.0	-0.12	+0.70	2130
8.0	+0.25	1.92	2420
9.0	0.53	3.18	2730
10.0	0.72	4.40	3020
11.0	0.86	5.50	3320
12.0	0.96	6.40	3620
13.0	1.03	7.02	3900
14.0	1.08	7.28	4200
15.0	1.11	7.09	4500
16.0	1.13	6.38	4780

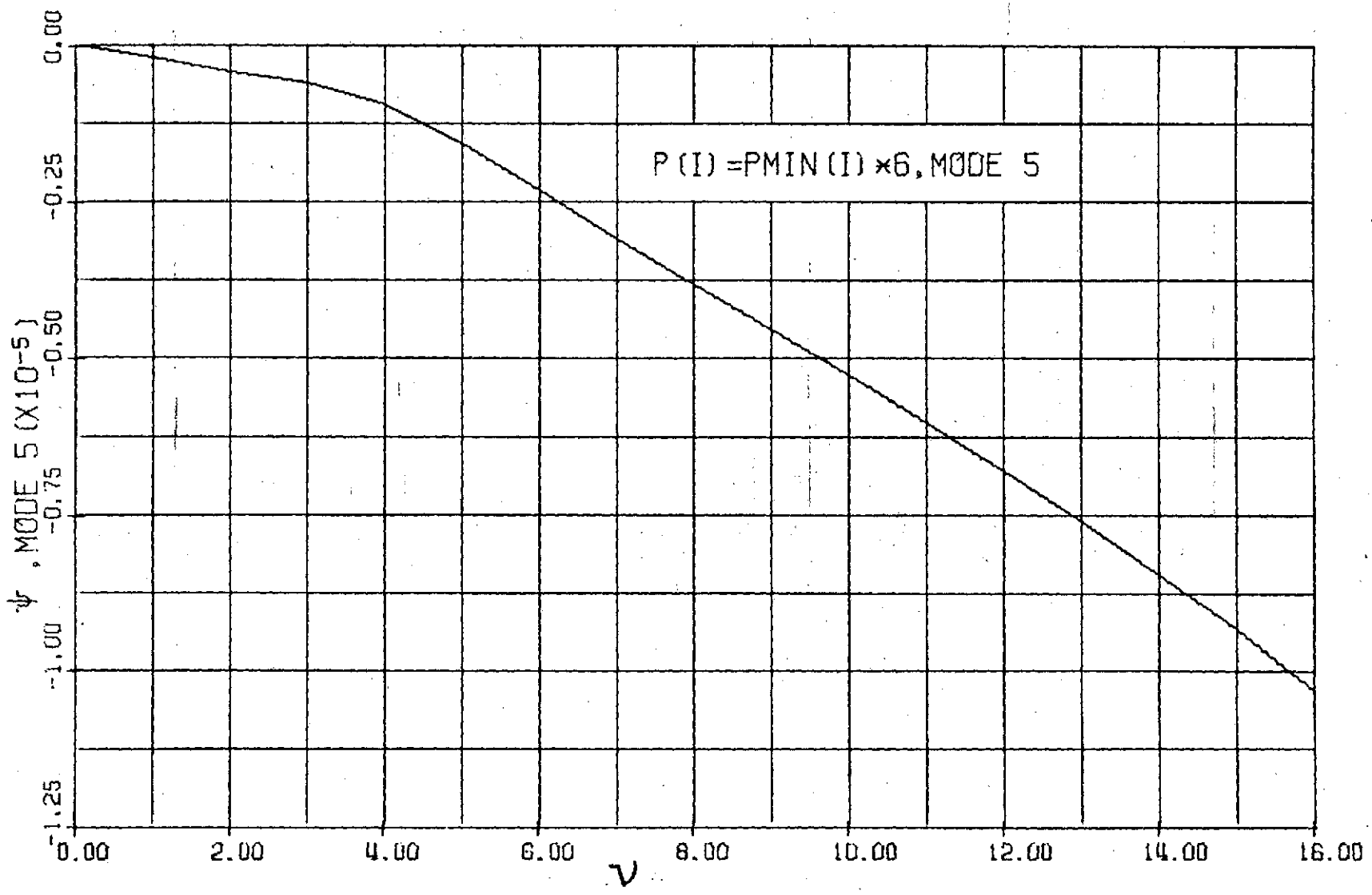

Figure 30. ψ_5 versus ν for Case 2.

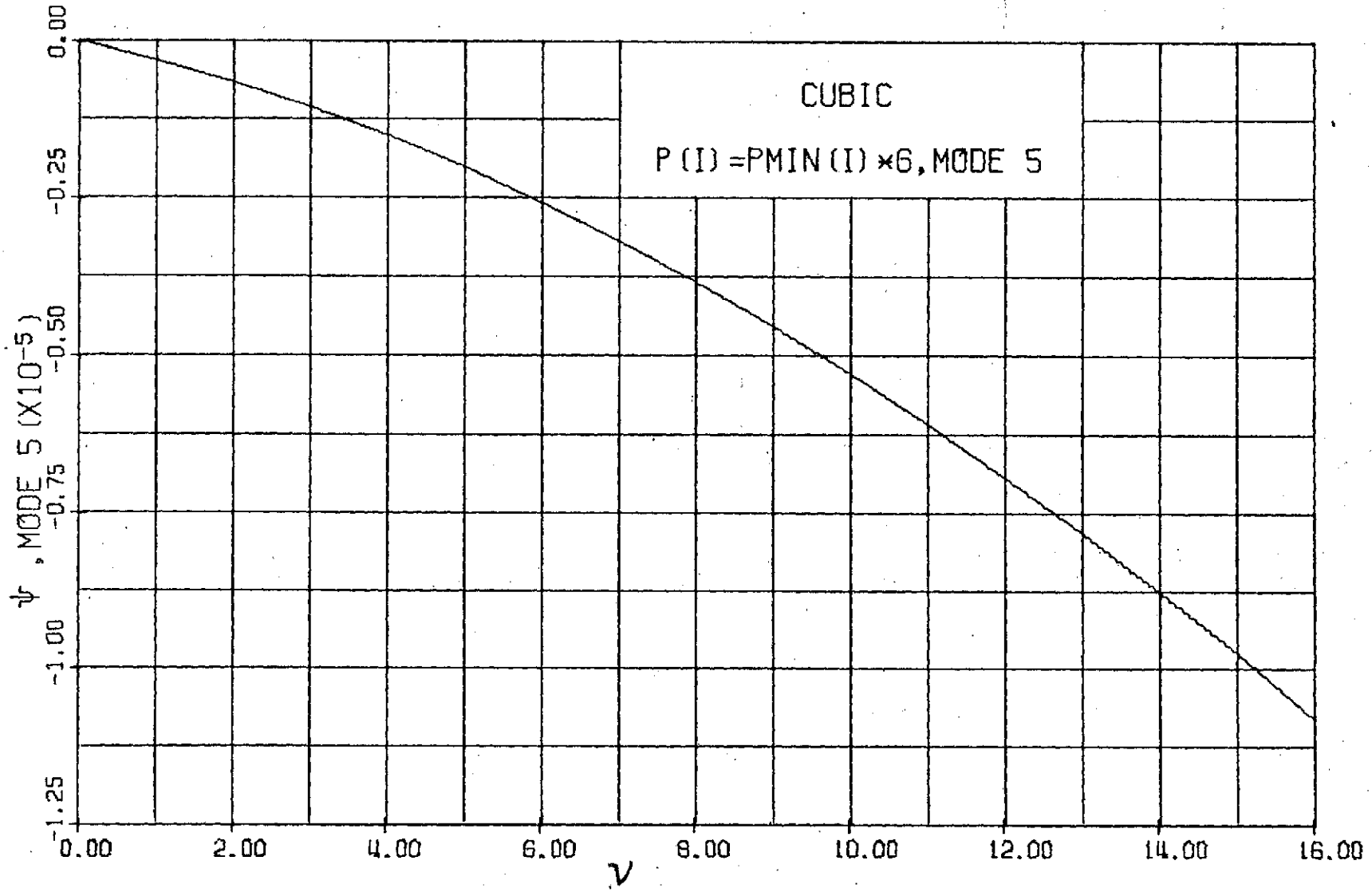

Figure 31. Cubic Approximation of ψ_5 for Case 2.

Table XV. Computed ψ_5 and Cubic Fit Values for Case 2 and $\nu_o = 9.0$.

ν ft/rad	COMPUTED CURVE ($\times 10^6$)	CUBIC FIT $\nu_o = 9.0$ ($\times 10^6$)	COMPUTED AIRSPEED ft/sec
0.0	0.0	0.0	0
1.0	-0.18	-0.31	414
2.0	-0.41	-0.66	830
3.0	-0.60	-1.06	1260
4.0	-0.93	-1.52	1680
5.0	-1.55	-2.02	2090
6.0	-2.32	-2.58	2430
7.0	-3.08	-3.18	2700
8.0	-3.81	-3.83	2910
9.0	-4.54	-4.54	3070
10.0	-5.27	-5.28	3200
11.0	-6.01	-6.08	3290
12.0	-6.78	-6.93	3350
13.0	-7.59	-7.82	3400
14.0	-8.43	-8.75	3430
15.0	-9.32	-9.74	3470
16.0	-10.30	-10.76	3490

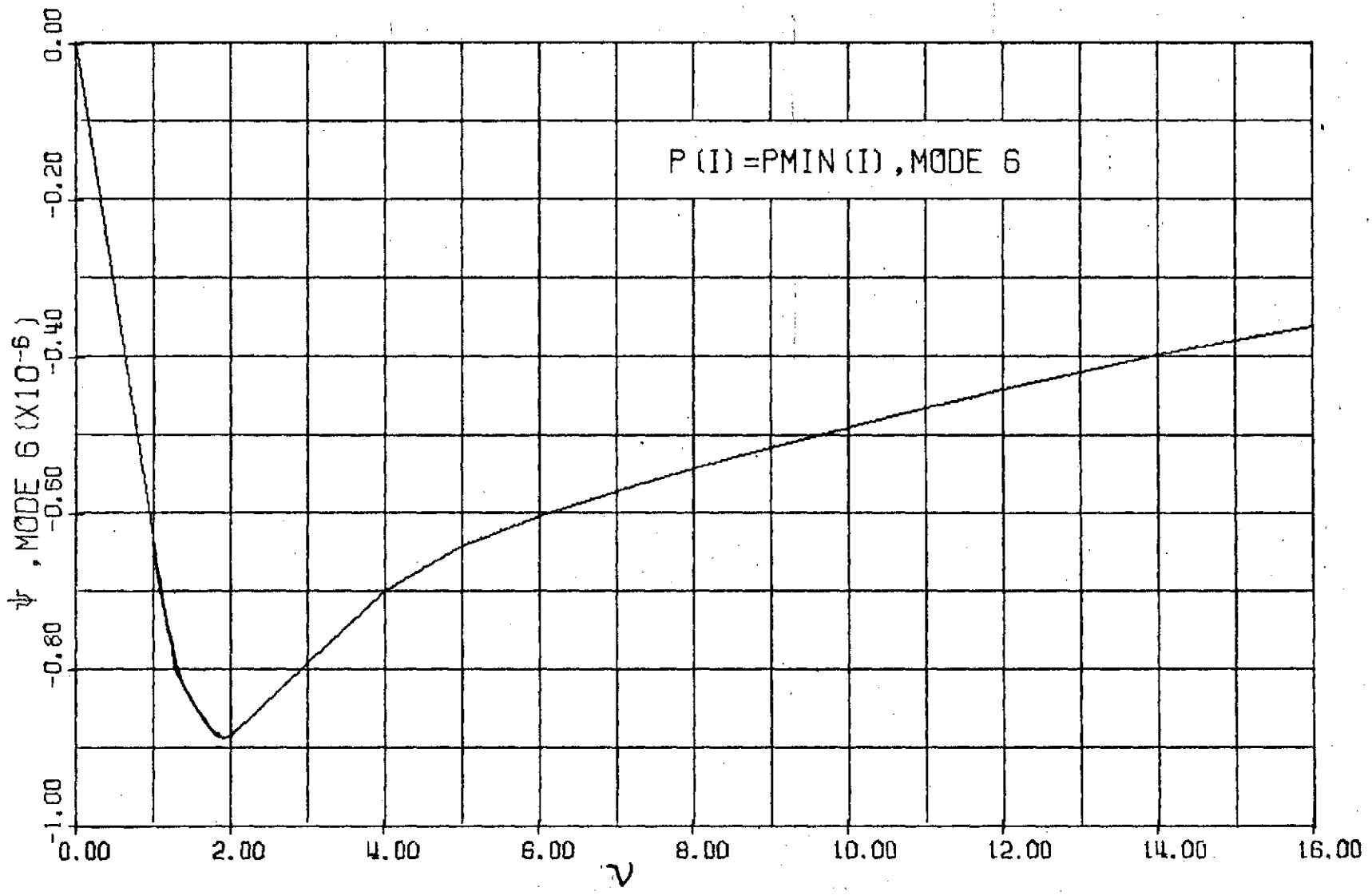

Figure 32. ψ_6 versus ν for Case 1.

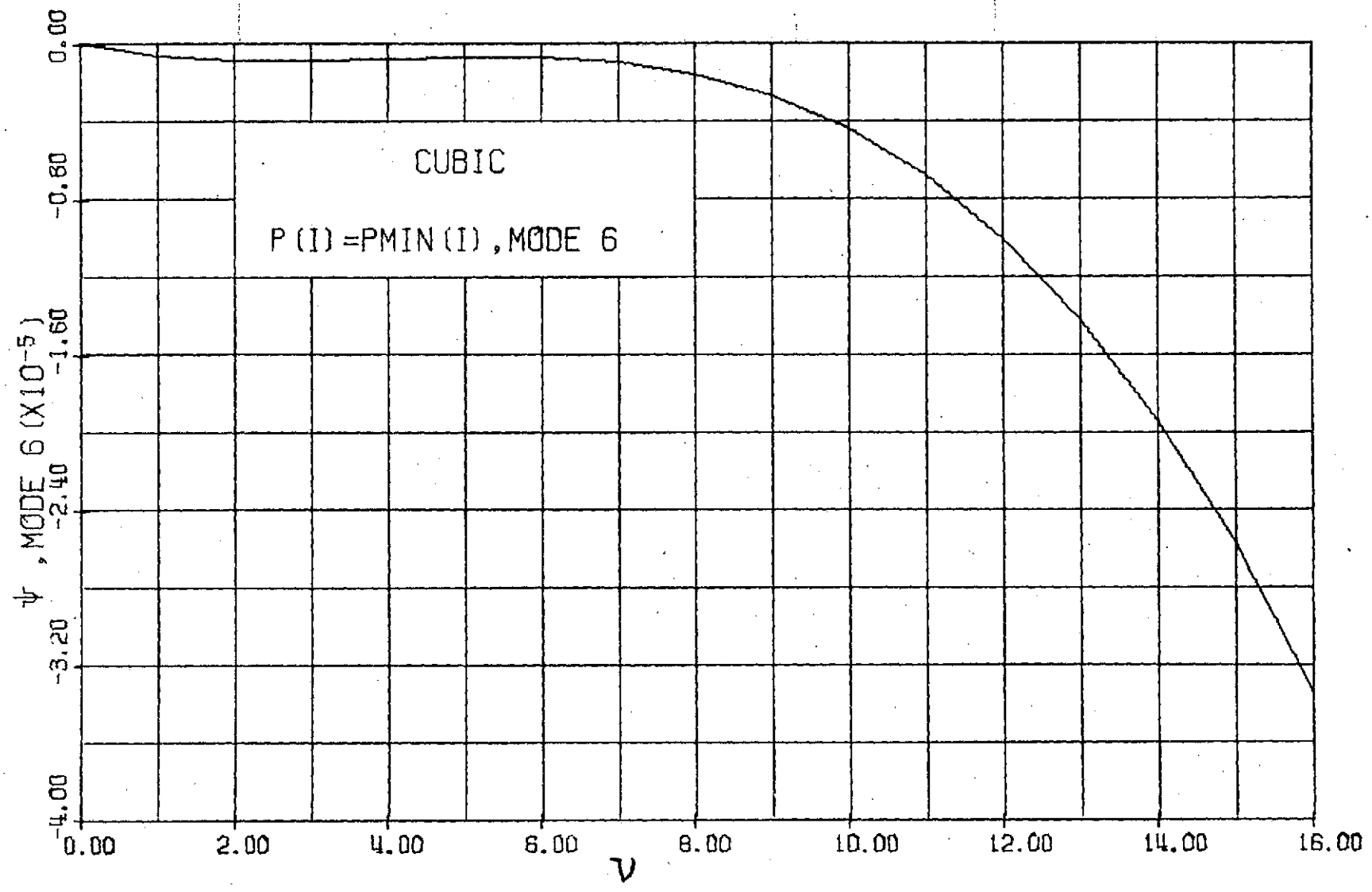

Figure 33. Cubic Approximation of ψ_6 for Case 1.

Table XVI. Computed ψ_6 and Cubic Fit Values for Case 1 and $\nu_o = 5.0$.

ν ft/rad	COMPUTED CURVE ($\times 10^6$)	CUBIC FIT $\nu_o = 5.0$ ($\times 10^6$)	COMPUTED AIRSPEED ft/sec
0.0	0.0	0.0	0
1.0	-0.63	-0.58	581
2.0	-0.88	-0.81	1090
3.0	-0.79	-0.83	1600
4.0	-0.70	-0.73	2160
5.0	-0.64	-0.64	2750
6.0	-0.60	-0.68	3360
7.0	-0.57	-0.95	4000
8.0	-0.54	-1.59	4650
9.0	-0.51	-2.69	5310
10.0	-0.49	-4.38	5990
11.0	-0.46	-6.78	6670
12.0	-0.44	-10.00	7360
13.0	-0.42	-14.20	8050
14.0	-0.40	-19.40	8730
15.0	-0.38	-25.70	9430
16.0	-0.36	-33.40	10100

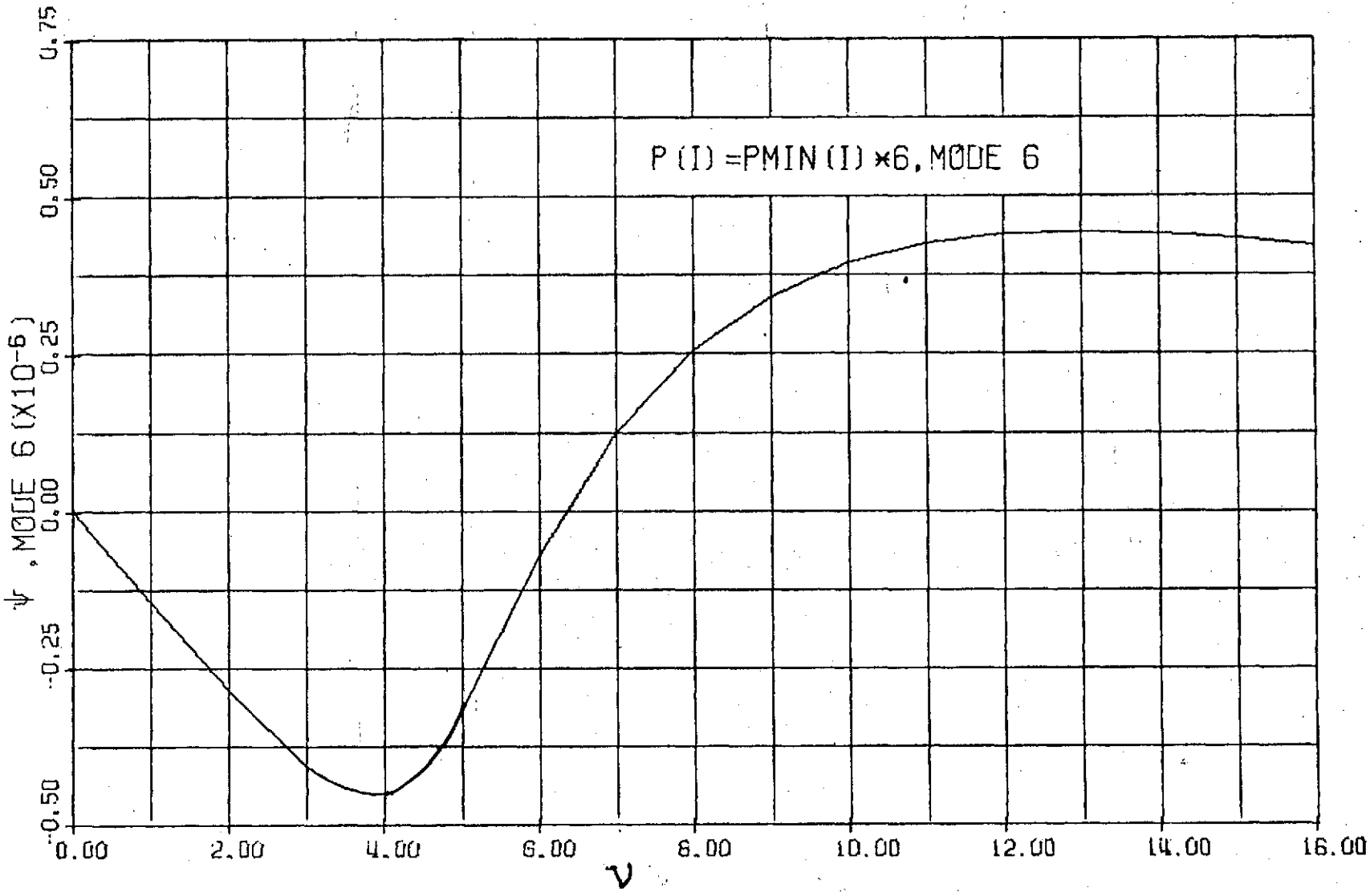

Figure 34. ψ_6 versus ν for Case 2.

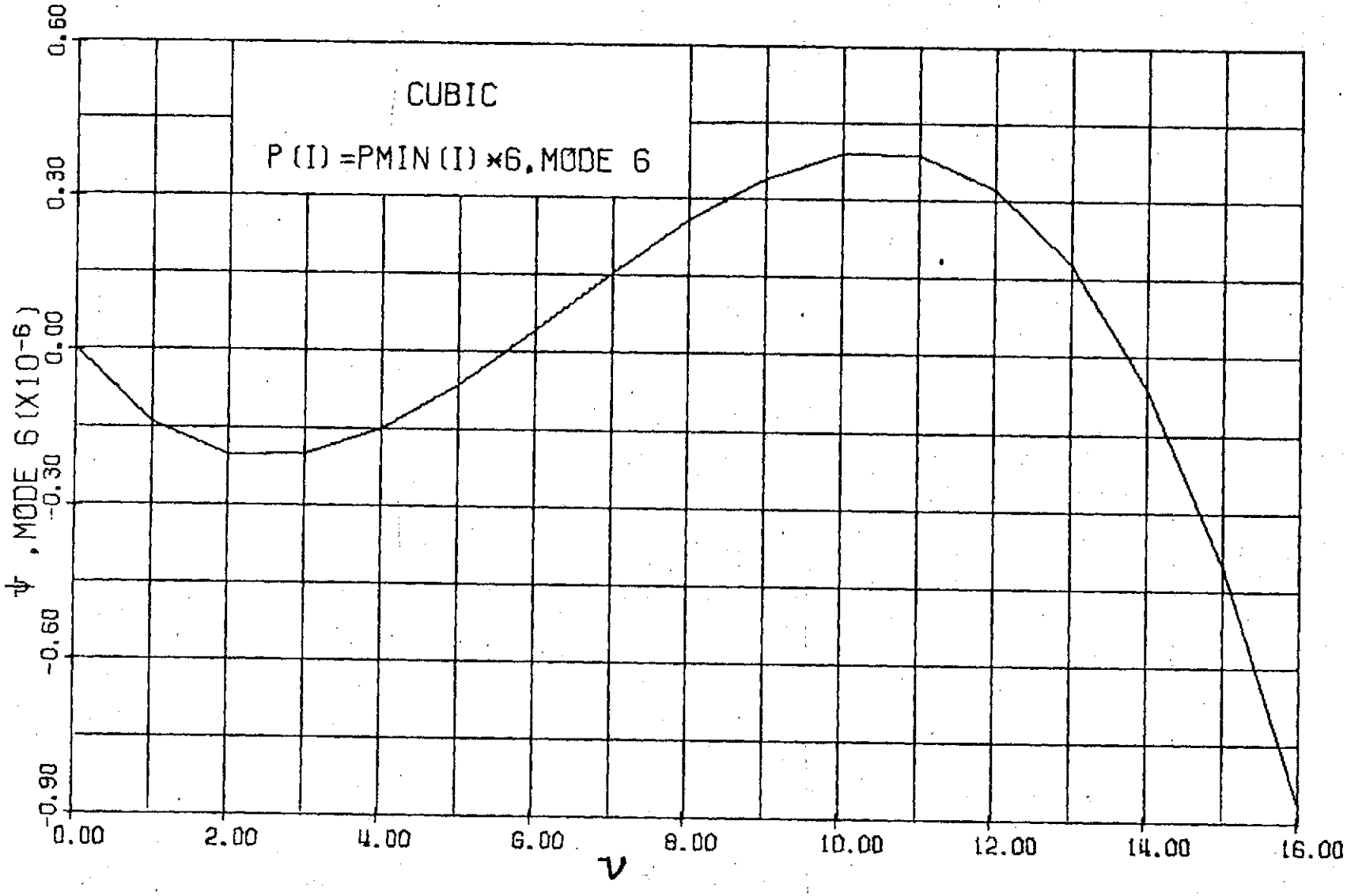

Figure 35. Cubic Approximation of ψ_6 for Case 2.

Table XVII. Computed ψ_6 and Cubic Fit Values for Case 2 and $\nu_o = 9.0$.

ν ft/rad	COMPUTED CURVE ($\times 10^7$)	CUBIC FIT $\nu_o = 9.0$ ($\times 10^7$)	COMPUTED AIRSPEED ft/sec
0.0	0.0	0.0	0
1.0	-1.43	-1.39	651
2.0	-2.84	-2.01	1260
3.0	-4.05	-1.99	1800
4.0	-4.48	-1.49	2250
5.0	-3.14	-0.64	2640
6.0	-0.70	+0.42	3050
7.0	+1.25	1.54	3470
8.0	2.56	2.59	3910
9.0	3.42	3.42	4350
10.0	3.95	3.90	4770
11.0	4.26	3.88	5200
12.0	4.40	3.22	5630
13.0	4.44	1.78	6060
14.0	4.41	-0.58	6490
15.0	4.33	-4.00	6930
16.0	4.22	-8.62	7360

ABSTRACT

ABSTRACT

The established method for solution of the critical flutter velocity of the equation of motion for an aircraft structure requires a plot of ψ versus ν where ψ is the imaginary part of the eigenvalue of the flutter equation and ν is the velocity divided by the circular frequency of oscillation or the dependent variable of the flutter equation. From this plot the crossover points, where ψ is zero, are sought from which the lowest or critical velocity, for which the structure will have divergent oscillations, may be computed. A curve fitting approach (which is rapid, simple, and direct in comparison to established methods) has been developed to solve the flutter equation for the critical flutter velocity.

The ψ versus ν curves are approximated by cubic and quadratic equations. The curve fitting technique utilized the first and second derivatives of ψ with respect to ν which are derived in the text.

The method was tested for two structures, one structure being six times the total mass of the other structure. The algorithm never showed any tendency to diverge from the solution. The average time for the computation of a flutter velocity was 3.91 seconds on an IBM Model 50 computer for an accuracy of five per cent. For values of ν close to the critical root of the flutter equation the algorithm converged on the first attempt. The maximum number of iterations for convergence to the critical flutter velocity was five with an assumed value of ν relatively distant from the actual crossover.